The Use of Nanostructures in Bioelectronics

Brendan George Casey

Submitted for the degree of Doctor of Philosophy
to the Department of Electronics and Electrical Engineering
at the University of Glasgow

June 1999

ProQuest LLC.
789 East Eisenhower Parkway
P.O. Box 1346
Ann Arbor, MI 48106 – 1346

After those halcyon days.....

Acknowledgements

Since day one of my PhD experience I have been helped, encouraged and most importantly befriended by many people within the Department of Electronics and Electrical Engineering and Glasgow University on a whole.

However, this thesis would not exist but for the influence of several of these people.
If it were not for Chris Wilkinson's Midas like ability to find money I would not have been given the opportunity to do this work at all.

The job of supervising my work also fell on the shoulders of Chris along with Geoffrey Moores.

I would also like to thank all of the technical staff who have helped and tutored me throughout the course of my work. Particularly, Bill Monaghan, Mary Robertson, John Cochrane, the dry etchers, the mechanical workshop and everyone in nano.

I am grateful to John Weaver, Adam Curtis, Douglas Macintyre, Steve Thoms and Jon Cooper for useful discussions and advice.

Thanks to the Friday Pub People who always help get things in perspective if out of focus.

I thank my friends for putting up with me to the end and to the one who didn't quite make it all the way, thanks.

Finally, I thank my family for standing by me and supporting me through thick and thin.

Thank you all.

Outline of Thesis

The Use of Nanostructures in Bioelectronics

During the period from October 1994 to October 1997, I was working towards a PhD investigating potential applications of nanofabrication in biomedical assays. Using standard fabrication procedures such as electron beam lithography, reactive ion etching and anodic bonding, devices were made which allowed direct, real time observation of DNA conformations under the influence of an electric field. Mechanical pattern transfer methods were developed which utilised polymer substrates to fabricate devices for biological tests. These polymer devices were used to extend the initial DNA work with a view to producing a device capable of separating large chain DNA molecules by length. The nanofabrication methods developed for these devices using polymer thermoplastics were used to test a series of nanometre scale topographies for uses in the areas of biological cell guidance and adhesion.

Contents

Abstract

This thesis describes research performed to investigate the use of nano and microstructures in bioelectronics. The nanofabrication techniques and developed processes are presented first in conjunction with the application design ideas at each stage. The results obtained by the application of these devices in bioelectronics are then described. The two application areas for nanotextured devices presented in this thesis are biological cell adhesion and DNA sequencing.

The nanostructure fabrication processes used throughout this project were electron beam lithography, reactive ion etching, electroplating and anodic bonding. These techniques have been used either to directly fabricate a working device or as donor processes for mechanical pattern transfer technology. The mechanical pattern transfer fabrication process developed for biological applications was based on polymer substrates and embossing to produce working devices from a nanofabricated master die. Three other novel polymer patterning procedures are presented in this thesis. It is shown that it is possible to pattern cellulose acetate using deep ultra violet exposure and that when applied to a previously embossed plastic substrate, it is possible to produce multilevel polymer devices. It is also shown that using electron beam lithography, solid sheets of polymethylmethacrylate can be patterned thus producing working devices in a single step. Following on from this, such perspex samples have been used as soft embossing masters for the fabrication of polystyrene devices.

ABSTRACT

Using the nanofabrication techniques developed during the course of this work, fractionating chambers for the direct, real time observation of migrating DNA molecules have been fabricated. The driving force behind this work was the Human Genome Project which is concerned with the mapping of all the genes in the human nuclear genome. The benefits of knowing this information are extensive, from applications in cloning to the discovery of which genes are responsible for hereditary illnesses and traits. However, the current method for sequencing the genetic code contained within DNA of gel electrophoresis is far from optimal and is very slow. Therefore, we have designed and fabricated a system on a chip which should be capable of rapid, high resolution DNA sequencing. The device works by passing the DNA molecules through an environment which presents different levels of retardation to molecules depending on their size. The genetic code contained within the DNA strands can then be calculated by comparing molecular migration rates. The DNA is moved through the device by an electric field using a process known as electrophoresis.

The devices used to analyse DNA motion under electrically induced migration were initially fabricated in SiO_2 using e-beam lithography and C_2F_6 reactive ion etching. They were then sealed using anodic bonding to produce a hermetic flow chamber for molecular observation. These samples consisted of 500nm diameter pillars on a 1μm pitch in arrays of 7,840,000 structures. The function of the pillar elements was to act as a retarding environment to DNA molecules which were passed through the chamber using electrophoresis. The migrating DNA was stained with ethidium bromide and observed using fluorescence microscopy. The conformational changes that the migrating molecules exhibited were compared to those predicted by the biophysical theory of DNA migration and a suitable geometry capable of producing highly dispersive mobilities was mathematically and electrostatically modelled. The geometry which produced the desired response was found to be an array of 'U' shaped elements.

Devices consisting of such features were fabricated using our embossing technique with the polymer cellulose acetate as the substrate. The DNA migration was again visualised using fluorescence microscopy and the results obtained with these devices are presented.

Biological cell adhesion to surfaces is an extremely important phenomenon in tissue and vascular repair. It is critical that platelet cells do not adhere to the inside of a plastic tube used to replace a diseased vascular section. The mechanisms for cell adhesion have been studied for many years, however the influence of topographical cues on adhesion is still uncertain. Cell adhesion to a surface is strongly affected by the roughness of that surface. However, studies into the effect of rugosity are inconclusive, mainly due to the

difficulty in characterising such surfaces. In this work, the embossing technique utilising perspex and silicon master samples was used for the fabrication of substrates to examine biological cell adhesion to rough surfaces. We fabricated large areas of 15nm and 60nm pillars which presented cells with a quantifiable surface roughness. These devices were made in cell culture grade polystyrene and cell adhesion to nanotextured areas was compared with that for smooth unpatterned areas. The results for such devices are presented and a mechanism for the cellular reaction is suggested.

Chapter 1

Introduction

The main body of work presented in this thesis is concerned with the development of new micro and nanofabrication processes primarily for biological applications. These procedures developed utilise polymer materials as substrates for the fabrication of devices for biological assays and prosthetics and for diffractive optics applications. Using plastic substrates it is possible to produce nanoscale patterns using a number of pattern transfer processes. The main area of development described in this thesis is in mechanical pattern transfer. The pattern is transferred to the final device by pressing a die or mould into a malleable substrate at elevated temperature. This embossing procedure is used in many areas of commercial manufacturing as a low cost, large scale method of producing plastic shapes and patterns but not at nanometre sizes. We have fabricated structures in fused silica and silicon at the resolution limit of electron beam lithography and found that it is possible to mechanically transfer these nanometre scale features into polymer substrates. This shows that the resolution of our mechanical pattern transfer process is at least as good as that of e-beam lithography. It is also possible to pattern some plastic materials using UV or electron beam irradiation and novel applications of these processes are presented in this thesis. Three novel patterning processes are presented here. Firstly it is shown that the polymer cellulose acetate can be patterned using deep ultra violet exposure [1]. If used in conjunction with embossing, multi-level plastic devices can be fabricated using this technology. Secondly, direct writing of polymethyl methacrylate(PMMA) is presented [2]. Normally, thin layers in

the region of a few hundred nanometres of PMMA are spin coated on substrates and then exposed using electron beam lithography. A new process has been developed in which solid sheets of PMMA are patterned. This form of fabrication allows the production of large area nano-patterned devices and efficient diffractive optics such as Fresnel lenses, zone plates and computer generated holograms. These are multilevel devices which under normal circumstances require nanometre scale alignment, however by direct writing it is possible to produce such devices in a single step. The direct writing of sheet PMMA is excellent for prototyping but is not suitable for mass production. Therefore, a novel method of embossing was developed whereby the direct written PMMA sample was used to pattern a polystyrene substrate [3]. Having optimised these processes, they have been applied to the production of optical devices and polystyrene replicas have been used to investigate biological cell interaction with nanometric topographies [3][4]. However, the initial application considered for these types of devices is in DNA sequencing. Initially samples for this function were made using standard fabrication techniques before embossed devices were tested.

In many areas of biological and medical research it is extremely desirable to minimise the quantity of sample required for an analysis. In medical practice it is important that assays can be carried out with minimum delay. The commonly used assays, such as DNA sequencing and blood tests were developed by scientists working within biological and medical laboratories and their methodology reflects this origin. Recently it has been realised that progress in nanofabrication and material science has presented the possibility of simplifying and accelerating such assays. The medical profession and researchers within the biological sciences have always been keen to embrace the introduction of engineered devices and materials, such as pacemakers, artificial valves, polymer sutures and biosensors. It is the object of this project to examine the possible applications of novel nano-engineering procedures and devices to both in-vivo and in-vitro situations, particularly in DNA sequencing, cell guidance and cell adhesion.

The separation of fragments of DNA by length is a crucial procedure in many areas of biological analysis, so it is therefore preferable if the method used for fractionating specific types of molecular samples is optimised for that application. Ideally, a consistent and repeatable process which can produce high resolution results from a small assay sample in a short time scale is required. At present there is no single method capable of delivering such results but the approach described in this thesis may alleviate some of the problems.

In order to understand the difficulty of length sequencing of DNA, it is worth considering the problem from a size viewpoint. Long, single, continuous strands of

deoxyribonucleic acid are found in the nucleus of cells. The DNA is arranged in base pairs which contain thousands of unique functional units called genes. Genes are the basic unit of heredity, i.e. they are responsible for the transmission of mental and physical qualities from parents to offspring. It is this nuclear genetic information, or genome as it is called, which is of interest and concern to the world wide Human Genome Project [5]. The nuclear genome contains approximately 3000 Mega basepairs, 50000 - 100000 genes and is made up of roughly a metre length of DNA. From these numbers it is possible to picture the enormity of the task to sequence the whole genome and with present methods it is not feasible to perform this task in one researcher's lifetime.

At present the standard method used to separate and identify deoxyribose nucleic acids is to drive them through gels using an electric field, with different lengths arriving at the end of the gel at different times [6][7][8][9]. This method is known as gel electrophoresis and allows DNA which has been removed from anything from fungi to humans to be separated into specific sizes in order to facilitate sequencing of the genetic code contained within. Currently in almost every step of gene cloning, DNA has to be sized or the length of a fragment has to be either analysed or controlled and this is done using gel electrophoresis with a constant field. During this procedure, DNA migrates under the electrophoretic force through the porous gel which retards the movement of the polymer strands. This migration occurs because DNA has a net negative charge associated with it as explained in §5.2.1 of this thesis. Essentially the gel works in a similar way to a sieve with greater resistance to longer strands, therefore the migration of different strand lengths occurs at different speeds and the length can be estimated by the arrival time at the end of the gel. However, the motion of biological molecules in these gels is very complicated and depends not only on the strength of the electric field being applied but also on the time sequence of applications of the field. This problem is best exemplified when considering large DNA strands, greater than 15μm in length, since it is not possible to fractionate these molecules using a simple continuous field. In this case it is necessary to use pulsed and non-uniform fields, commonly known as contoured fields, since the field is now used to steer the strands through the gel or retarding medium. This complicates the procedure and does not allow a simple model of its operation to be used. This is explained in detail in §5.2.1.

The development of such techniques has been one of the main focus points of research in improving separation of DNA along with a number of other procedures such as capillary electrophoresis, which uses gel set in a capillary tube. However nearly all of the common areas of development involve small adjustments to the constant field method in ways such as those described by [10][11] and [12]. Many changes in the

technique have been tried. However, changing the retarding medium to something other than a gel has not been tried until recently. Until now all separation techniques have used agarose, a natural polymeric carbohydrate, or acrylamide as the sieving medium. This appears to place a huge constraint on procedures since the pore size of the gel is controlled by gel concentration and therefore the upper limit is determined by the mechanical resistance of the gel. This is very unfortunate since reptation theory, as described in §5.2.1, suggests that it should be possible to extend the sieving regime to separate large DNA using constant fields if the pore size of the medium is large enough.

We have designed and fabricated an alternative to gel electrophoresis which should be capable of rapid sequencing of long strand DNA using a simple, constant electric field set up. The method employed involves the use of nanofabrication techniques to produce obstacle courses which will act as restrictive environments for the migrating molecules, an idea first described by Volkmuth et al [13]. In the work described in this thesis obstacle arrays of identical pillar like structures were initially made in silicon dioxide using electron beam lithography (EBL) and reactive ion etching (RIE). The DNA was visualised using fluorescence microscopy thus allowing observation of the conformational changes that DNA undergoes during electrically induced migration.

The desire to change and develop new device topographies means that it would be preferable if the nanofabrication method used for the chamber fabrication was as flexible and simple as possible. If a device such as this is to integrated into a currently existing, relatively successful laboratory set up, then it must be available as a cheap option. Therefore, in order to fulfil all of these requirements a cheap fabrication method has to be employed. These restrictions immediately eliminate EBL, since this is a very expensive way to produce working samples. However, by developing a mechanical pattern transfer method which can produce hundreds of devices from one beam written sample it is possible to make devices with a high throughput and a very low cost. Embossing allows fractionation chambers to be made economically and quickly in thermoplastics. This is immensely useful as it allows fabrication of structures which should facilitate fractionation of very large molecular weight polymers in a parallel system thus greatly accelerating the rate of sequencing. The advantages that these lattices allow over gels are extensive. The microfabricated chambers for separating DNA are cheap, small, easy to use and reusable. Due to their regularity and known structure, they are potentially more accurate than gels and avoid the need for complicated field configurations which require expensive equipment.

The development of the previously mentioned embossing fabrication technique presents the possibility of producing a wide variety of devices. It is this flexibility that

mechanical pattern transfer methods allow which helps to alleviate some of the problems faced in the area of biological cell guidance and adhesion experimentation.

The mechanism of cell adhesion has been studied by cell biologists for many years, but is not yet fully understood. In the body, biological cells adhere to each other and to prosthetic devices. Cell adhesion is important in tissue repair; in many cases it is desirable that cells adhere to each other and to other tissues. In other situations it is essential that cells do not adhere to surfaces. A good example of this is in vascular repair and vascular prostheses: here it is very important that platelet cells do not adhere to the inside of the plastic tube used to replace a diseased vascular section. In 1911 Harrison [14] observed that cells in vitro are strongly influenced by topography. Since then, it has been shown that it is possible to guide cells and affect their behaviour by placing them in environments which present topological cues [15][16][17]. Recently, there have been problems in producing devices for cell observations. This is because biologist now require large areas of either uniform or varying features over the device area and in a biocompatible material. If the features required are in the nanometre scale, then production of many samples with structures over large areas using standard fabrication techniques is very expensive and time consuming. However, embossing combats this problem and facilitates the production of large area devices which can in turn be used to perform extensive biological tests. It is the results from such devices which allow new insight into cell adhesion and guidance and which are described in this thesis.

Chapter 2 presents a brief review and explanation of the fabrication procedures of electron beam lithography, reactive ion etching and anodic bonding which are used to produce fused silica and silicon devices. The second part of chapter 2 describes the ideas behind choosing a suitable retarding feature for electrophoresis and presents the results of the electrostatic modelling of the optimally shaped structure. Chapter 3 describes embossing and general plastic fabrication methods and applications. This chapter reviews and presents devices made during the course of this work for use in DNA electrophoresis and cell adhesion tests as well as devices which are not applicable to bioelectronics, but do provide an insight into the expanse of devices capable of being produced using mechanical pattern transfer methods. Chapter 4 contains explanations of the biology and cell structure associated with cell guidance and adhesion and presents preliminary cell adhesion results obtained using embossed topographies in polystyrene substrates. Chapter 5 presents a brief review and explanation of the background biology, biochemistry and biophysics of DNA electrophoresis and presents the initial results obtained in DNA conformational control obtained using SiO_2 devices and describes DNA electrophoresis in plastic flow chambers. Finally, chapter 6 summarises the work and ideas presented in this thesis.

1.1 References

[1] Casey, B.G., Monaghan, W., and Wilkinson, C.D.W., Embossing of nanoscale features and environments, Microelectronic Engineering, vol. 35, pp. 393-396, 1997.

[2] Cumming, D.R.S., Khandaker, I.I, Thoms, S. and Casey, B.G., Efficient diffractive optics made by single-step electron beam lithography in solid PMMA, Journal Of Vacuum Science & Technology B, vol. 15, pp. 2859-2863, 1997.

[3] Casey, B.G., Cumming, D.R.S., Khandaker, I.I, Wilkinson, C.D.W., Nanoscale Embossing of Polymers using a Thermoplastic Die, To be published in Microelectronic Engineering, 1998.

[4] Curtis, A.S.G., Macdonald, K., Wojciak-Stotard, B., Casey, B.G., Wilkinson, C.D.W., The Reaction of Cells to Nanometric Topography, To be published 1998.

[5] Strachan, T., The Human Genome. UK: BIOS Scientific Publishers Limited, 1992.

[6] Turmel, C., Brassard, E., Forsyth, R.K., Slater, G.W., Noolandi, J.,. High Resolution Zero Integrated Field Electrophoresis of DNA. In: Lai E, Birren, B.W.,, ed. Electrophoresis of Large DNA Molecules : Theory and Applications. New York: Cold Harbor Press, 1990:

[7] Smith, L.M., DNA Electrophoresis. Current Opinion in Biotechnology 1993;4:37-40.

[8] Viovy, J.L., Duke, T., Caron, F., The Physics Of DNA Electrophoresis. Contemporary Physics 1992;33(1):25-40.

[9] Guszczynski, T., Chrambach, A., Electrophoretic Separation of S. Pombe Chromosomes in Polyacrylamide Solutions Using a Constant Field. Biochemical and Biophysical Research Communications 1991;179:482-486.

[10] Heller, M.J., Tullis, R.H., Microelectrophoresis for the Separation of DNA Fragments. Electrophoresis 1992;13:512-520.

[11] Brumley, R.L, Smith, L.M., Rapid Dna Sequencing By Horizontal Ultrathin Gel-Electrophoresis. Nucleic Acids Research 1991;19(15):4121-4126.

[12] Grossman, P.D., Soane, D.S., Capillary Electrophoresis Of DNA In Entangled Polymer-Solutions. Journal Of Chromatography 1991;559(1-2):257-266.

[13] Volkmuth, W.D., and Austin, R.H., "DNA Electrophoresis In Microlithographic Arrays," Nature, vol. 358, pp. 600-602, 1992.

[14] Harrison, R.G., On The Sterotropism Of Embryonic Cells. Science 1911;34:279.

[15] Clark, P., Connolly, P., Curtis, A.S.G., Dow, J.A.T., Wilkinson, C.D.W., Topographical Control Of Cell Behaviour - I Simple Step-Cues. Research Development Biology 1987; 99: 439-448.

[16] Clark, P., Connolly, P., Curtis, A.S.G., Dow, J.A.T., Wilkinson, C.D.W., Topographical Control Of Cell Behaviour: II. Multiple Grooved Substrata. Development 1990; 108: 635-644.

[17] Clark, P., Connolly, P., Curtis, A.S.G., Dow, J.A.T., Wilkinson, C.D.W., Cell Guidance In Ultrafine Topography in Vitro. Journal of Cell Science 1991; 99: 73-77.

Chapter 2

Electrophoresis System : Technical Background

This chapter is concerned with the design and fabrication of a retarding environment which will allow direct, real time observation of DNA strand conformations under electrophoretic migration. The initial sections describe the fabrication procedures of electron beam lithography, etching and anodic bonding. These processes are used to fabricate the preliminary SiO_2 devices for DNA observation. The full fabrication details are described and a suitable sample mounting set up for microscope visualisation is explained. The second section of work presented in this chapter describes electrostatic modelling of retarding environments. The structures modelled are considered to be plastic coated with metal. The reason for this is that after testing the SiO_2 devices, the actual molecule fractionation chambers are fabricated using embossing for the reasons explained in chapter 1. The field patterns for these plastic devices are modelled using Vector Fields computer package PC-OPERA.

2.1 Micro and Nanofabrication Procedures

In order to fabricate silicon and SiO_2 devices for electrophoretic studies, nanofabrication processes developed at the University of Glasgow have been used. However, not only are these fabrication methods necessary to produce such devices, they are also essential in the production of patterned dies for the mechanical pattern transfer techniques described in chapter 3 of this thesis. Thus, the processes of electron beam lithography, lifting off of thin metal films, wet and dry etching and substrate sealing are the foundations for all of the devices fabricated and tested during the course of this project. These techniques are detailed in the following sections of this chapter and form the basis for all the following fabrication developments presented.

2.1.1 Electron-beam Lithography

Electron beam lithography is a technique used to produce extremely fine patterns primarily required by the electronics industry for integrated circuits. The first electron beam lithography machines were developed in the late 1960s and were made by converting scanning electron microscopes (SEM) [1]. The process of e-beam lithography has several main attributes. It has very high resolution, is an extremely flexible technique, but is slow, expensive and requires sophisticated equipment. Figure 1a shows a block diagram of a typical e-beam system. The part of the system which produces the beam is known as the column. This column contains the electron source or gun, lenses, beam control mechanisms and a detector for focusing and position detection of the beam. The process for pattern transfer involves coating the sample with an electron sensitive resist, typically the polymer polymethyl methacrylate (PMMA).

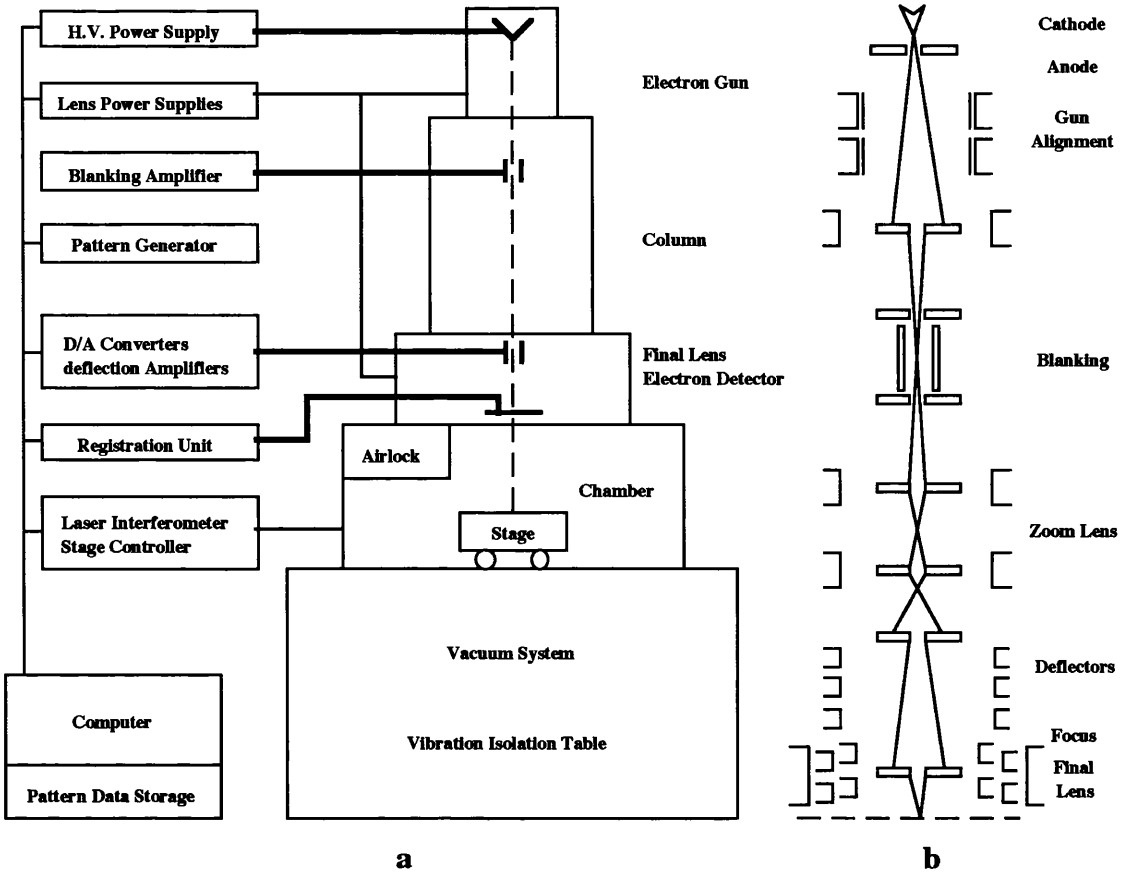

Figure 1. *(a) Block diagram of a typical electron beam lithography system [1]. The column forms and controls the beam. Under the column is a chamber containing the stage for moving the sample and facilitating loading and unloading. A set of control electronics supplies signals to the various parts of the machine, while a computer controls the overall running. (b) Diagram of the electron optics of the chamber. These are mainly lenses used for focusing and deflection, apertures to control beam passage and a blanking set up to turn the beam on and off.*

Figure 1b shows the constituent parts of the electron beam column. The electron source is made from a piece of conducting material and can be one of two types. Firstly, there are thermionic sources whereby electrons are emitted by heating the element to a point where the electrons have sufficient energy to overcome the work function barrier of the conductor. The other type of source is known as a field emission source, which produces electrons due to the application of an electric field sufficiently strong to allow the electrons to tunnel through the barrier [1].

After being emitted from the source the electrons are focused using electron lenses which can be either electrostatic or magnetic. The blanking section of the column is responsible for turning the beam on and off and is carried out by a pair of plates used as an electrostatic deflector. This deflector in conjunction with an aperture - a small hole through which the beam passes on its way down the column - allows the beam to be

switched on and off. The lower section of the column contains more lenses for focusing and deflection and a Faraday cup which measures the beam current to ensure correct dosage for resist exposure. The bottom of the column contains the stage where the sample is located and an airlock valve to allow loading and unloading of samples while keeping the gun under vacuum.

E-beam lithography is used for a number of purposes. It is used extensively to make masks for photolithography and X-ray lithography. It can write directly upon resist on a semiconducting substrate to produce prototype devices for the electronics industry. It is utilised for researching nanofabrication limitations and applications in areas outwith the electronics industry.

Throughout the course of this work electron beam lithography was used for all of the above applications. All the electron beam lithography was carried out on two machines within the department at Glasgow. A LEICA Cambridge Beamwriter EBPG 5 HR 100 which can operate at 20, 50 and 100kV and is capable of writing high resolution patterns as small as 20nm, and a converted Jeol 100CXII electron microscope which is capable of sub 10nm lithography [2].

The obstacle arrays fabricated for the initial stages of this work have small volumes and low dimensionality and were designed after consideration of the pore sizes in agarose. The maximum pore size possible in a gel before loss of structural rigidity is approximately 0.3μm, therefore a pillar with a diameter of 0.5μm was chosen. This size was selected since it was relatively large but still comparable with gel dimensions and thus makes it possible to compare the results obtained with those of agarose. This size of feature can be easily made using electron beam lithography and corresponds to an 'unphysical' agarose gel with a concentration of 0.1%.

2.1.2 Resists and Metalisation

A necessary component of every form of lithography is a recording medium. In photolithography and electron-beam lithography this medium is known as a resist. A commonly used e-beam resist is the polymer PMMA(polymethyl methacrylate) which has properties well suited for many areas of device fabrication [3]. PMMA is a positive resist, however there are also many negative resists available. A resist is categorised by how it reacts when it is exposed to the electron beam. In a positive resist, when the e-beam is scanned over it, the polymer chains in the area exposed are broken down into smaller chains which are more soluble in a particular solvent for that resist. The solvent, or developer as it is known, used for PMMA is methyl isobutyl ketone (MIBK). However, in order to make the development process more controllable the MIBK is often diluted down using isopropyl alcohol (IPA). This process is based on a solvent/non solvent solution which dissolves the molecules of lower molecular weight produced by the e-beam exposure preferentially. For negative resists the process is inverted. The scanning of the electron beam induces cross-linking in the resist and therefore exposed areas become less soluble in the relevant developer. The negative resist used in this project is Hoechst AZ PN114 and it is developed in AZ400K developer. The mechanism of this resist will be explained in detail in chapter 3.

For most applications, and indeed in this project, the main use of thin PMMA layers is as a mask for a process known as "lift-off" [4]. This procedure facilitates the transfer of a metal pattern onto a substrate surface which can then be used directly or as a mask for further processing. The best way to do this is by using a resist bilayer [5]. This means that two resist layers are spun onto the sample with a short bake in between each coat. Initially, a low molecular weight PMMA layer is spun onto the sample and baked. A layer of high molecular weight PMMA is then added and the sample is written. The effect of the different sensitivities of the two layers is to produce an undercut or overhang profile. This is shown below in figure 2.

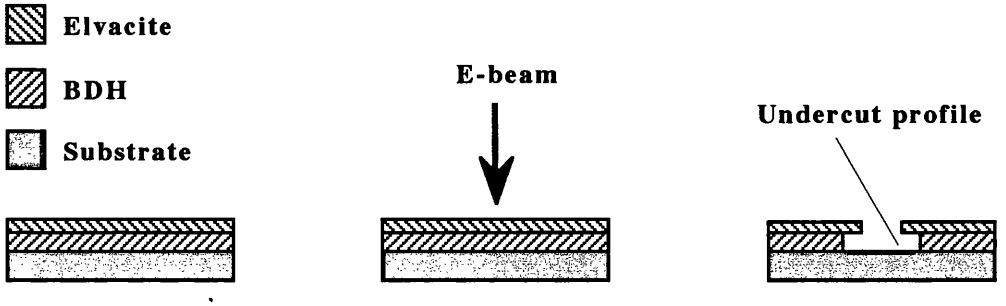

Figure 2. *E-beam exposure of a resist bilayer. The different sensitivities of the two layers causes the overhang or undercut profile.*

Once the sample has been written and developed, a thin metal layer is evaporated vertically onto the substrate. The resist which remained after development is then removed using acetone and it is found that a metal pattern identical to the original resist pattern is left on the surface of the sample. This is shown diagramatically below in figure 3.

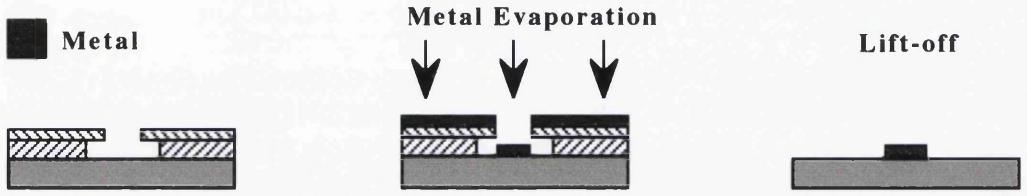

Figure 3. *The "lift-off" process. The overhang resist profile facilitates the easy removal of the resist even though it is coated with metal.*

The metal used in the this project for lift-off is nichrome, which is in turn used as an etch mask for the substrate.

In order to utilise resists for e-beam lithography, it is necessary to be able to coat substrates with a thin, uniform layer. This is done by spin coating. The sample is placed on a vacuum spinner and a few drops of resist are applied to the surface. The sample is then spun at several thousand revolutions per minute (rpm) for approximately 1 minute. The thickness of the resist layer obtained is controlled by the viscosity of the resist and by the acceleration of the spinner to the set spin speed. The viscosity of the resist is controlled by the amount of polymer dissolved in a volume of the complementary solvent. In the case of PMMA the solvent is either chlorobenzene or o-xylene. Since the resist is applied in a liquid phase it is necessary to bake it in an oven before using it so that it becomes solid. The ease with which PMMA is broken down by an electron beam, *its sensitivity*, is controlled by the molecular weight of the polymeric chains present. In the fabrication processes explained here two molecular weights are used. These are commercially known as Elvacite, which is high molecular weight (Mwt = 350000), and BDH which is of a lower weight (Mwt = 85000).

2.1.3 Etching

Etching is a process which involves the removal of layers of a sample in a similar way that rain, wind and waves erode a cliff face. There are two main methods used for etching, namely wet and dry etching. Wet etching utilises chemical solutions which react with the surface to remove the exposed material. Dry etching, on the other hand, removes surface layers by bombarding the sample with ions. The two processes are very different and give rise to wide variation in results. If a sample is exposed to a wet chemical etch, in general the material erosion progresses uniformly in all directions. This type of reaction is isotropic. Thus, when applied to a masked semiconductor material which requires selective patterning by etching, the final result is an undercut profile. In many cases this is undesirable but can be avoided by using dry etching. This method of substrate patterning works by sputtering off the surface material. It can either be a purely physical process or it can be a combination of physical and chemical etching. The later of these two is known as reactive ion etching (RIE). Both of the dry etching processes occur predominantly in the vertical direction and can thus be regarded as anisotropic. Figure 4 shows typical profiles obtained using wet and dry etches.

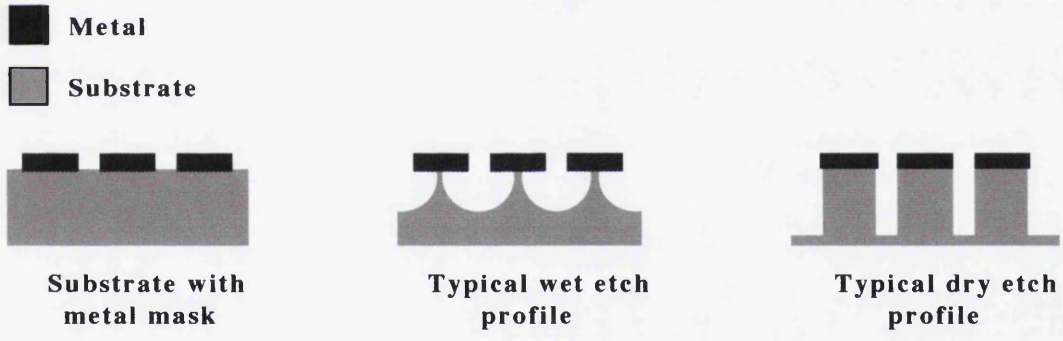

Figure 4. *Typical wet and dry etched profiles. The isotropic quality of wet etching results in a characteristic undercut profile. Conversely, the anisotropy of dry etching results in a vertical etch profile.*

It is dry etching's anisotropy that makes it the method of choice for many semiconductor applications, especially for small features. However, before selecting a wet or dry etch it should be noted that the sputtering action of dry etching can, in some cases, produce undesired effects.

For the application required here, namely the fabrication of 500nm pillars in SiO_2, reactive ion etching is the preferred method. RIE can be performed using a wide variety of gas species. The gas is chosen so that it reacts chemically with the substrate to form a

volatile product. However speed, etch damage and mask damage are also important considerations when selecting a suitable gas. A schematic representation of a RIE system is shown in figure 5.

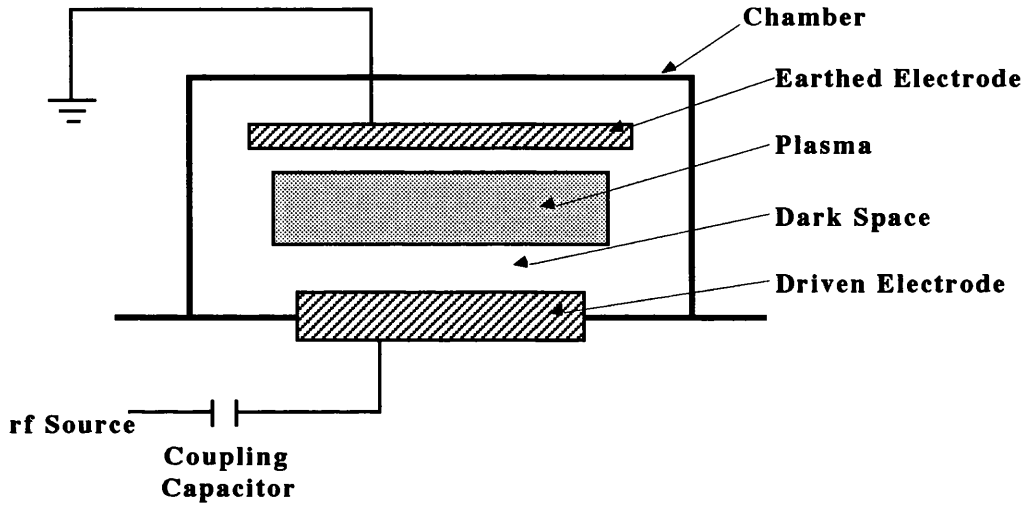

Figure 5. *Diagram of a simple RIE system. Ions are accelerated across the dark space and hit the surface of the sample. The etching then occurs due to sputtering and the reaction of the ions with the substrate.*

The system in figure 5 works as follows. Once the chamber is under vacuum, the reactive gas is introduced into the chamber under a set flow rate until a predefined constant pressure is obtained. Fluorine based chemistries are usually used to etch SiO_2. The gas used in the process described here is C_2F_6. The top electrode is grounded and the cathode at the bottom of the chamber is driven by an rf signal. This electrode set up generates a plasma in the chamber which in turn induces a dark space near the cathode. The rf discharge forms a plasma which contains reactive ions and electrons. Since the electrons travel faster than the ions, there is a rectifying action which produces a dc voltage which in turn accelerates the ions across the dark space. The sample to be etched is therefore placed on the cathode and is vertically bombarded by reactive ions. This reaction results in etching of the semiconductor substrate and thus production of volatile species which are in turn pumped out of the chamber.

The mask used for the patterning of the SiO_2 pillars in this instance was nichrome(NiCr), which has very good chemical resistance to the C_2F_6 etch.

2.1.4 Anodic Bonding

Anodic Bonding, first reported by Pomerantz and Wallis [6][7], is a process which permits the sealing of sodium rich glass to a metal or semiconductor at a temperature well below the softening point of the glass. The actual mechanism of the bond is as yet unknown although it is believed to be governed by ionic flow at the interface and in the glass, as explained in references [8][9][10][11] and [12]. Before the glass and silicon are bonded they are brought into physical contact by electrostatic attraction. This is done by heating the glass in order to increase its electrical conductivity. A potential is then applied across the elements, thereby producing an electric current through the stack and creating an electrostatic field in the gap. This field brings the elements into intimate contact. This can be explained by considering the conductivity of the glass is considered. At a temperature of approximately 500^{o}C the glass contains mobile positive ions and almost immobile negative ions. Thus, when a d.c. voltage is applied across the glass the positive ions move towards the cathode and become neutralised. At the same time, the area adjacent to the anode becomes depleted of positive ions and acquires a negative space charge. Therefore the side of the glass in contact with the silicon has a net negative charge while the silicon, which is in contact with the anode, has a positive charge. The pyrex and the silicon are drawn together by the electrostatic attraction which has built up and at this point the bonding itself takes place.

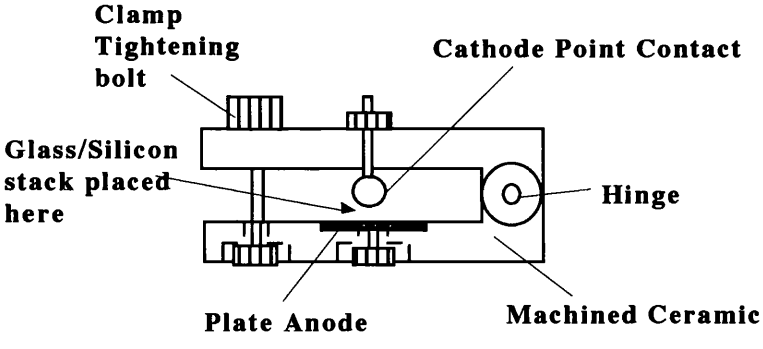

Figure 6. *Clamp used to perform anodic bonding. The silicon/pyrex stack is placed between the two electrodes which are integrated into the ceramic clamp. The clamp is then closed, tightened and placed in a furnace tube. Two nichrome wires are attached to the electrodes and connected to the high voltage power supply.*

In order for bonding to occur under laboratory conditions, the silicon and the glass are held in close contact using the clamp shown in figure 6 and heated to a temperature of 450^{o}C. A voltage of approximately 1kV is then applied across the stack with the glass at a negative potential to the semiconductor. The actual voltage applied is dependent on the thickness and area of the samples used. It should be noted that the voltage used is that

which gives a suitably high current to initiate the bond. This will, however, be discussed after explanation of the ionic flow involved in this process. A schematic representation of the experimental apparatus used to perform the bonding is shown in figure 7.

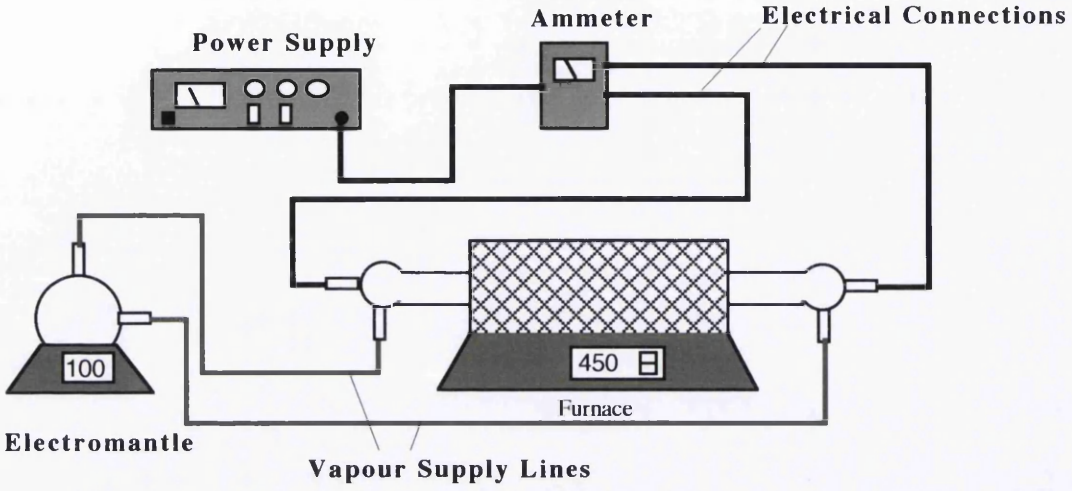

Figure 7. *Anodic bonding apparatus. The clamp described in figure 6 is placed in the furnace at 450^{O}C. The current produced through the stack is measured on the ammeter and the electromantle introduces water into the reaction by passing steam through the quartz furnace tube.*

This set up is used in this project in order to make the fabricated silicon flow chamber into a fully sealed unit. The height of the fully finished array is between 2 to 20nm higher than the silicon posts themselves due to the formation of a thin oxide layer at the interface of the SiO_2 and the borosilicate glass. The pyrex glass used for the bonding was initially a BDH supplied glass cover slip of thickness 200μm which had a SiO_2 content of 64.1%, however this was replaced by polished Corning code #7740 glass which has a SiO_2 content of 80.5%, a Na_2O content of 3.8% and has a melting point of 776^{O}C.

The important ions for the formation of the bond appear to be Na^+ ions contained as Na_2O in the pyrex which migrate out of the glass towards the cathode. The interfacial bond itself is believed to be a Si-O-Si type bond with the main chemical reactions represented by

$$Si + 2H_2O \rightarrow SiO_2 + 4H^+ + 4e^- \qquad (a)$$

$$Na_2O \rightarrow 2Na^+ + 1/2\ O_2 + 2e^- \qquad (b)$$

$$Na_2O + H^+ \rightarrow 2Na^+ + OH^- \qquad (c)$$

Reaction (a) takes place at the silicon surface with reactions (b) and (c) proceeding in the glass and at the cathode [8]. After considering these reactions it was felt that the bonding

procedure could be improved if water was introduced into the furnace tube. The reason for this is that if excess water is introduced, reaction (a) can progress at a faster rate thus producing more hydrogen ions. The increased concentration of these ions produces a higher reaction rate of the H^+ ions with the Na_2O in reaction (c), thus resulting in faster production of Na^+ ions. This in turn means that there is a greater number of Na^+ ions migrating towards the cathode, thus increasing the electrostatic attraction at the glass/semiconductor interface. The excess water is introduced into the system using an electro-mantle to pass steam through the tube and it was found that the quality and time of bonding was indeed improved.

Several experiments were carried out using the bonding apparatus and parameters were adjusted to gain the strongest hermetic seal. In all of the experiments, a point cathode was used since it was found that trying to bond whole areas simultaneously with a disk electrode resulted in bonded surfaces with trapped air bubbles. With a point contact, the bond initiates from an independent point relative to the point cathode on the glass surface and radiates from that point. Therefore, the time for the bonding to take place is dependent on the surface area of the glass. Figure 8 below shows examples of bonding times for various glass areas. The values are calculated using the relation $\mathbf{R} \propto \sqrt{t}$ where **R** is the distance the bonding front has to move.

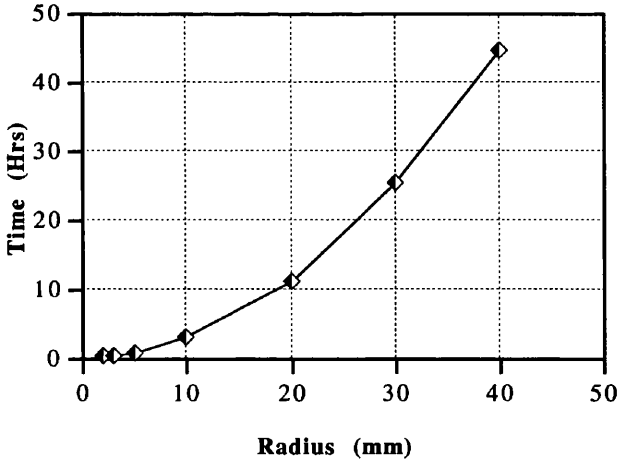

Figure 8. *Plot shows times required for bonding to take effect for different areas of glass. Bond times calculated using the relation* $R \propto \sqrt{t}$.

When the bonding voltage is applied, an ammeter reads the current through the stack and it is found that the current drops with an exponential style decay as shown in figure 9. Comparing graph 1 and graph 2 in figure 9, it can be seen that the measured current for a constant voltage varies depending on the thickness of the pyrex used. The initial current in the samples is due to ion migration and is therefore higher in the thicker

sample since it has a larger ion volume. It is believed that the voltage causes transport of sodium ions thus forming a depletion layer about the interface. The current then decreases as this grows. The current, however, levels off at approximately 9μA for both samples. This occurs when the ionic migration ceases and is the produced by the voltage source through the large area, resistively dominant silicon sample. A current decay of this type is a good indication that the bonding has worked.

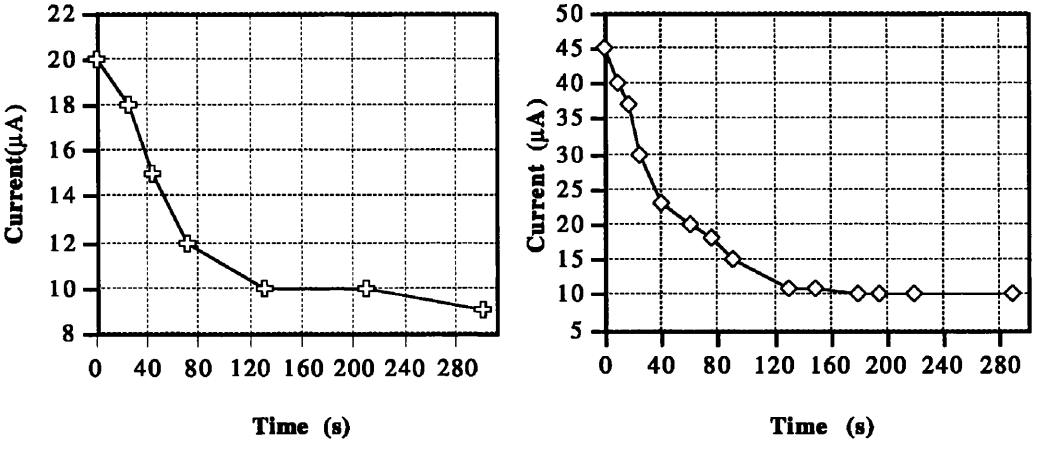

Graph 1 Graph 2

Figure 9. *Graph 1 shows the current decay against time for a piece of pyrex 0.17mm thick. Graph 2 shows the current decay versus time plot for a pyrex sample 1mm thick. Bonding conditions of 450°C and 800V were used in each case.*

However, figure 10 shows the two time/current plots superimposed and it can be seen that the rate of decay is very similar for the two sample thicknesses. This confirms that the bonding time is independent of pyrex thickness.

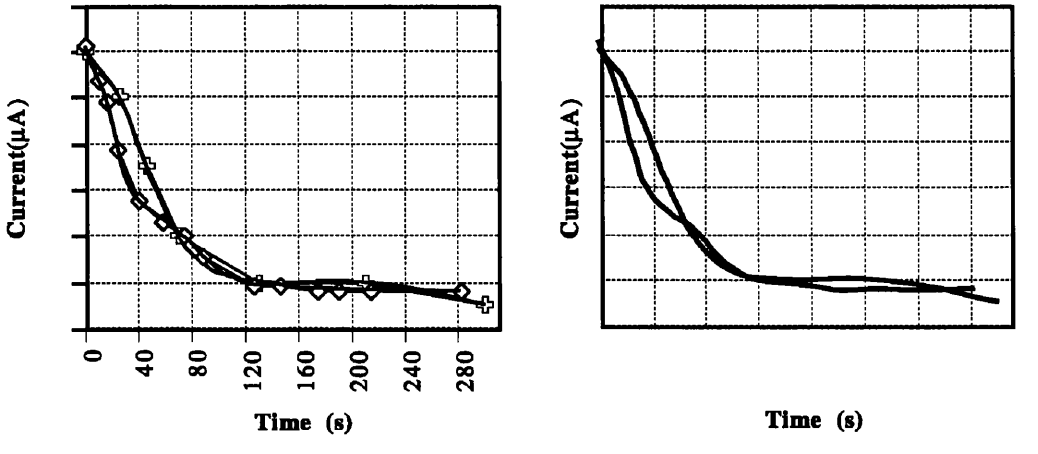

Graph 1 Graph 2

Figure 10. *Superimposed current/time plots for 1mm thick (◊) and 0.17mm thick (+) glass samples. The rate of current decay is extremely similar thus showing that the bonding time is independent of glass thickness. Bonding conditions of 450°C and 800V were used in each case.*

In order to produce the currents shown in figure 10, a voltage of 800V was used. Tests were also carried out to observe the effect that glass thickness has on the bonding parameters and the results obtained are shown in figure 11. Graph 3 shows the required voltages to maintain a constant current of 25μA through 0.5mm and 1mm thick glass samples. The pyrex sample areas were 6mm by 6mm. The silicon samples used for the voltage observations were the same size as the glass. The reason for this being that in order to draw conclusions concerning the effect of the glass on the voltage, the pyrex must be the dominant resistive species. It can be observed that a higher voltage is required for the thicker sample. Thus, to avoid arcing, the glass should be kept as thin as possible.

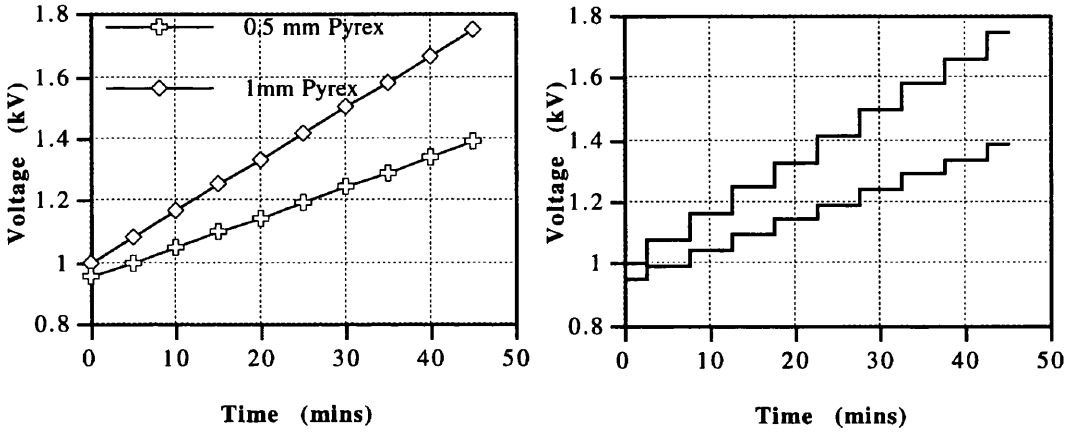

Graph 3 Graph 4

Figure 11. *Graphs of voltage required to produce constant currents during bonding. Graph 4 shows the results obtained displayed as step increases.*

Graph 4 displays the voltage steps required to produce a constant 25μA in the two samples. While the starting voltages are very similar, the step increase for the 1mm thick glass sample is double that required for the 0.5mm thick one. From consideration of the current results obtained for a constant voltage as shown in figure 9 it is expected that the initiation voltage for the bonding should be similar for the two thicknesses of glass. However, the reason for the step increase is not so obvious. This phenomenon can be understood by considering what happens when a voltage increase is applied to an already bonded silicon/pyrex stack. Assuming that the bonded interface is a Si-O-Si type region, then the effect of applying a secondary voltage would be to initiate a similar depletion region in the glass as before but in the area immediately above the bond. If increased voltages are then periodically applied the phenomenon is repeated and progresses through the glass. Therefore, with the application of every voltage increase, a new ionic current is produced which decays until the next voltage increase. The reason for the step variations are that after the initial bond, the voltage to induce another ionic

current is controlled by the relation V=IR. Since the 1mm sample has double the resistance of the 0.5mm one, then the voltage required to produce each further current would be double.

During all of the bonding experiments a white amorphous material appeared between the cathode and the glass. It was observed that the material had a pH of 9 and appeared to etch into the glass. Initially it was thought that this powder substance may be sodium hydroxide (NaOH) formed by migrating sodium ions leaving the glass and reacting with moisture in the furnace or it could be sodium borate ($Na_4B_{10}O_{17}$) formed by either migration or by reaction of NaOH with the glass. A sample of the material was examined using X-Ray diffraction and the plot obtained is shown below in figure 12.

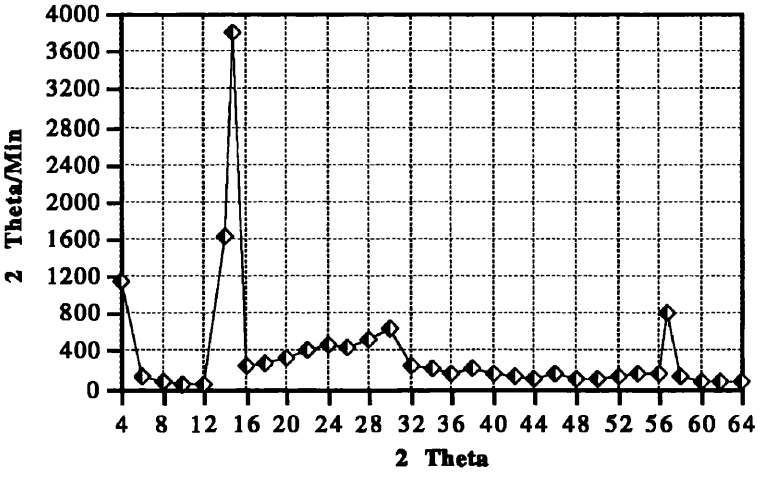

Figure 12. *X-Ray Diffraction Plot obtained for unknown amorphous material.*

The intensity peak at 14.8 corresponds to the intensity peak for sodium borate as found in 'Diffraction from Materials' [13], however the rest of the plot is not in agreement. These results are therefore inconclusive. It is not certain if the substance comes from the bonding reactions and is a mixture of materials or if it is produced by impurities on the cathode surface reacting with the glass. No further test were carried out to identify this material since it was discovered that damage to the glass surface could be removed by post bonding polishing. Further, the problem could be avoided completely by placing a thin sacrificial piece of borosilicate on top of the real glass sample thus protecting it at the expense of the waste piece.

After the procedure for bonding was finalised a pyrex cover was bonded onto the top of a finished post sample. This produces a sample ready to use for electrophoresis.

2.1.5 Electrophoresis Medium : Fabrication Process

The electrophoresis retarding medium is fabricated using the procedures described in §2.1.1 to §2.1.4. The material used for the experiments is n-type Silicon with a 1μm thick oxide layer grown on it. The pyrex glass used for each device is Corning #7740 polished to a thickness of 200μm. The pillars are fabricated using e-beam lithography, lift-off and reactive ion etching. Glass is then bonded onto the pillars to seal the chamber. The full fabrication process is :

1) Clean Silicon sample by immersing in an ultrasonic bath and successively washing in Opticlear™, acetone, methanol for 5 minutes each. Rinse in RO water for 3mins.

2) Spin first layer of resist: 8% BDH @ 5000rpm for 60s and bake for 1 hour at 180°C. Spin second layer of resist : 4% Elvacite @ 5000rpm for 60s and bake for at least 2 hours at 180°C.
Evaporate 30nm of nichrome to act as a charge removal layer during e-beam exposure.

3) Sample submitted to beamwriter. Pattern consists of 500nm circles with a 1000nm centre to centre spacing. The area covered is 2.8mm by 2.8mm, giving a 2800 by 2800 array of structures. Thus the area written contains 7,840,000 structures for fractionating the DNA. The job was run at 50kV with a resolution of 50nm, a spot size of 112nm, a dose of 250μC/cm^2 and the run time was 1.42 hours.

4) Remove nichrome layer. Develop sample in 2:1 IPA:MIBK for 45s. Rinse in IPA and blow dry.

5) Lift-off. Evaporate 30nm of nichrome on top of developed sample. Then place sample in warm acetone for 30 mins with agitation.

6) Dry etch. The sample is etched using reactive ion etching and the Nichrome as a mask. The gas used is C_2F_6 at a pressure of 15mTorr, a flow rate of 20sccm, a self bias of -400V and an rf power of 100W. Etch rate is 50nm/min.

7) Remove nichrome mask using wet etch. Nichrome etch is made from 150g ceric ammonium nitrate, 35ml acetic acid(conc. 98%), 1l water.

8) The final step is Anodic bonding. Bonding is carried out using the process described in §3.1.4.
This is the last fabrication step in producing the retarding medium.

Figure 13 shows a micrograph of 500nm SiO_2 Pillars etched to a depth of 150nm. These features were made using the procedures described in this section.

These features are then anodically bonded to a 200mm thick pyrex glass cover slip in order to seal the chamber. Figure 14 shows a photograph of the posts taken through the bonded glass at x40 magnification.

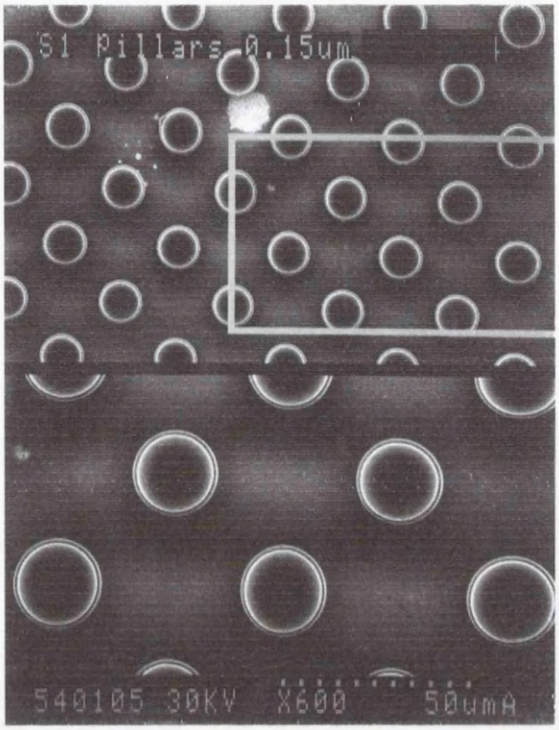

Figure 13. *500nm diameter pillars etched into SiO_2. The etch depth is 150nm.*

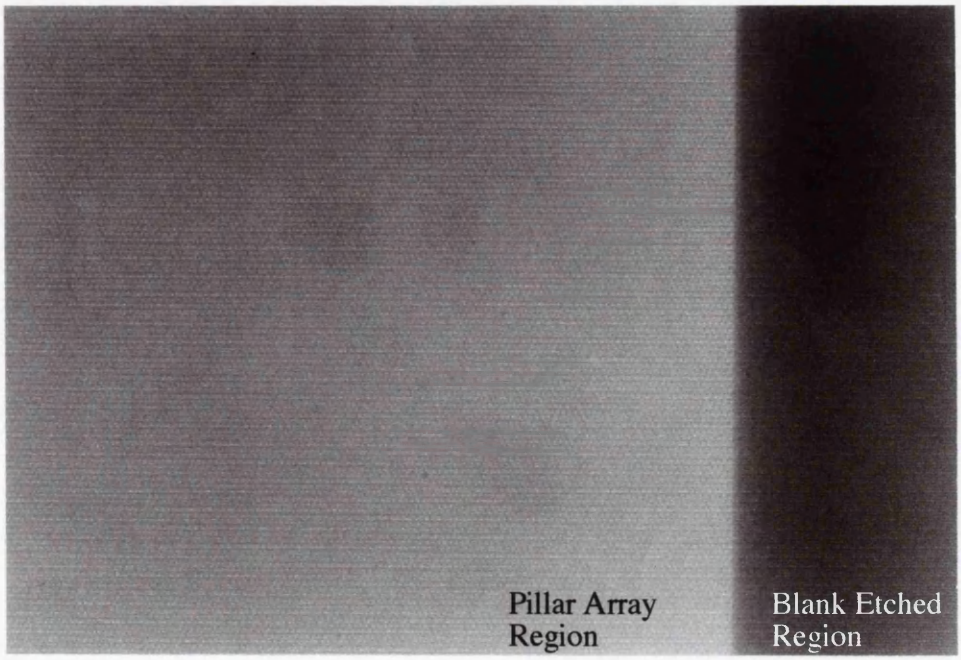

Figure 14. *500nm pillars as viewed through the anodically bonded glass. The dark region on the right is etched but not patterned and is therefore not bonded. The uniformity of the colour in the post region suggests excellent uniformity in bonding over the area.*

2.1.6 Design of a Suitable Electrophoresis Environment

A standard gel electrophoresis box is approximately 30cm by 15cm by 10cm and is used on a laboratory bench. However, in order to observe DNA conformations in real time, a small experimental set up is required which will allow direct observation using a microscope. Therefore, a small electrophoresis box was made which allows the actual migration of the DNA molecules through the fabricated lattices to be observed under a fluorescence microscope. The new 'gel' box was made from a plastic which was tested for biocompatability using B.H.K. cells and was found to have no adverse effects on the cell culture. The electrophoresis apparatus is essentially a box with platinum wire electrodes at each end and a sample mounting area in the centre where the pyrex capped silicon dioxide array is clamped. Figure 15 shows the lay out of the electrophoresis box.

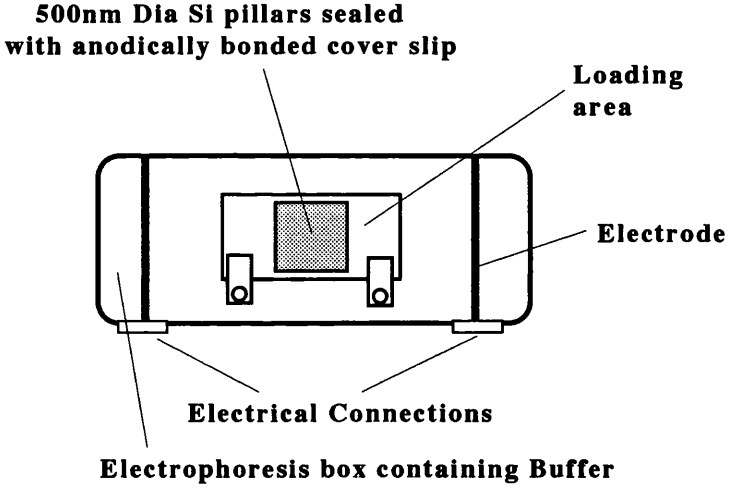

Figure 15. *Microelectrophoresis box. The nanofabricated flow chamber is clamped to the base of the box which is in turn filled with the electrophoresis buffer. The electrodes are used to apply a field of 1V/cm. The box is 5cm long, 3cm wide and 1cm high.*

The silicon dioxide fractionation array is placed on the base of the micro-electrophoresis box and held in place by the clamps. Once the device is securely in place and the walls of the chamber are running parallel to the direction of the field, the buffer is poured into the box so that it does not cover the top of the glass.. The reason for keeping the fluid presence at a minimum is to make visualisation as easy as possible since observing DNA is a difficult task without complicating the process with fluid films on top of the chamber. The electrophoresis buffer used is tris-borate which maintains the required pH of 8. This buffer is made into a working solution which is composed of 89mM tris-borate, 89mM boric acid and 2mM EDTA (ethylenediaminetetraacetic acid). The electrophoresis can now be performed either in the open lab or under the microscope which facilitates observation of the polymer stretching in the arrays.

2.2 Field Requirements for Highly Dispersive Mobilities

The optimal DNA molecular conformation to produce highly dispersive mobilities within any retarding medium is the random walk form. At this stage this can be considered as a tangled ball conformation, however the physical explanation for this is given in §5.2.2. As a strand of DNA travels through a nanofabricated lattice its shape becomes distorted as it interacts with each row of obstacles. This distortion is dependent on the length of the strand and on the action of the obstacle, which in turn is controlled predominantly by feature shape and how the electric field interacts with said feature. It is this distortive effect that causes the DNA to reptate or 'snake' and thus renders the fractionating medium useless.

The simple pillar arrays described in this chapter allow observation of DNA conformational changes during migration. However because they are based on gel dimensions they produce reptative motion which makes them unsuitable for a real fractionating medium, as explained in chapter 5. However, if the obstacle array is designed in such a way that the DNA can return to its random walk after each interaction, then it is possible to control the molecular migration. This effect can be obtained by ensuring that the field strength between rows of obstacles is very weak. The biophysics of this is explained in detail in §5.2.2. If the field is weak then the action on the DNA is slight and the strand, which has been extended by the first feature, will move very slowly and start to retangle before it reaches the second obstacle. With the correct choice of feature shape and material this is obtainable and allows production of a chamber capable of producing long chain migration without reptation. This is the form of migration required to produce dispersive mobilities and in turn allows length fractionation of long chain polymers.

Therefore, the purpose of modelling retarding media is to find a suitable geometry which insures that the relaxation time is length dependent and that the physical interaction between the DNA and a lattice element obeys the relation :

$$v_o T_R \sim Nb$$

where v_o is the migration velocity, T_R is the relaxation time, N is the number of chain segments and b is twice the persistence length. This equation is true for low electric fields where the thermal forces acting on the polymer become comparable in size to the electric forces.

With this relation in mind, obstacle geometries and sizes were modelled for optimum performance in controlling DNA molecular conformations during electrophoretic

migration. By considering the biophysics of the molecular interaction with an array element and the initial modelling results, it was decided that a simple 'U' shape could be a suitable feature for this purpose and so the modelling results of such features are detailed in the following sections.

During the development stage of the molecule retarding environments, their interaction with an electric field was modelled using a computer simulation package. Since the long term plan for these devices was to fabricate them using embossing, the structures modelled were considered to be made from plastic coated with metal. The metal covering improves conduction which is necessary in a large lattice as explained in §2.3.3 and §5.5.

2.3 Electrostatic Modelling of Electrophoresis Arrays

Plastic shapes coated in metal were modelled using Vector Fields software PC-OPERA, which is a package for 2-dimensional electromagnetic field analysis. The programs use the finite element method to solve partial differential equations that describe the behaviour of the fields[14]. The main equations used by the package are Poissons, Helmholtz and the diffusion equations[15]. The basic field equations used for electrostatic analysis are :

the displacement current ($\vec{D}$) is related to the charge density (ρ) by

$$\nabla \cdot \vec{D} = \rho \tag{1}$$

and the electric field strength and permittivity (ε) by

$$\vec{D} = \varepsilon \vec{E} \tag{2}$$

The electric scalar potential (v) is defined by

$$\vec{E} = -\nabla v \tag{3}$$

Before any analysis can be done, the problem data must be supplied. This is done through a graphical preprocessor where the model space is divided into a continuous set of triangular elements. Once the problem space has been prepared, the solution is calculated using the analysis program. The results can then be examined using the postprocessor. The postprocessor allows the graphical and numerical observation of the system variables, including potentials, currents, fields, forces and temperature. Numerical errors due to the inaccuracies in the mesh definition are also analysed at this point to allow refinement for improved accuracy. A full and concise explanation of the

2.3.1 Design of Traps and Obstacles

The PC-OPERA suite of programs allows the user to model electromagnetic fields for a wide variety of applications. In this instance, we model the electric field as it interacts with our 'U' shaped retarding obstacle. The graphical preprocessor used allows the user to simply draw the shape and specify its physical and electrical qualities. In order to coincide with an embossed feature coated with metal, the modelled feature consists of a dielectric(plastic) centre surrounded by metal. Figure 16 below shows the simple form used throughout the electrostatic analysis.

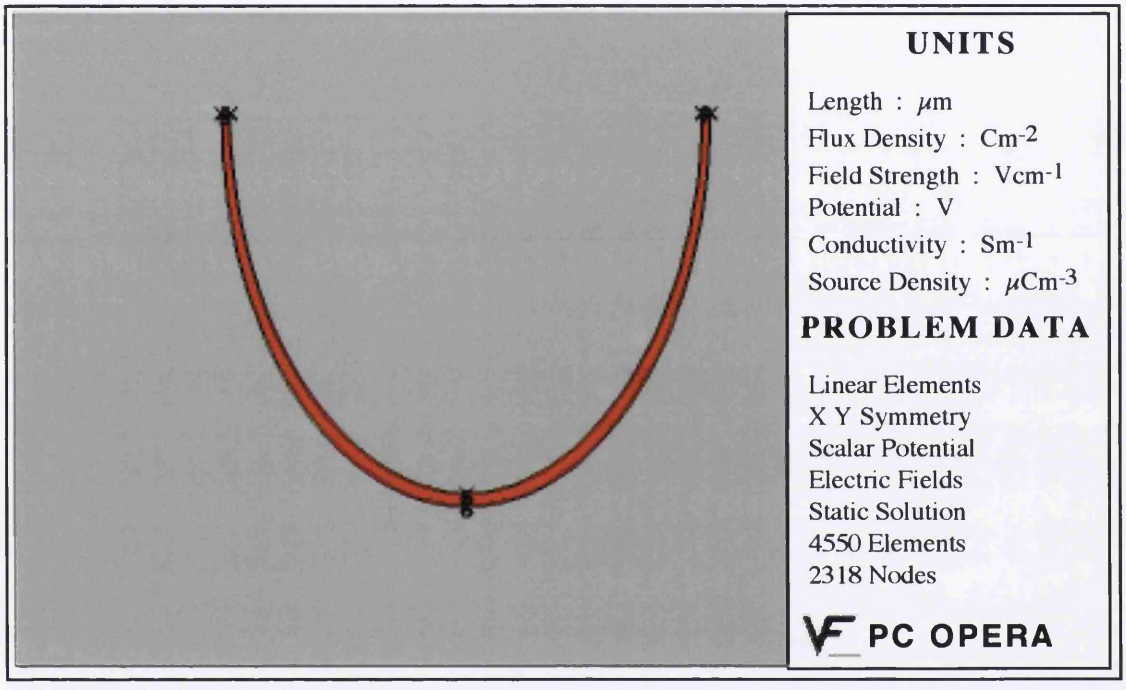

Figure 16. *The simple 'U' shape used for modelling the electric field in a retarding array. The shape consists of a dielectric(plastic) centre covered with metal.*

The 'U' shaped feature has a line width of 500nm and a total length of 30μm from point to point. The material properties which can be specified in PC-OPERA are, mu or epsilon, current density, conductivity, phase/angle and velocity. Not all of these properties need be specified for every application.

Once the feature has been drawn and specified, the boundary conditions are set. The field strength is 1V/cm and the feature has no independent boundary condition assigned to it. The overall boundary condition is a zero normal derivative condition and encloses the analysis space. The mesh is now automatically generated but can be manually adjusted to produce a more accurate modelling space. This forms the data necessary to

analyse the problem and observe the results. Figure 17 shows the finite element mesh generated for the retarding obstacle geometry.

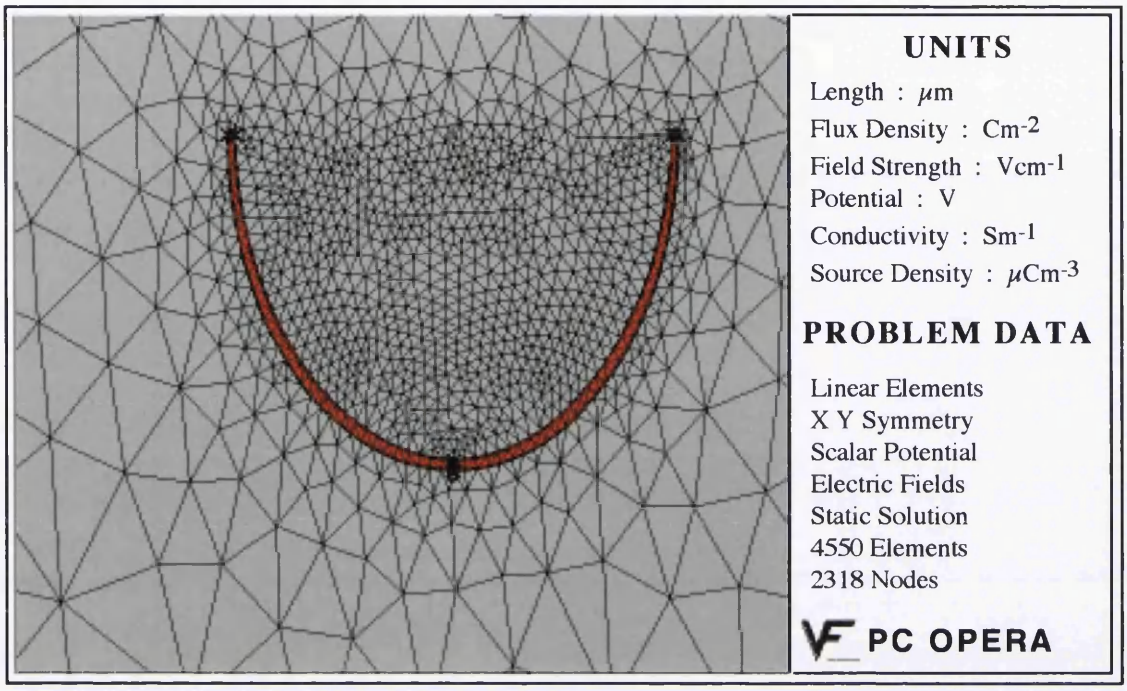

Figure 17. *Finite element mesh. The mesh is generated automatically by the program, however it can be manually refined for a more controlled specification.*

Once the mesh has been generated and refined, the postprocessor is used to produce graphical representations of the electric field around the obstacle. Initially a plot of the field equipotential lines is produced, as shown in figure 18.

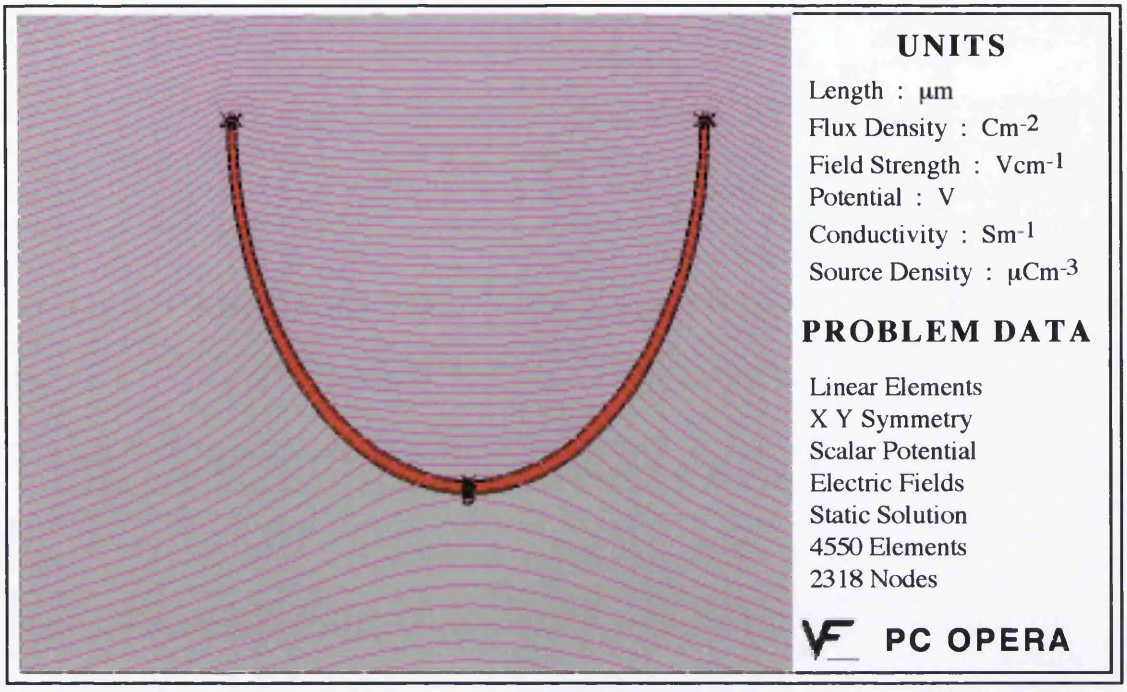

Figure 18. *Plot of equipotential lines as the field interacts with the 'U' shaped obstacle.*

It can be seen from figure 18 that a metal coated embossed feature has little effect on the electric field. This is ideal since we require the field to pass through a large lattice of such structures. The next plot produced is of the field strength at a field point. This is shown in figure 19.

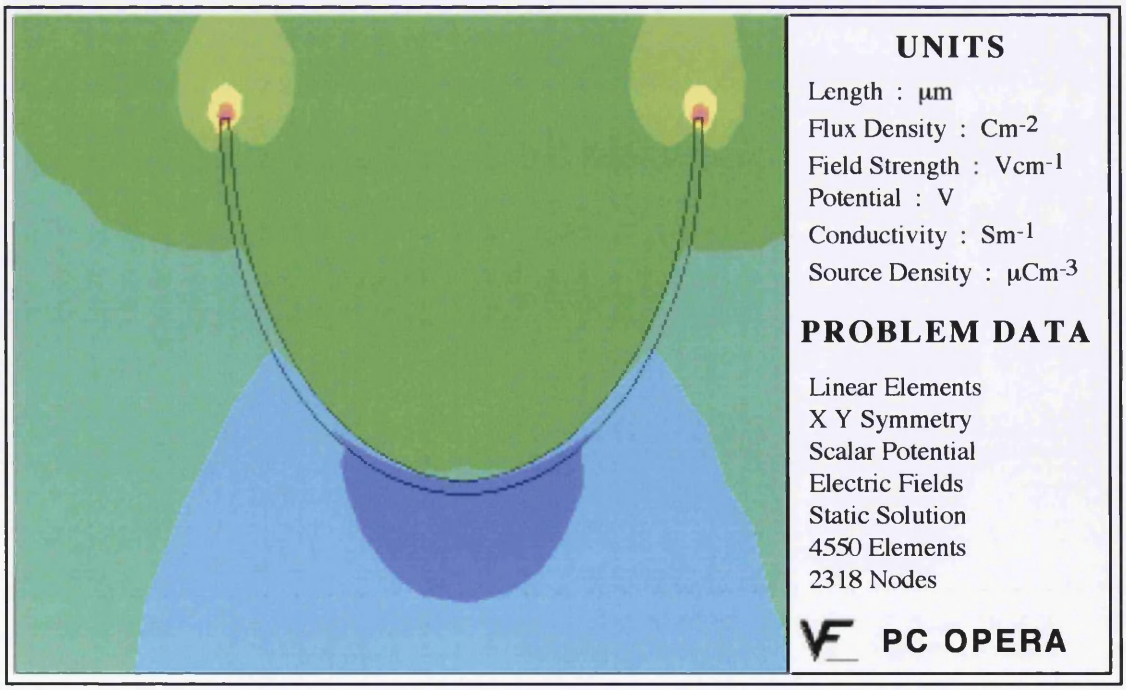

Figure 19. *Graphical representation of field strength on and around the array obstacle. The darker the colour the weaker the field strength.*

From this plot it can been observed that the field is weakest immediately behind the trap, but is relatively strong within the obstacle. This is a good field structure for encouraging DNA into the 'U' trap and also for directing strands which pass this particular feature into the traps behind.

However, in order to understand how a lattice of these features would work, it is essential to model an array of several identical features. This would allow observation of the electric field pattern to see if it is suitable to produce non-reptative migration of DNA molecules. This array modelling is now described in §2.3.2.

2.3.2 Effect of Large Lattices on the Electric Field

In order to observe how a large array of 'U' shaped obstacles will behave, a model was made which consisted of 7 structures aligned in the same way as a real array. Figure 20 below shows such a set up.

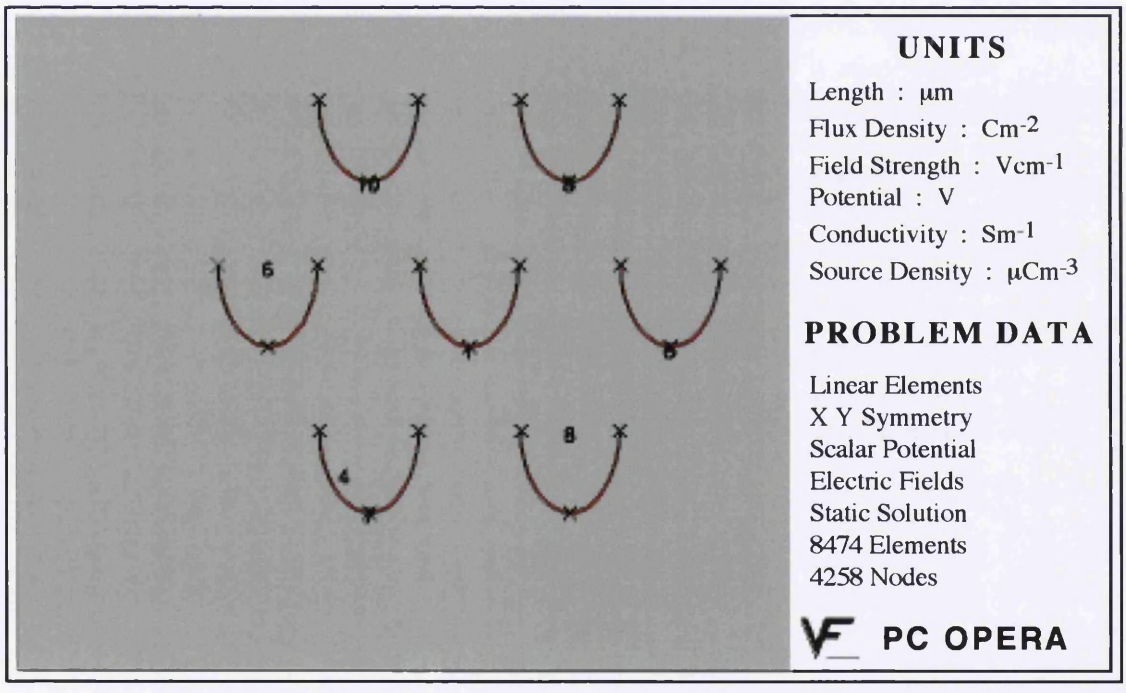

Figure 20. *Small array of obstacles to observe how the field disturbance by an obstacle affects its neighbours.*

As before, the PC-OPERA postprocessor is used to produce graphical representations of the field strength on and around the array and of the equipotential lines at the features. Figure 21 shows the later of these plots.

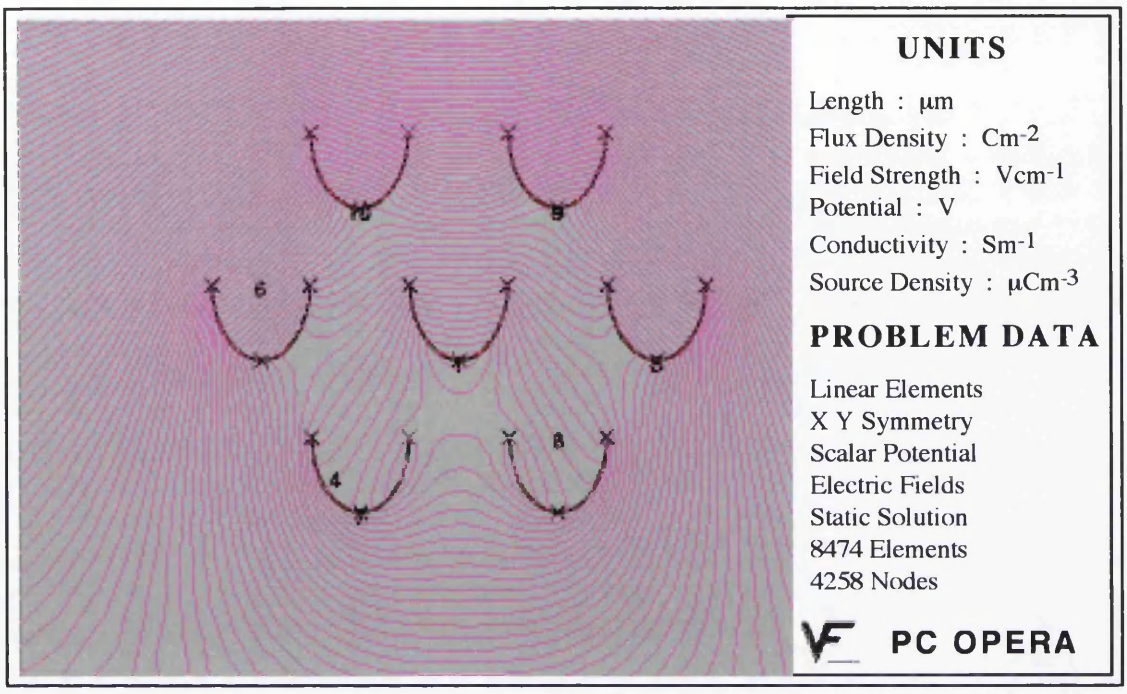

Figure 21. *Plot of equipotential lines as the field interacts with the obstacles.*

From figure 21 we can see that the field becomes less ordered between the obstacles. The effects at the side of the array are exaggerated and would not be as noticeable in a larger array. If we now look at the field strength plot in figure 22, we can see the real effect that the obstacles are having on the field.

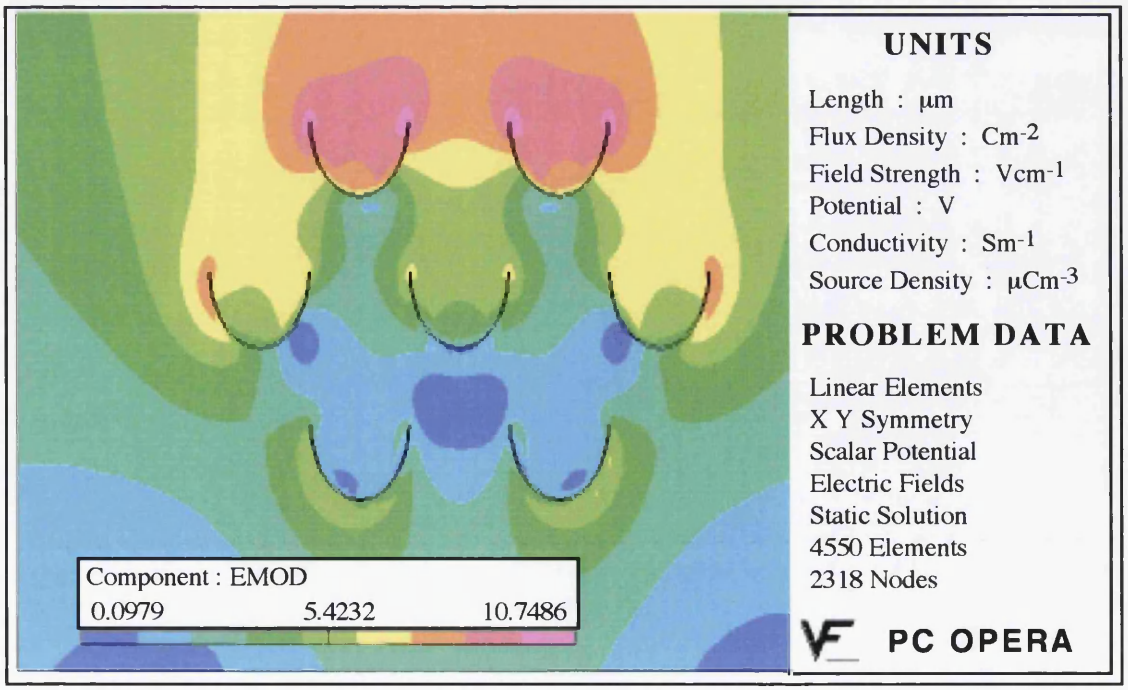

Figure 22. *Graphical representation of the field strength on and around the array of obstacles.*

Again as before, dark blue represents a weak field whereas pink represents a strong field. It can be seen from this plot that the area where the field is at its weakest is in between the rows of structures. This is ideal for random walk migration as explained in §5.2.2 and §2.2.

This model suggests that such an array of features would produce the required field structure for non-reptative migration. Therefore, after considering these results along with the theoretical response of an open lattice and the experimental results, it was decided that this type of feature is a promising starting point for production of retarding arrays which are capable of length fractionation of long chain polymers such as DNA.

Before actual experimental work can be carried out using these devices, they must be fabricated. Chapter 3 describes the plastic fabrication procedures used to make them.

2.4 References

[1] Rai-Choudhury, P., Handbook of Microlithography and Microfabrication : Volume 1., SPIE. Web page : http://www.cnf.cornell.edu/SPIEBook/toc.HTM.

[2] Beaumont, S.P., Bower, P.G., Tamamura, T., Wilkinson, C.D.W., Sub-20 nm wide metal lines by electron beam exposure of thin poly(methyl methacrylate) films and liftoff, Applied Physics Letters, 38, 6, 436-439, 1981.

[3] Haller, I., Hatzakis, M., Srinivasan, R., High resolution positive resist for electron beam exposure, IBM Journal of Research Development, 12, 251, 1968.

[4] Hatzakis, M., Semiconductor metallising process, IBM Tech. Disclosure Bull., 10, 494, 1967.

[5] Beaumont, S. P., Tamamura, T., Wilkinson, C. D. W., Two-layer resist system for efficient lift-off in very high resolution electron beam lithography, Microcircuit Engineering 80, Elsevier, Amsterdam 1981.

[6] Pomerantz, D.I., Anodic Bonding. U.S. Patent No. 3,397,278. U.S.A: Aug. 13, 1968:

[7] Wallis, G., Pomerantz, D.I., Field Assisted Glass-Metal Sealing. Journal of Applied Physics 1969;40:3946-3949.

[8] Kanda, Y., Matsuda, K., Murayama, C., Sugaya, J., The Mechanism Of Field-Assisted Silicon Glass Bonding. Sensors And Actuators A Physical 1990;23(1-3):A-Physical.

[9] Anthony, T.R., Anodic Bonding Of Imperfect Surfaces. Journal Of Applied Physics 1983;54(5):2419-2428.

[10] Anthony, T.R., Dielectric Isolation Of Silicon By Anodic Bonding. Journal Of Applied Physics 1985;58(3):1240-1247.

[11] DeNee, P.B., Low Energy Metal-Glass Bonding. Journal of Applied Physics 1969;40:5396-5397.

[12] Henmi, H., Shoji, S., Shoji, Y., Yoshimi, K., Esashi, M., Vacuum Packaging For Microsensors By Glass Silicon Anodic Bonding. Sensors And Actuators: A Physical 1994 ; 43 (1-3).

[13] Schwartz, L.H., Cohen, J.B. Diffraction from Materials. Springer-Verlag, 1987.

[14] Vector Fields, PC-OPERA User Guide, Software for Electromagnetic Design, 1994.

[15] Cheng, D.K., Field and wave electromagnetics, Addison-Wesley, New York, 1989.

[16] Vector Fields, PC-OPERA Reference Manual, Software for Electromagnetic Design, 1994.

Chapter 3

Development of Plastic Fabrication Methods

Since its conception, engineers have been steadily and diligently improving and developing the art of nanofabrication. In recent years there has been a great deal of interest in producing devices over large areas with high throughput at reduced cost. At present the ultimate fabrication resolution is obtained using electron beam lithography (EBL). However, this is a serial process in which every picture element has to be defined, one at a time. This is inevitable in a machine for the primary definition of an arbitrary pattern. For rapid production of structures with nanometric resolution, some form of replication must be used. Printing using X-rays is a possible route [1][2][3] which has the desired resolution [4][5][6]. However the capital cost is high; the most suitable source of X-rays is a synchrotron. An alternative approach is to use mechanical methods of pattern transfer. In these methods, a die formed at high resolution using electron beam lithography and dry etching is transferred using heat and pressure into a suitable substrate. Chapter 3 describes work done into new materials and methods for mechanical pattern transfer which have produced very encouraging results. It has been found that using mechanical transfer methods and polymer materials, it is possible to obtain features of the same scale as EBL but in a parallel process and in a fraction of the time.

3.1 Plastic Patterning Techniques

There are four main methods of mechanical pattern transfer capable of producing nanometre scale features. These are casting, molding, resist stamping and embossing. The work described in this chapter covers the embossing and resist stamping processes and explains several plastic fabrication techniques developed during the course of this project.

In many areas of commercial manufacturing mechanical pattern transfer is used as a low cost, large scale method of producing polymer shapes and patterns. The most common uses of embossing are in the manufacture of holograms and compact disks, where metal dies are used to repeatedly and uniformly stamp out plastic features. The advantages of a process like this are that it is cheap, allows large area coverage of small features, has a high speed yield and can produce many identical samples from one master sample. These properties are strongly desirable in the microfabrication industry and recently encouraging results have been obtained whereby 25nm features have been produced in PMMA using imprint technology [7].

The work presented here demonstrates that it is possible to produce nanometre scale features in a variety of polymers using embossing. It is possible to combine embossing and photolithography to produce multilayered devices the results of which are presented along with the plastic handling procedures required to produce such devices.

3.2 Embossing : The Process

Embossing is a mechanical pattern transfer process whereby features can be easily and uniformly transferred into a thermoplastic from a master die. For nanofabrication purposes the master is made using electron beam lithography, reactive ion etching and electroplating. Figure 23 below describes the process diagramatically.

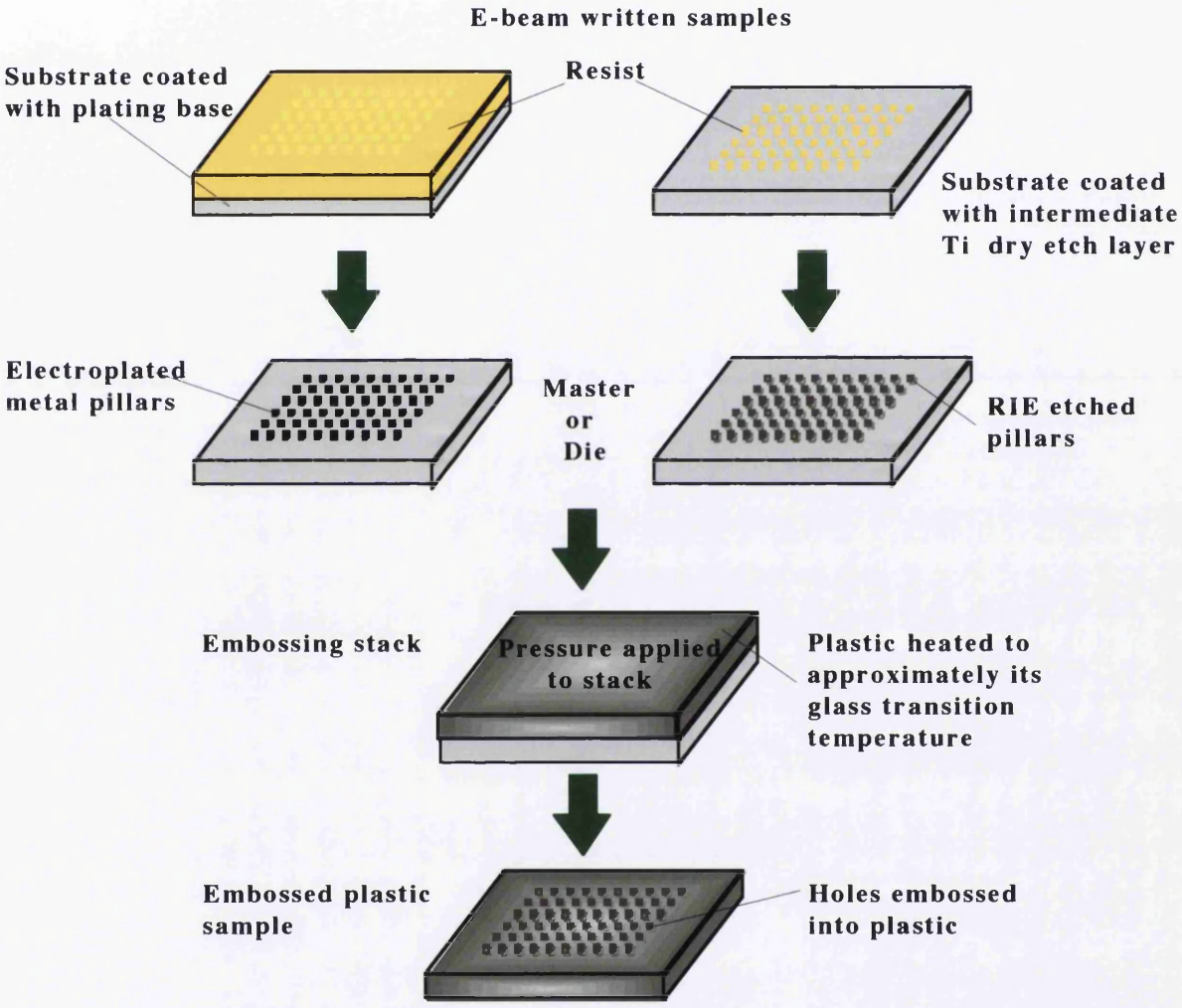

Figure 23. *Embossing Process. Initially the master is made using e-beam lithography and electroplating or reactive ion etching. The plastic is then pressed against the die and heated to approximately the glass transition temperature of the polymer. Pressure is maintained throughout the process. The embossed stack is then allowed to cool before the patterned plastic is peeled off from the master.*

This is the basic embossing technique. This procedure and variations on it were utilised during the course of this work. The details of each part of the process will be described in full in the following sections of this chapter.

3.2.1 Embossing Materials and Considerations

In order to ensure a good quality dimensionally accurate pattern transfer through embossing, it is essential to choose the process elements carefully. Firstly, the master die must be strong, dimensionally and structurally stable at elevated temperatures, and should be chemically inert under the process conditions.

The most important element in the process is the polymer which is to be embossed. There are many considerations when choosing a suitable polymer, some of which are application dependent. It should be noted that not all polymers/plastics are suitable for this type of process due to chemical or structural instability, toxicity, adhesion problems and a variety of other reasons. For best results it is necessary to be extremely selective when choosing the polymer and its related processing temperature and pressure. In the work described here, the following polymers were used : polymethylmethacrylate, polystyrene, cellulose acetate and photoresist .

These materials were chosen because of their temperature/compression properties. If heat is applied to a polymer it is possible to obtain expansion or shrinkage depending on the particular material [8]. Thus when choosing a plastic for embossing it is necessary to select a polymer which will, after being heated and compressed, maintain a high level of dimensional 'memory'. That is, it will maintain its shape and dimensions. This dimensional stability is the main problem facing all forms of polymer moulding. It is therefore difficult to achieve complete dimensional stability during processing.

This dimensional problem manifests itself in moulding because polymers exhibit a property known as viscoelasticity. If a polymer has been held under stress, upon release of the stress the molecules slowly recover their spatial configuration and the strain returns to zero. This effect is known as creep. The polymer creeps under load and recovers when the load is removed. Creep is a manifestation of the viscoelastic nature of polymers. That is, the solid is elastic in that it recovers but is viscous in that it creeps. Viscoelasticity is also highly temperature and time dependent since mechanical stress leads to time effects in the strain as the mobile sections of the macromolecule flow. This builds up a back stress which upon removal of the original stress causes the polymer to recover its original dimensions in due time. In the lifetime of the devices fabricated during the course of this work, no long term creep related phenomena were recorded.

In most cases a dimensional difference of approximately 0.5% between the mould and the master is as good as can be expected and is sufficiently accurate to cause no

significant problem. However, at a nanometre scale this can be unacceptable. Therefore, care must be taken to reduce this error further as will be explained in §3.3. A fuller explanation of the causes of dimensional instability for the specific polymers used here can be found in 'Plastic Materials' [9] and 'Principles of Polymer Engineering' [8].

3.2.2 Characterisation of Hoechst PN114 E-beam Resist

In order to produce features in a polymer using a mechanical pattern transfer method it is necessary to produce a master die which has the inverse of the required features. If the master is going to be made using electroplating, then the resist pattern obtained should be identical to the required plastic one. To this end, a negative electron beam resist is used. The resist used in the work presented here is Hoechst AZ PN114 chemically amplified negative tone resist [9]. In AZ PN114, a Novolak matrix is insolublised in an acid catalysed crosslinking reaction. Upon radiation, a strong Bronsted acid is produced which activates a melamine type crosslinking agent during the thermal bake step. Unlike conventional solvent developed negative tone resists, AZ PN114 resist is developed in an aqueous alkaline developer. Using this type of development chemistry, swelling, snaking and other resolution limiting phenomena are not observed due to the comprehensive reduction in the gel layer which is produced at the resist/developer interface during conventional development [10].

Using a spin speed of 3000rpm, the thickness of PN114 is approximately 1.6μm. This thickness can be reduced by dilution with Hoechst EBX thinner (ethyl lactate) down to a layer of 30nm. The resist thickness is measured using a Dek-Tak surface profiler. The handling procedures for this resist are different from that of PMMA and are as follows. Substrates of either glass, quartz or silicon are coated with Ti/Pd/Au. This acts as a plating base and as a charge conduction layer during EBL exposure. The substrates are then spin coated using a Headway resist spinner with hexamethyldisilazane (HMDS), an adhesion promoter, and oven baked at 80°C for 20 mins. The resist is then applied by spin coating and immediately softbaked at 120°C for 2 mins on a vacuum hotplate. The resist is then exposed using the Leica Cambridge EBPG 5HR beamwriter after which it is given a post exposure bake at 105 ± 1°C for 5 mins before being developed at 20°C in Hoechst AZ400K developer diluted 1:4 with RO water [11]. AZ 400K developer is a potassium hydroxide based developer which gives high contrast pattern definition when diluted 1:4 with water.

AZ PN114 is an extremely sensitive resist with exposure doses 10 to 20 times lower than that for PMMA, so reducing the time required for writing a pattern by EBL. The 'U' shaped features described in chapter 2 were written using this resist and resolution tests were carried out using dot arrays.

It was found that the required dose to write a 'U' feature is 15μC/cm^2. An array of these features is written over an area of 6mm by 6mm producing an exact replica of the required plastic device. Two micrographs of such features are shown in figure 24.

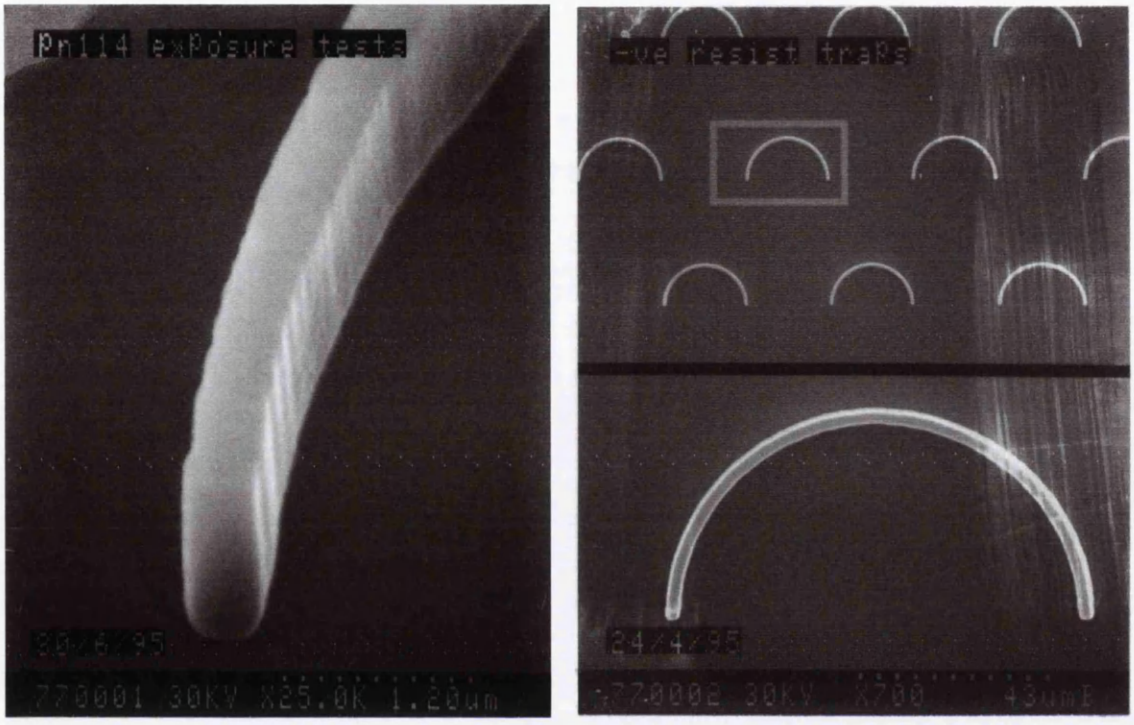

a **b**

Figure 24. *Micrograph* ***a*** *shows the resist profile of a 500nm wide feature 1.6μm high. The dose is 15μC/cm^2. Micrograph* ***b*** *shows an array of these features. This is an exact replica of the required plastic device.*

In order to make an embossing die the device shown in figure 24 must be electroplated. However, before electroplating can take place the metal plating base must be cleaned to remove any remnants of resist and adhesion promoter which may be present on the surface. This is done using reactive ion etching. The sample is placed in a CHF_3 plasma for 30secs and then removed. This etch does not affect the resist or the metal base but does remove HMDS/resist residues. The etching parameters are CHF_3 at 20sccm, 16.4 mTorr, 100W and a DC bias of -410V.

It is difficult to clean the sample surface adequately. It was found that after dry etching in CHF_3 or O_2 it is extremely difficult to remove PN114 by either wet or dry etching. It is suspected that there is a reaction between the resist and the CHF_3 and that a hard polymeric layer is formed. When contacted, the vendors of the resist said that it suffers from sidewall polymer redeposition which makes it impossible to remove the resist using reactive ion etching. Therefore, several wet etches were applied. It was found that neither Nanostrip (sulphuric acid and hydrogen peroxide), acetone or MIBK (methyl iso

butyl ketone) removed dry etched PN114 so a more rigorous process was required. Samples with PN114 which had been patterned and cleaned using dry etching were refluxed in Opticlear W™ and N-methyl pyrrolidone at 100°C for 1 hour. N-methyl pyrrolidone does not remove dry etched resist. It was found that the resist was completely removed from samples that were treated in this way with Opticlear W™. Thus, with this problem eliminated, tests could be carried out to observe the resolution limits the AZ PN114 resist.

The resolution of the resist was tested by etching features obtained with it into quartz. The fabrication procedure for this is as follows. A quartz slide was coated with a 50nm film of Ti and 60nm thick PN114 resist spun onto the sample at 3500rpm for 35secs. The resist is diluted using EBX thinner (ethyl lactate) to give a 60nm film. The ratio is 15:85 PN114 : EBX thinner. The sample was prebaked, written, postbaked, developed and CHF_3 cleaned as explained earlier. The Ti was etched using $SiCl_4$ in a Plasma Technology ECR machine at a pressure of 4mTorr, 150W of microwave power and 24W of rf power at a bias of -79V. This process has an induction time of 1.5 mins. before etching the Ti at a rate of 50nm/min. This produces a Ti mask for the CHF_3 etching of the quartz. This process is carried out using a Plasma Technology BP 80 RIE machine with a flow rate of 20sccm, a pressure of 13mTorr, 100W rf power and a bias of -420V. This procedure etches the quartz to a depth of 50nm in 3.5 mins.

A process has been developed in the department which allows relatively large dot arrays to be written in a reasonable time scale[12]. This method works by using the beamwriter to write a large square using a small spot size and a large pixel step size. For example if a 20nm spot was used to write a square of side length 200μm then the square was written using a raster scan method with this small spot. However, the distance that the spot moves between exposures was set by the pixel step size. Therefore, if the pixel step size was set to 300nm then the spot only exposes the resist every 300nm as shown in figure 25.

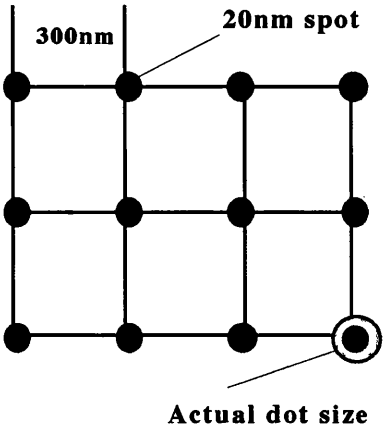

Figure 25. *Method for producing dots. The beam spot of 20nm exposes the resist in steps of 300nm. The actual dot size obtained depends on both the spot size and the dose.*

The actual size of the dot obtained depends on the dose as well as the spot size. Using AZ PN114 it is possible to write 60nm dots over areas of 1cm by 1cm in approximately 1.5 Hrs. This is 10 times faster than when using PMMA and instead of using lift off, a difficult procedure, it is possible to dry etch an intermediate metal layer underneath the resist. This method allows the production of posts of different diameter and on different pitches, see figure 26. It should be noted that the dose vs size plot is a particular example valid only for 100kV writing with a 12nm spot size and is not a universal rule.

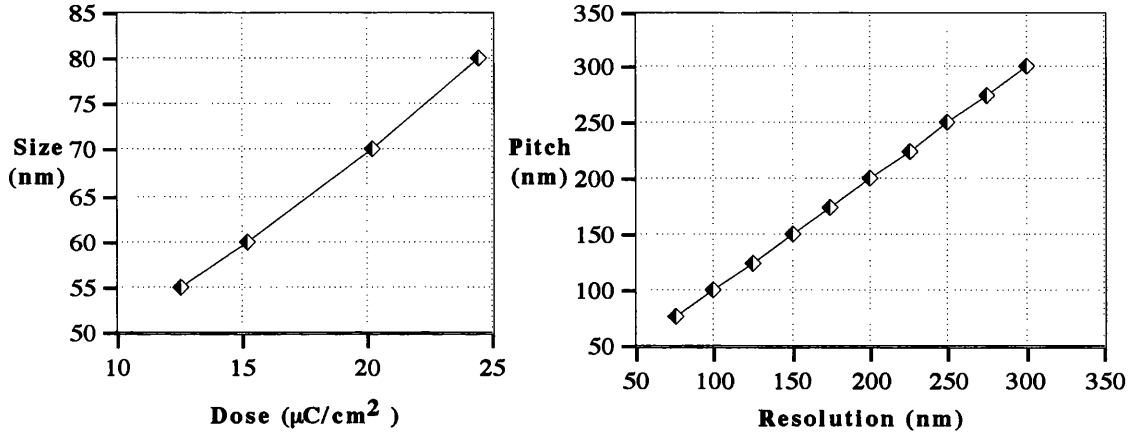

Graph 1 Graph 2

Figure 26. *Dot parameters. Graph 1 shows the variation between dose applied and diameter of dot obtained for a 12nm spot size. Graph 2 shows the relation between dot centre to centre spacing and the pixel step size.*

Extensive e-beam exposure tests were carried out to observe the diversity of dot sizes and separations possible with this resist. A typical exposure test consists of 240 tests covering beam spot size, dose, resolution and beam step size. A micrograph of 100nm dots on a 300nm pitch fabricated in PN114 using electron beam lithography are shown in figure 27a. The smallest posts made using the beamwriter were 40nm in diameter with a centre to centre spacing of 70nm, as shown in figure 27b. These were written at 100kV using a pixel step size of 70nm and a dose of 20μC/cm^2. It is not possible to produce pillars smaller than this because if the dose is reduced below a threshold level it is found by SEM inspection that the array becomes randomised since many of the features are dissolved in the developer.

Using the resist pattern as a dry etch mask, dots were transferred into quartz using CHF_3. A micrograph of 80nm diameter quartz pillars with 125nm pitch is shown in figure 27c and a picture of an array of 100nm dots on 125nm centre to centre spacing is shown in figure 27d.

The next step in the fabrication of a master die for embossing is electroplating of the resist sample.

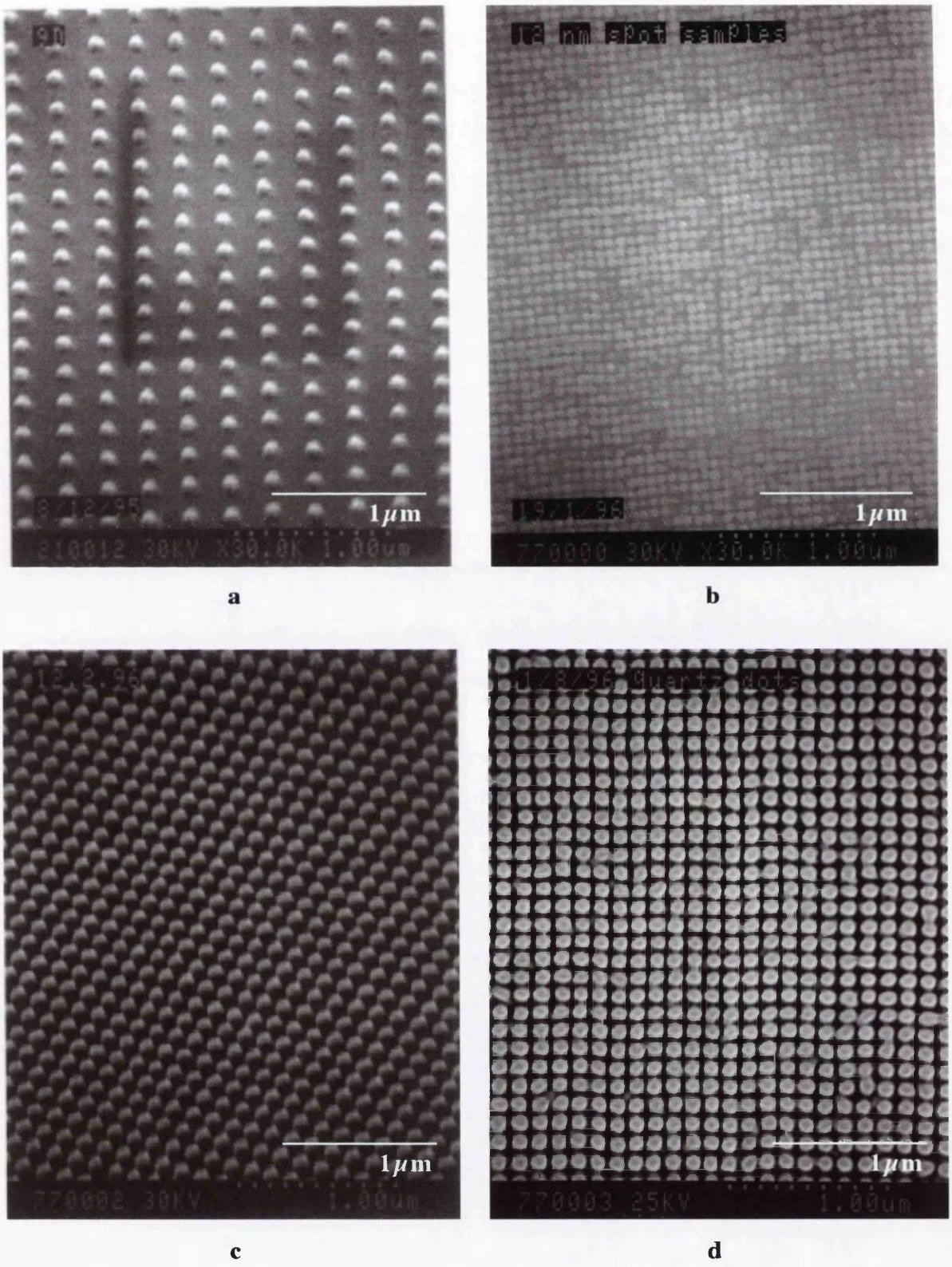

a **b**

c **d**

Figure 27. *Micrograph* ***a*** *shows 100nm PN114 resist dots produced using electron beam lithography. Micrograph* ***b*** *shows 40nm dots made in the same resist. This is the resolution limit of PN114 and it can be seen that at this scale there is some randomisation of the pattern. Micrograph* ***c*** *shows 80nm dots on 125nm pitch etched into quartz. Micrograph* ***d*** *shows 100nm diameter dots on 125nm pitch. These features were produced using e-beam lithography, RIE and Hoechst AZ PN114 resist. These dots were written using 50kV, 125nm pixel step size and a dose of 7μC/cm^2.*

3.2.3 Electroplating

Electroplating is carried out using a commercial nickel sulphamate based chemistry [13]. The solutions are supplied from a company called Ethone-OMI Ltd and are used in a home made laboratory apparatus. A diagram of the lab set up is shown below in figure 28.

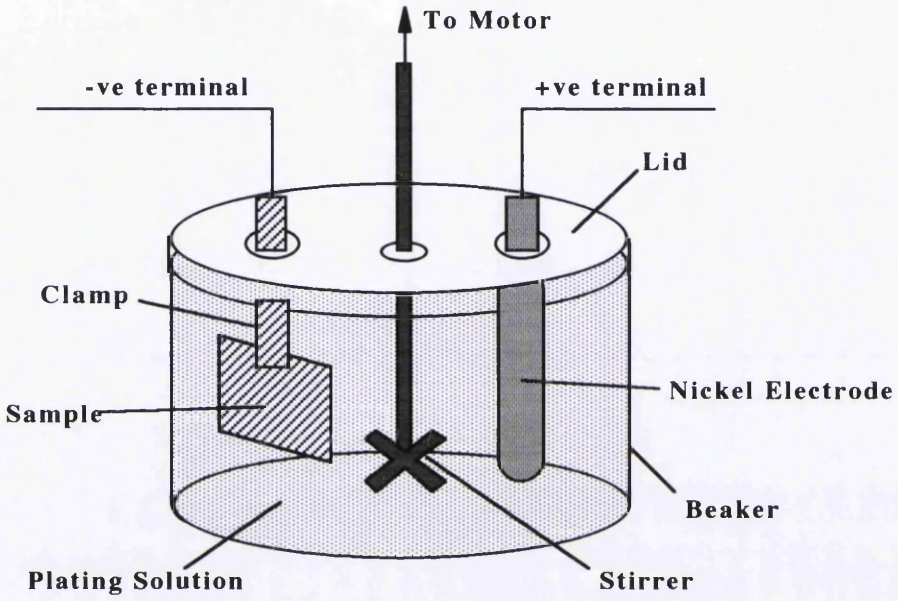

Figure 28. *Apparatus for nickel electroplating.*

The oxidation reaction at the anode is $Ni \rightarrow Ni^{2+} + 2e^-$.

The reduction reaction at the cathode is $Ni^{2+} + 2e^- \rightarrow Ni$.

During plating the pH is 3, the temperature is approximately 54°C, and the stirrer spins at 100rpm. The sample to be plated is attached to a copper board and the plating is carried out using a current density of 13μA/mm^2 . The actual current used is calculated as follows.

Area of Copper plate =3979mm^2 (63mmx63mm)
Area of sample = Xmm^2
Plating Current Density=0.013mA/mm^2

Plating Current required (ZmA):
Area of Copper Plate - Area of Sample x Current Density
3979mm^2 - Xmm^2 x 0.013mA/mm^2 = ZmA

The sample is then plated for 5mins at this current to produce a 500nm thick nickel layer. The nickel is deposited on the plating base but not on the resist. The nickel is plated to approximately 500nm which is 1/3 of the resist height of 1.6μm. The resist is then removed using Opticlear W™ and the embossing master die is ready to use. Figure 29 below shows two micrographs of nickel masters used to produce embossed DNA fractionation chambers.

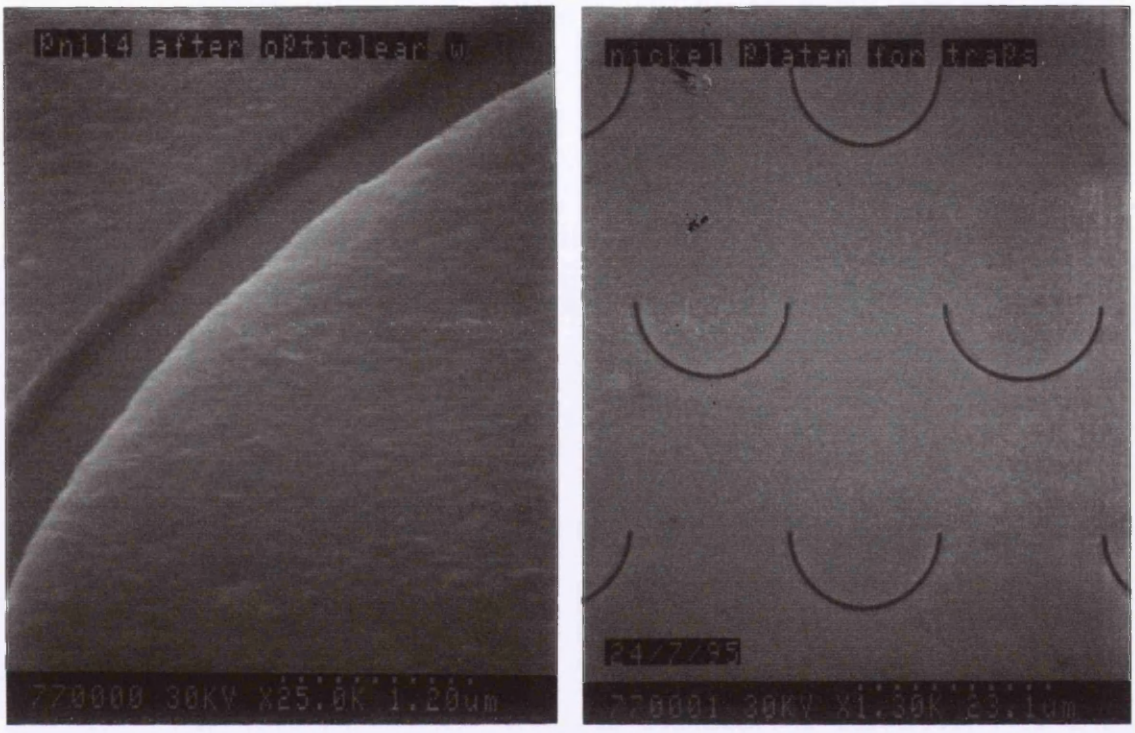

a **b**

Figure 29. *Micrograph* ***a*** *shows a section of a 500nm curved line produced in nickel by electroplating. Micrograph* ***b*** *shows a section of a die for producing an array of 'U' shaped features for DNA fractionation.*

Electroplating is the final stage in producing a master embossing die. Now that all of the relevant processes required to produce a die have been described, §3.2.4 details the fabrication processes used to produce a finished master.

3.2.4 Fabrication of Master Dies

There are essentially two methods used for producing master dies for embossing. One utilises the electroplating method, the other reactive ion etching. The plating method is ideal for feature sizes of a few hundred nm or greater whereas the RIE method is optimal for smaller nanometric feature sizes. The reactive ion etching method is as follows in figure 30.

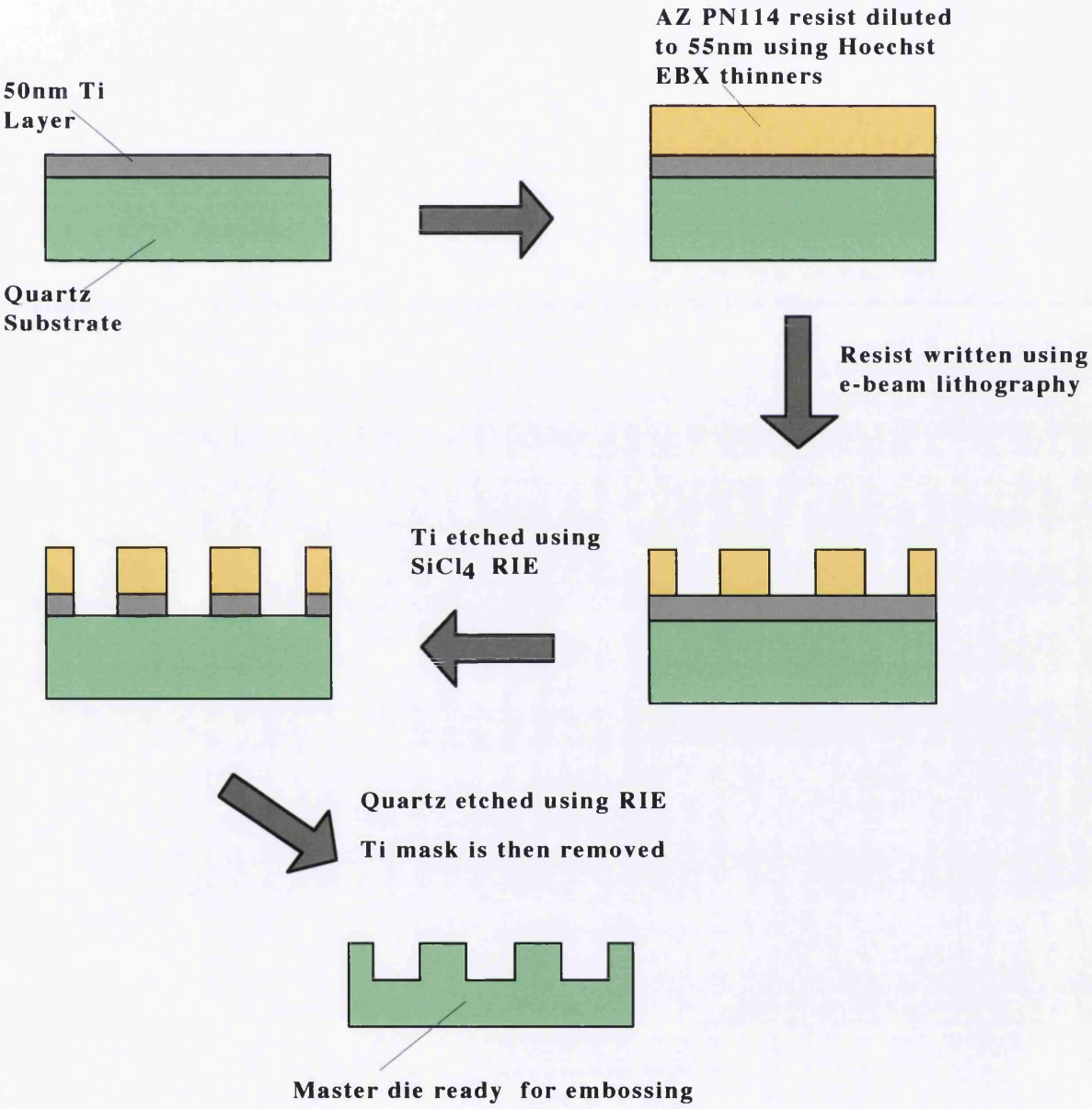

Figure 30. *Fabricating a master die using reactive ion etching. A quartz substrate is coated with 50nm of Ti and then a resist layer of AZ PN114 is spun. The resist is exposed and developed and used as a dry etch mask for the Ti. The Ti is then etched and used as a mask for etching the quartz in CHF_3. The Ti is removed and the quartz master is left.*

The die fabrication process using electroplating is shown below in figure 31.

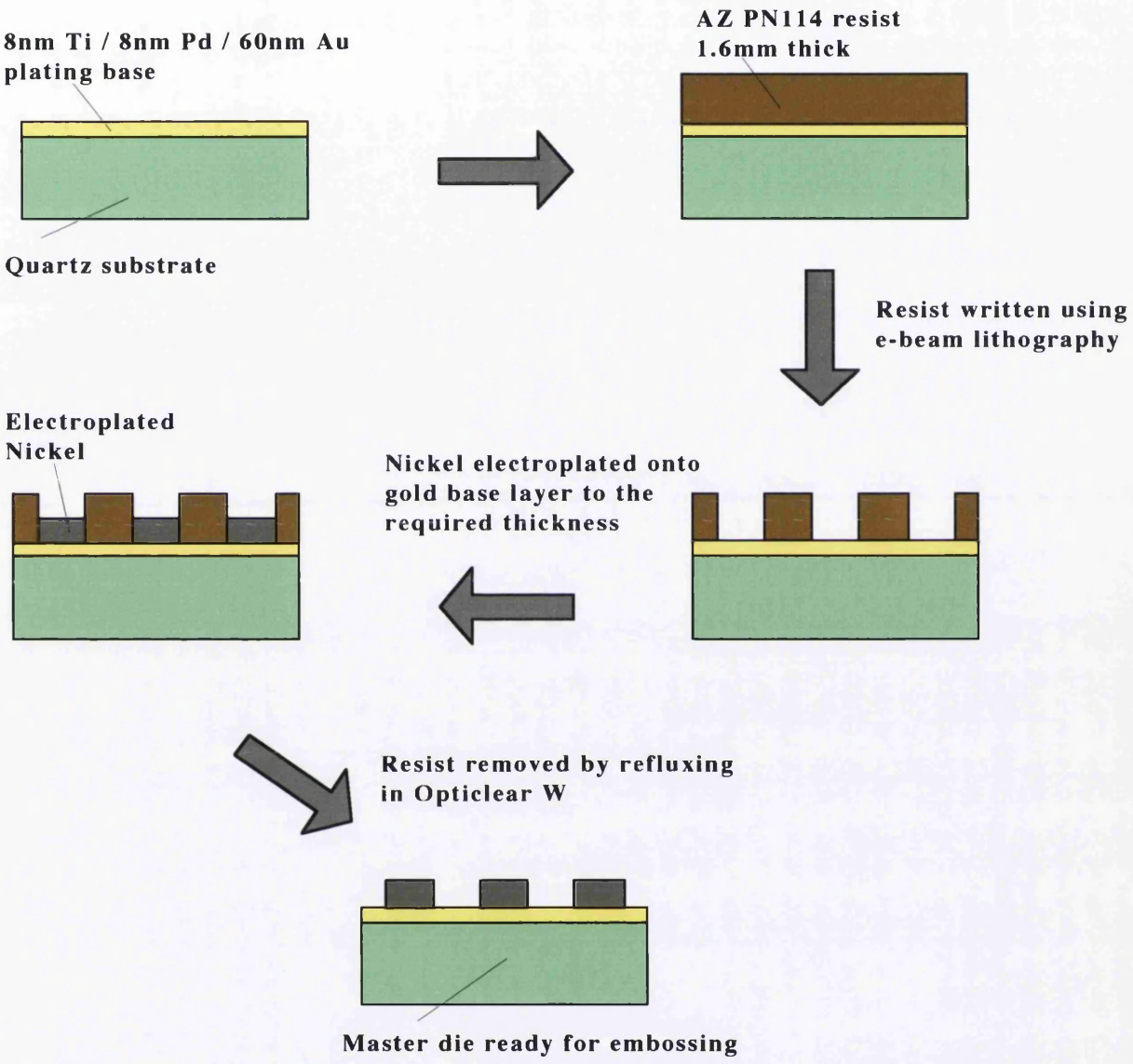

Figure 31. *Fabricating a master die using electroplating. A quartz substrate is coated with a metal layer structure of 8nm Ti, 8nm Pd and 60nm Au which acts as a plating base and as a charge removal layer during electron beam exposure. The substrate is then coated with AZ PN114 to a thickness of 1.6μm. The resist is exposed and developed before the sample surface is cleaned using a CHF_3 dry etch. The sample is now electroplated to the required thickness using the process described in §3.2.3. The resist is now removed by refluxing in Opticlear W™ producing the finished master sample.*

Having fabricated the dies it is now possible to make plastic devices using embossing and to study the limiting factors of this process.

3.3 Embossing Resolution and Results - Imaging Plastics

Currently, the highest resolution structures are made using electron beam lithography and dry etching. The aim therefore must be to achieve such fidelity of transfer that the resolution of the electron beam written master is transferred to the copy. The devices and the fabrication processes based on the Leica Beamwriter and described in the earlier sections of this chapter were used to test the fidelity of mechanical pattern transfer. To test it to the full, devices were fabricated using a converted Jeol 100CXII TEM which offers the highest resolution currently available using EBL.

Arrays of pillars and holes with diameters of 15nm were fabricated in Silicon substrates. These were fabricated using 40nm thick PMMA resist and reactive ion etching. The holes were fabricated using $SiCl_4$ dry etching and PMMA as a mask for the silicon. The pillars were made using lift off of a 12nm gold layer, which in turn was used as the dry etch mask. The ion etching was carried out on a Plasma Technology microP 80 RIE machine using $SiCl_4$ and HBr in a ratio of 20/20 sccm, with a pressure of 30mTorr, an rf power of 100W and a bias of -275V. Figure 32 below shows micrographs of these features.

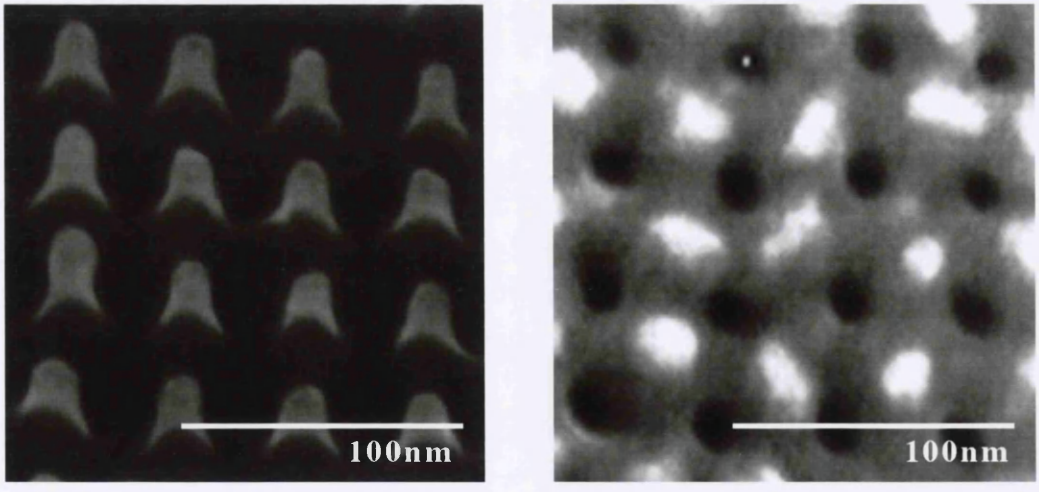

Figure 32. *Micrograph* ***a*** *shows 15nm pillars etched into silicon. Micrograph* ***b*** *shows 15nm holes etched into silicon. The white areas are the remains of the PMMA etch mask. These devices were used to test the ultimate resolution of the embossing process.*

The features obtained with embossing were examined using scanning electron microscopy and atomic force microscopy, the results from which are presented in the following two sections.

3.3.1 SEM Imaging of Plastic Features

When analysing the results of embossing, it is important to remember that many plastics are sensitive to ultra-violet and electron radiation and are consequently degraded upon exposure to such rays. Most electron beam resists are solutions of thermoplastic polymers. Therefore, when observing plastic samples using a scanning electron microscope (SEM) the substrate material becomes damaged even if it is coated with a metal protection layer. Figure 33 below shows an example of the damage caused to a cellulose acetate sample during SEM observation.

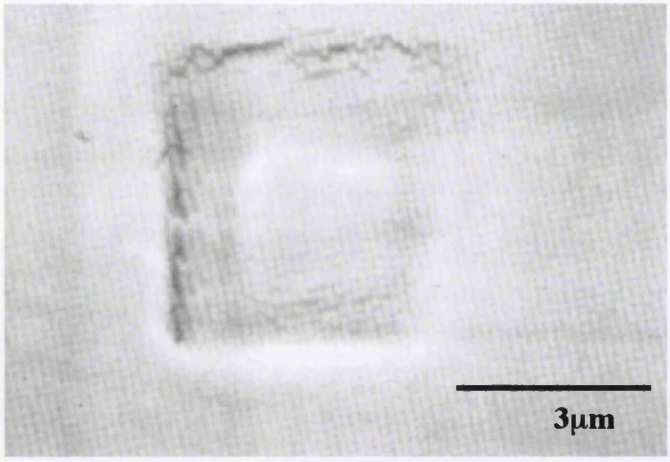

Figure 33. *Electron beam damage of cellulose acetate caused by SEM observation of the polymer. The sample was examined using a Hitachi S800 SEM with an accelerating voltage of 5kV.*

This electron beam damage is a problem when observing polystyrene, cellulose acetate and PDS. It is impossible to look at PMMA (Perspex) using this form of microscopy. However, it is possible to minimise this damage affect by sputter coating the sample with between 5 and 30nm of Au/Pd and by using a low accelerating voltage on the SEM.

Bearing this in mind, the results shown in this section contain some microscopy artefacts and damage. The first devices which were embossed were the arrays of 'U' shaped features required for the fractionation of DNA. These plastics features were made in cellulose acetate using a master die fabricated by electroplating. The linewidth of the features is 500nm and the area coverage is 6mm by 6mm. Micrographs of these features are shown over in figure 34.

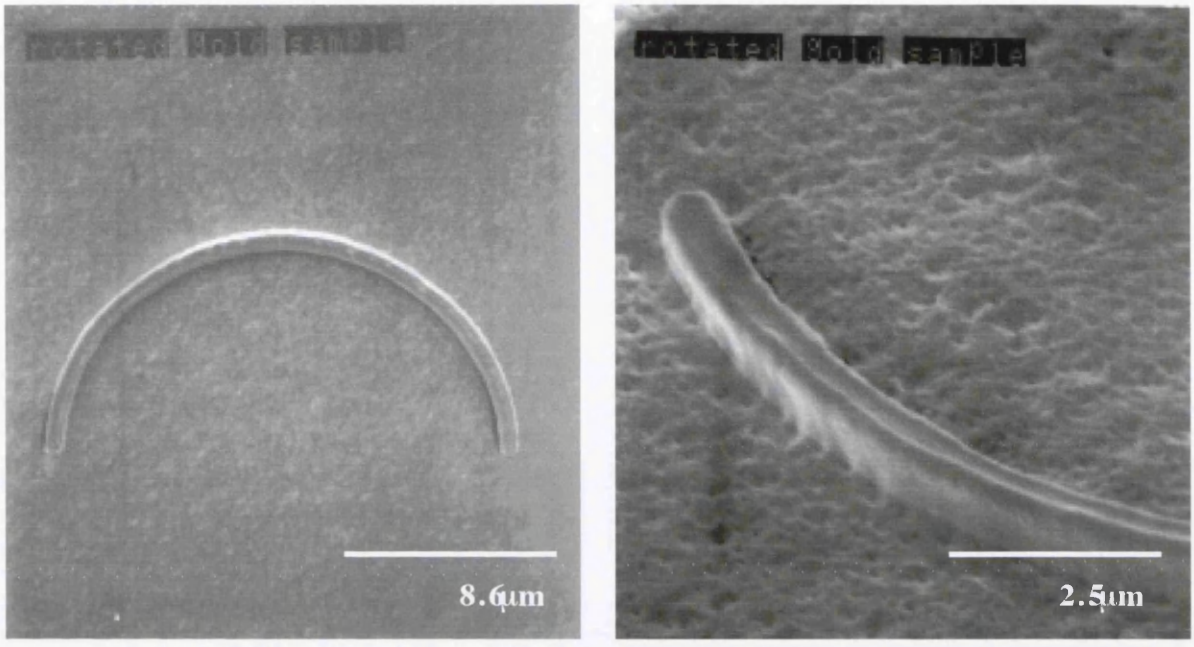

a **b**

Figure 34. *500nm features embossed into cellulose acetate viewed using scanning electron microscopy. Micrograph* ***a*** *shows a 500nm wide curved line used for DNA fractionation. Micrograph* ***b*** *shows a magnified section of this line.*

Continuing investigation of the resolution limits of this process showed that it is possible to produce features with dimensions in the realms of 50nm without any significant problem. Taking this one step further, it was found that not only can this mechanical pattern transfer method produce features at the limit of the beamwriters capabilities but also works for features at the resolution limit of the Jeol beamwriter, i.e. 15nm pillars and holes. Figure 35 contains a micrograph of 60nm diameter holes and 15nm diameter holes embossed into cellulose acetate.

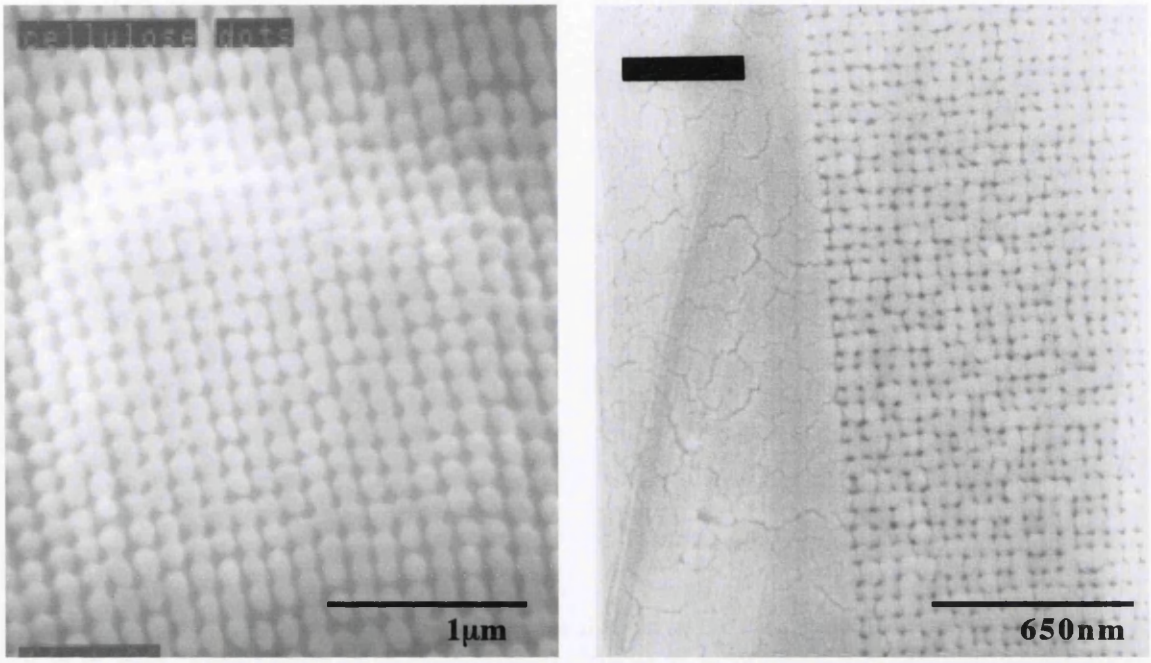

a **b**

Figure 35. *Micrograph* ***a*** *shows 60nm holes embossed into cellulose acetate. Distortion can be seen on the micrograph caused by the SEM observation. Micrograph* ***b*** *shows 15nm holes embossed into cellulose acetate.*

From the results shown here it can be seen that embossing is capable of producing feature sizes at the limit of present nanofabrication capabilities. There are, however, problems visualising polymer samples with scanning electron microscopy as can be seen from the figures presented in this section. Ideally a visualisation method which does not require the use of radiation or polymers which are not affected by radiation is required to give a more accurate representation of the actual properties of embossed features. An example of such a microscopy method which does not irradiate the sample during observation is scanning probe microscopy, or more specifically atomic force microscopy (AFM). This visualisation technique is the subject of the following section.

3.3.2 AFM Imaging of Plastic Features

Atomic force microscopy is a form of sample visualisation which maps the surface of the substrate by scanning a probe over it. Towards the end of this project access was gained to a Digital Instruments Nanoscope III Multimode AFM in the Department of Cell Biology within the University. Figure 36 below shows a cartoon of the Nanoscope AFM used.

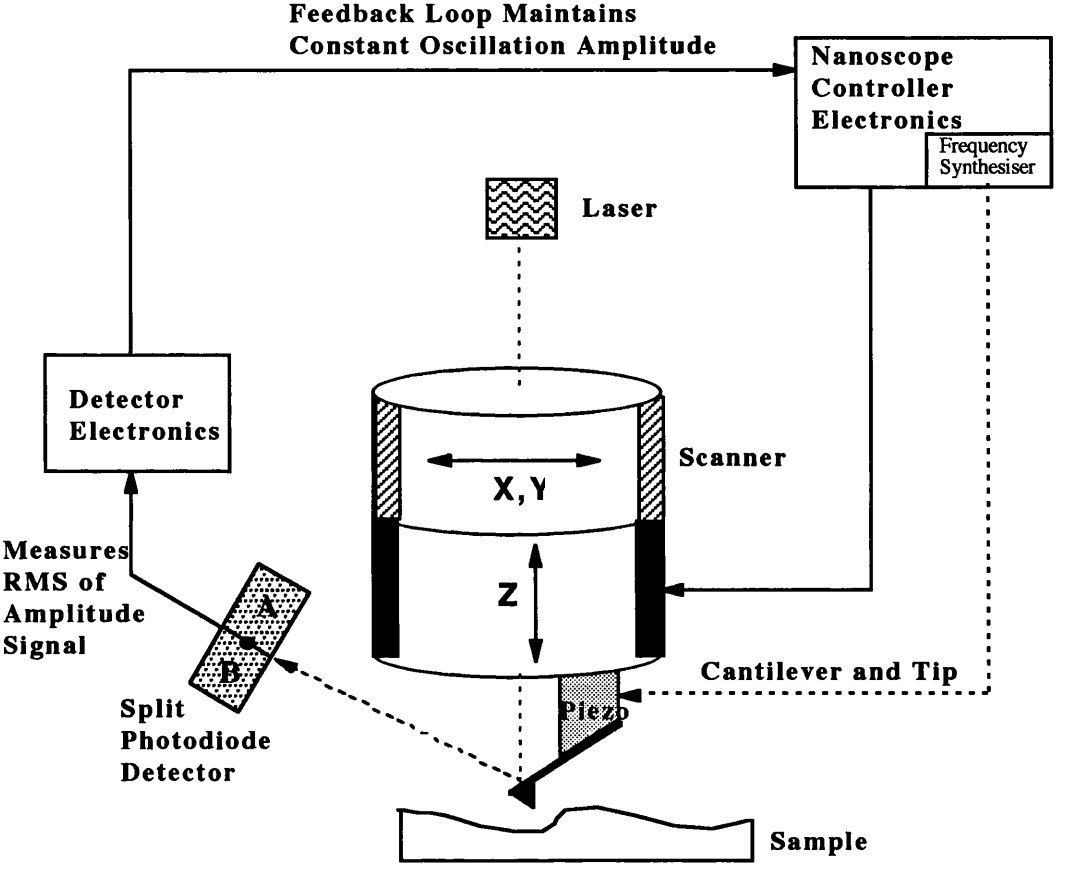

Figure 36. *Schematic diagram of the Digital Instruments Nanoscope III Multimode AFM used for examination of the samples presented in this thesis [14].*

For polymer examination, the AFM is used in TappingMode™ form. During this process a tip attached to an oscillating cantilever is scanned across the sample surface. The cantilever is oscillated at or near its resonant frequency with an amplitude ranging from approximately 20nm to 100nm. The amplitude of oscillation allows the tip to contact the sample surface through the adsorbed fluid layer without getting stuck. The tip lightly taps on the sample surface and touches the surface at the bottom of its swing. The feedback loop maintains a constant oscillation amplitude by maintaining a constant RMS of the oscillation signal measured by the split photodetector. A constant tip-sample

interaction is thus maintained during imaging. The vertical position of the scanner required to keep a constant, user defined, setpoint amplitude is stored by the computer to form the topographic image of the sample surface.

While this microscope offers atomic resolution, it can produce images which contain a variety of artefacts. To this end, it is important that the results obtained using AFM are analysed with care.

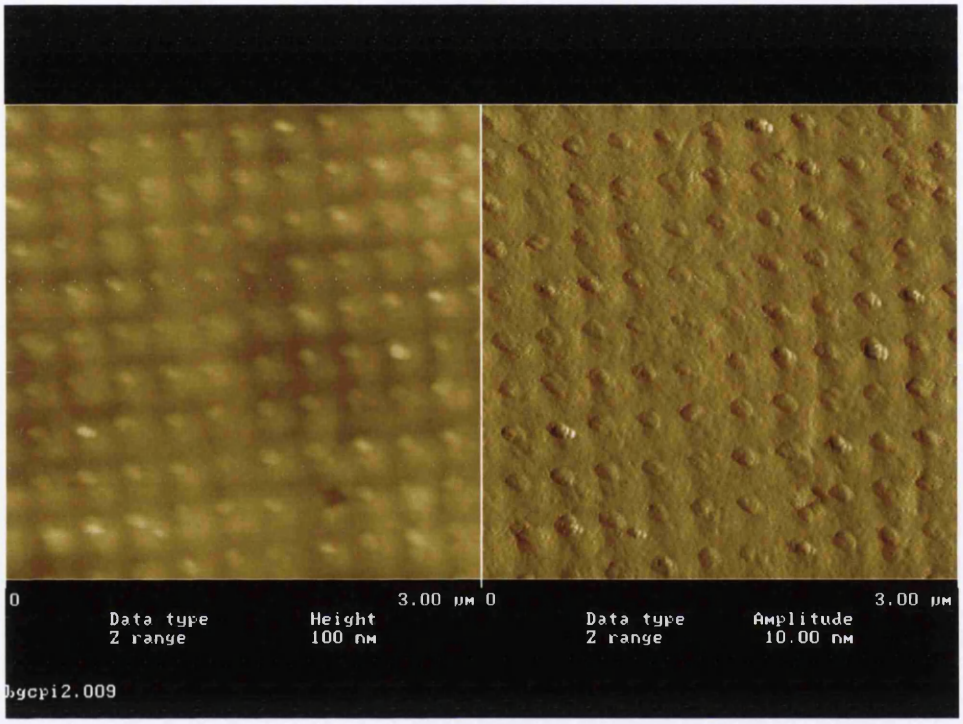

Figure 37. *Tapping mode AFM scan of a polystyrene sample patterned by embossing. The features are 60nm diameter pillars with a height of approximately 50nm. The image on the left is the surface topography and the image on the right is the cantilever deflection.*

The image shown above, figure 37, displays two sets of information. The image on the right represents the cantilever deflection and the image on the left is a representation of the actual surface topography. This is the standard and initial plot which is output after a scan. However it is possible to get a more realistic surface plot by plotting the scan information in the form of a 3-dimensional plot. Figure 38 and figure 39 on the next page show 3-dimensional scan images taken for 15nm and 60nm embossed pillars in polystyrene.

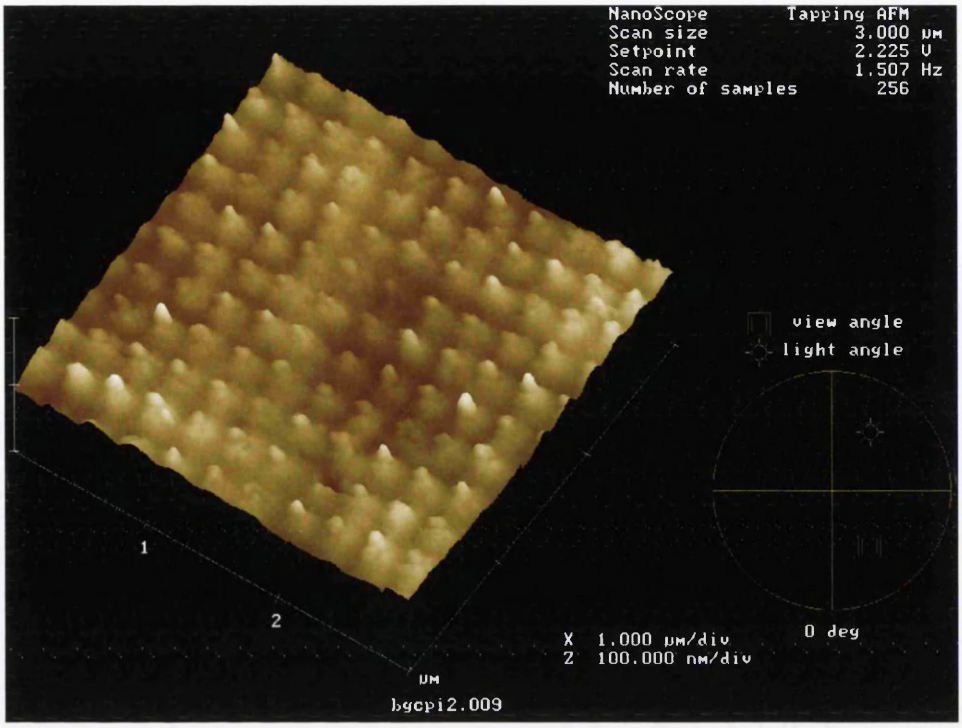

Figure 38. *3-dimensional plot obtained by tapping mode atomic force microscopy. The features shown are 60nm polystyrene pillars.*

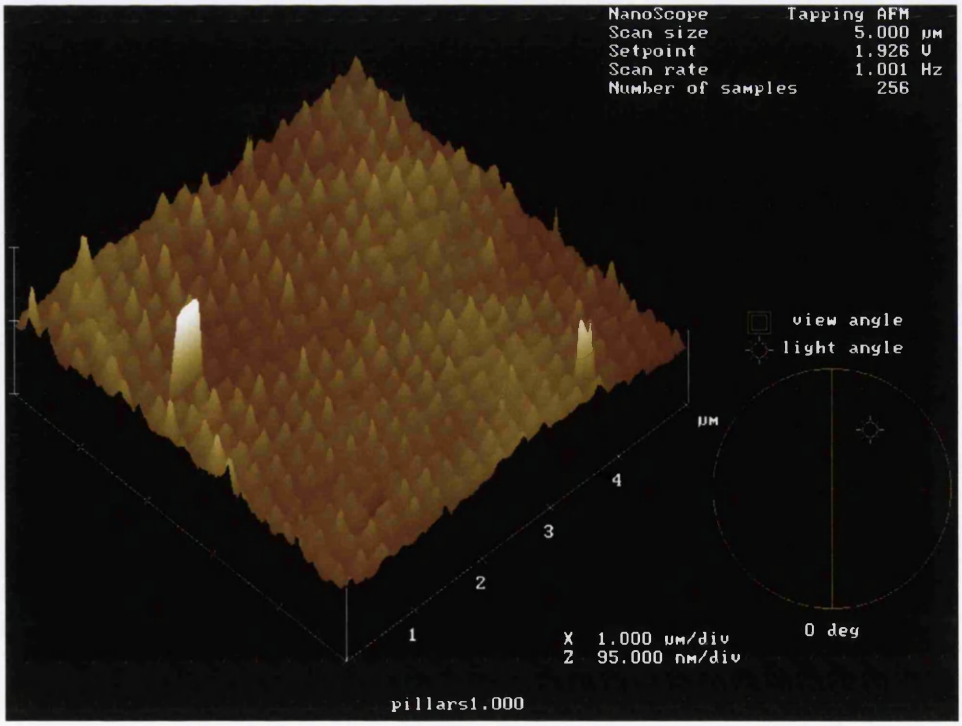

Figure 39. *3-dimensional plot obtained from tapping mode atomic force microscopy. The features are 15nm diameter polystyrene pillars.*

3.3.3 Embossing Resolution Limits

As explained in §3.3.1 embossing transfers the pattern written by electron beam lithography with apparently complete fidelity. There is however another factor which controls the ultimate resolution of mechanical pattern transfer technology. Most thermoplastic sheets are produced by a method known as casting. During this process, hot liquid polymer (or solvent dissolved polymer) is poured onto a cool flat surface, usually a fluid, and allowed to set (or left for the solvent to evaporate). During this cooling, or setting process nanometric cracks appear in the surface of the polymer which for most applications go un-noticed. However, when fabricating structures of 15nm in dimension these cracks become a serious problem. Figure 40 below shows a micrograph of a cellulose acetate surface which has been embossed with 15nm holes. Cracks can be seen on the unpatterned surface but where there is patterning it can be seen that the dots join together along these cracks.

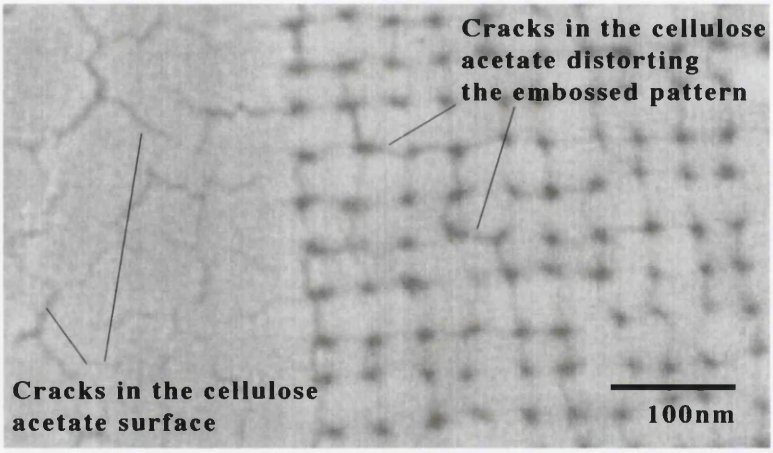

Figure 40. *SEM image of a cellulose acetate surface patterned with 15nm holes. Cracks in the surface can be seen and distortion of the dots is also visible.*

There is nothing that can be done to overcome this problem in materials such as cellulose acetate and polystyrene since it is a side effect of the material production process. Thus it is a limiting factor when considering polymers for high resolution applications.

The only other limiting factor when considering embossing as the pattern transfer method of choice is that the overall dimension of the replica is not exactly the same as the master. This phenomenon occurs at the mould release stage of the process. Since the plastic has been heated under pressure, when it is cooled and the pressure is released, the mould shrinks slightly. In general this shrinkage is between 5% and 0.5% which is acceptable in many applications. However, in nanofabrication this is too large an error which must be reduced. It has been measured during the course of this work that the worst shrinkage obtained was 0.04%. This is a more reasonable value and does not

effect the working of the devices fabricated here. This value is obtained by careful correlation of temperature, time and pressure during the embossing process and by ensuring that the sample is cooled completely before releasing from its mould. See §3.2.1. In order to measure the size variation between the original electron beam written lithographic pattern and the embossed pattern, the mask shown below is used.

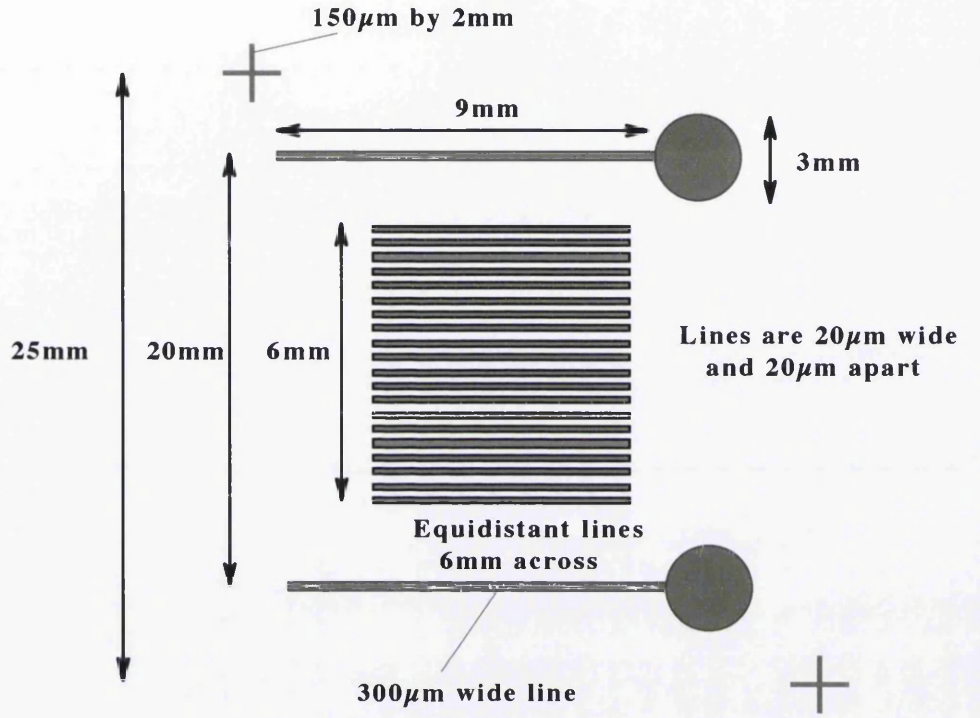

Mask 1. *Mask used to measure master and replica correlation (Not to scale). This is the mask used for the selective metalisation of the embossed flow chamber. See §3.6.1.*

The mask pattern is embossed into the polymer substrate and is then compared to an identical optical mask on a mask aligner (HTG Mask Aligner). Shrinkage of test polymer samples was measured for substrates with the pattern embossed on one surface and for samples with the pattern embossed onto both sides of the sample. Double sided samples were produced with the test patterns either parallel or perpendicular to each other. No difference in dimensional instability was found for these substrates. The embossed patterns were compared to the optical mask over the area shown in *mask 1* and it was using this comparison that the value of 0.04% for the shrinkage of the embossed samples was obtained. Polymer samples were tested for dimensional stability no later than three weeks after fabrication. Since the experimental lifetime of the embossed samples was short (1-4 weeks), so no long term shrinkage measurements were made.

The two constraints on the resolution of embossing described here are not major problems but are inconvenient and it is felt that with work both could be greatly reduced if not removed completely. However, even allowing for these problems, embossing is still one of the highest resolution forms of pattern transfer available today.

3.4 Plastic Fabrication for Bioelectronics and Beyond

Embossing is a very useful method of transferring surface topographies into plastics for applications in bioelectronics and cell engineering. However, during the development of the embossing process, other devices and patterns were fabricated which are applicable in optoelectronics and transistor fabrication.

For optical applications, lens and grating devices were fabricated to test the extent to which the embossing process could replicate structures which are difficult to make at a reasonable cost using conventional nanofabrication methods. Fresnel lenses were stamped into polystyrene using a master device which had been made using e-beam lithography and reactive ion etching. Also, blazed diffractive gratings were replicated from master samples fabricated in solid PMMA. This process will be described in detail in §3.5.1. A photograph of the Fresnel lens replica is shown in figure 41 below.

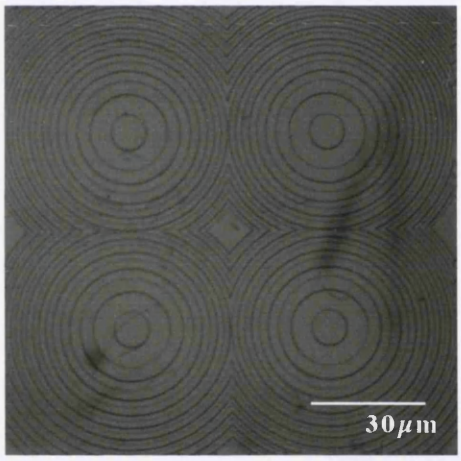

Figure 41. *Photograph of a Fresnel lens produced by embossing polystyrene with a quartz master.*

Having discovered that it is possible to transfer these patterns into plastics it was decided to attempt to imprint lenses into photoresist. At present Fresnel lenses are made by multilevel EBL, lift-off and reactive ion etching. However, if photoresist was used it would be possible to use this as the RIE mask directly. Imprinting would also allow many samples to be made in one step from one master rather than in a serial multistep fashion. The imprint is made by taking a polished quartz substrate, spinning photoresist (Shipley S1818) on it and baking at 90°C for 30mins. Shipley S1818 is a microposit photoresist consisting of a photoactive compound (PAC) in a Novolak resin. The solvent used for this resist is propylene glycol monomethyl ether acetate This resist coated sample is then pressed against the master and heated to 135°C for 45mins. At this temperature the photoresist flows and is patterned by the quartz die. The excess

resist produced by this process flows to the outer edges of the sample where the pressure is lower and thus leaves a thicker resist film at the edges than in the middle. This is a more difficult process than embossing since it is essential that every component used is optically flat. If the samples are not polished then a patchy pattern transfer is obtained when using large surface area patterns. Thus, the results obtained for this process were mixed. It is possible to produce excellent replica areas in the photoresist, however over large areas of a device the uniformity is poor. Figure 42 shows two micrographs of lenses imprinted into Shipley S1818 photoresist (1.8μm thick).

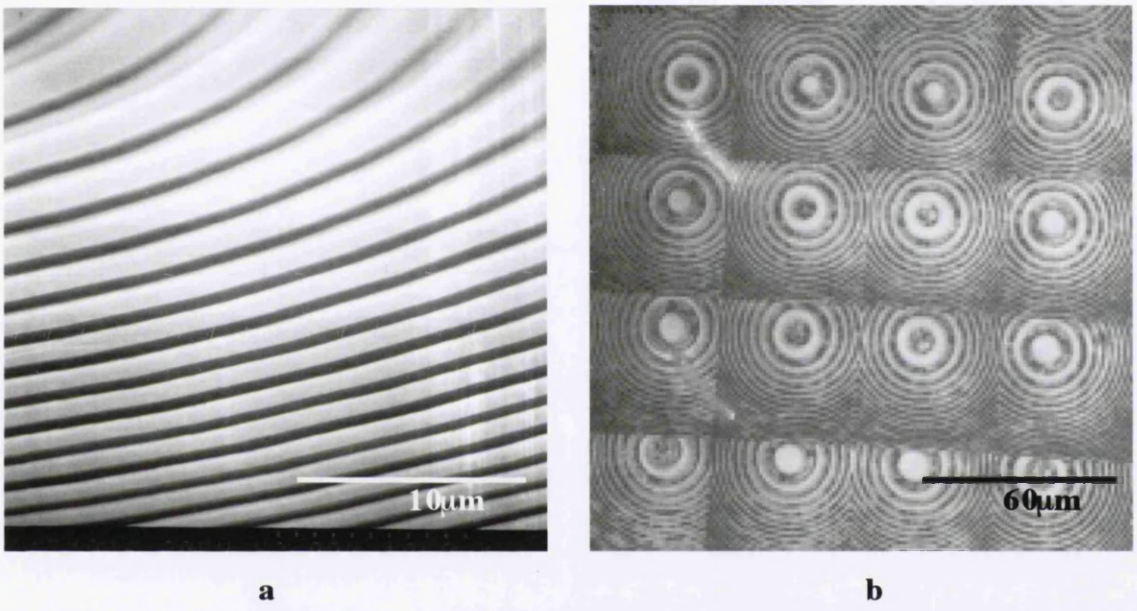

Figure 42. *Micrograph* ***a*** *shows a section of a Fresnel lens imprinted into photoresist. The quality of the pattern transfer is excellent. Photograph* ***b*** *shows a large area of a device. It can be seen that there are sections missing where the resist has been removed from the surface. The overall pattern transfer is poor.*

The actual integrity of the pattern transfer in all devices made using resist imprinting was good. However, the resist adhesion is the problem. Since photoresist is made to stick to surfaces it sticks to both the master and the platen during imprinting. This is why the device shown in figure 42b has sections missing. It is this adhesion difficulty that is the restricting factor in resist replicas. It should however be possible to overcome this problem by a different selection of resist or by using mould release agents. This is a possible area for future work in this field. Resist imprinting is a process worth developing since it has the same pattern transfer qualities as embossing but allows any substrate material to be used.

3.4.1 Lithography Processing for Plastics

When fabricating plastic devices for DNA fractionation it is necessary to perform photolithography on top of the embossed features. See §3.6.1. However, since the plastics used here; cellulose acetate, polystyrene and perspex, are polymers which dissolve in a variety of solvents they have to be handled with care when doing photolithography. Therefore, during this project, new procedures have been developed which allow the use of plastic substrates in photolithography.

Let us consider a full photolithography process leading from resist spinning to exposure to metalisation to lift off to finished sample. Firstly, when selecting a photoresist to use with a plastic substrate care must be taken to ensure that the resist solvent will not attack the plastic surface as this makes lithography impossible. Secondly, it is not possible to bake the resist to remove the solvent after spinning. The reason for this is that at the resist baking temperature of 90°C many plastic substrates will begin to soften and expand, where upon cooling they will contract and cause defects in the resist surface. This problem can be overcome by leaving the sample for 24 hours in a fume hood to allow the resist solvent to evaporate. The photoresist used throughout the course of this work was Shipley S1818. The solvent for this resist is propylene glycol monomethyl ether acetate which does not attack the polymer substrates used here. After the resist has been 'cold baked', UV exposure and development can be performed as normal. If lift-off is to be performed then the metal layer must be evaporated by an electron beam evaporator since a normal thin film evaporator heats the stage to the point where the plastic sample will melt. It is also important to choose the metal carefully. With plastics adhesion is a problem. However it has been found that nichrome gives best results, although this varies from plastic to plastic and application to application. Now moving on to lift-off. This is normally performed in acetone but acetone dissolves plastics very readily. Therefore, when working with plastics lift-off is performed in resist developer. This is done by flood exposing the resist immediately after pattern development and before the metal evaporation. The flood exposure makes it possible to perform lift-off in developer by making the remaining resist soluble in the developer. The metalised sample is then placed in developer and the flood exposed resist is dissolved in the solvent without harming the substrate.

These are now standard handling procedures used within the department for handling plastic samples during photolithography.

3.5 Direct Patterning of Plastics

Many plastic polymers are sensitive to various forms of radiation. Some are degraded by exposure to ultra violet light, some are degraded by an electron beam and some are damaged by X-rays. From an engineering view point it is of interest to control and utilise this polymer characteristic. Resists used in the microfabrication industry are, in general, simply specialised plastics. Therefore, it should be possible to use nanofabrication techniques to pattern directly onto plastics. This is an important process in the battle to overcome the problem of embossing being useful only for single layered devices. In the following sections two specific examples of direct patterning of plastics are presented and results are shown where a second patterned layer is superimposed on a previously embossed substrate.

3.5.1 Electron Beam Patterning of Solid PMMA

Perspex (polymethyl methacrylate-PMMA) has long been used as a high resolution positive electron beam resist [15]. Normally thin layers in the region of a few hundred nanometres of PMMA are spin coated on substrates and then exposed using EBL. At Glasgow, David Cumming et al. have developed a process which patterns solid sheet PMMA [16]. The driving force behind this work is the fabrication of efficient diffractive optics such as Fresnel lenses, zone plates and computer generated holograms. These are multilevel devices which under normal circumstances require nanometre scale alignment, however by direct writing it is possible to produce such devices in a single step. Therefore, this fabrication method is ideal for rapid device prototyping as well as making devices suitable for embossing into other materials.

The PMMA sheet used had an average molecular weight of 1.5-4.5 x 10^6 amu, was 1mm thick and is made by a casting process. Before e-beam exposure the sample is coated with 30nm of nichrome (60/40) to act as a charge conduction layer. The NiCr is deposited using an electron beam evaporator with a working distance of 0.6m, so as not to melt the PMMA. After exposure the NiCr is removed by dipping the sample in commercial Cr etch for 30s, before rinsing in water and blowing dry.

Using this technique blazed diffraction gratings were fabricated for use in transmission or reflection with efficiencies as high as 83% at a wavelength of 514nm. Tests were also carried out to observe the resolution of this process and it was found that features with dimensions of 60nm could be easily produced using this technique [17].

As mentioned earlier it is possible to emboss the features contained within these devices into a material with a lower flow temperature or a longer polymer relaxation time [17]. Polystyrene was chosen as the replica material since although it has a similar glass transition temperature to PMMA (~100°C) it has a longer relaxation time by approximately 3mins. Therefore, the PMMA samples were sputter coated with 5nm of Au/Pd to avoid any chemical reaction between the two heated surfaces. The samples are then pressed together and heated to 97°C for 9 mins. Since this process depends on polymer chain relaxation time it is crucial that the time is closely observed. Figure 43 below shows polystyrene features made from direct written perspex masters.

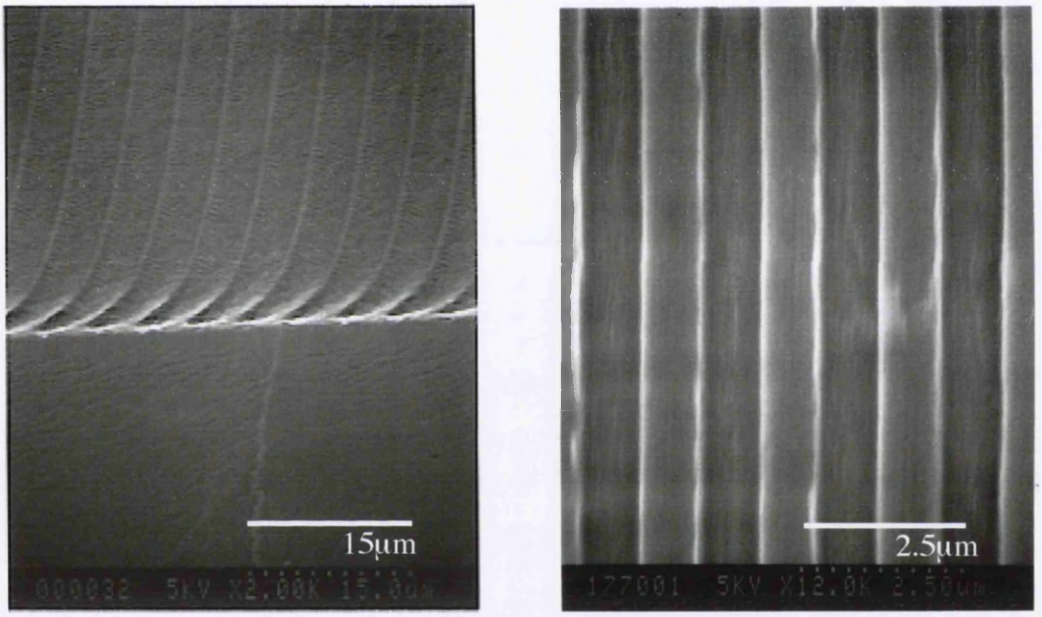

a **b**

Figure 43. *Micrograph* ***a*** *shows blazed diffraction gratings embossed into polystyrene using a perspex master. Micrograph* ***b*** *is of a 850nm 1:1 grating embossed into polystyrene using a perspex die.*

It can be seen from figure 43 that this process is capable of producing high resolution results with good correlation between replica and die.

While direct writing of perspex is not suitable for mass production of devices, using such devices as dies for pattern transfer is. The yield, repeatability and efficiency of the perspex samples are excellent and these characteristics are carried over into the replicas. Both of the fabrication techniques demonstrated here are of great value in optoelectronic and topography dependent devices. The results have shown that the quality of sample produced is at least as good as any other fabrication method but with cost and throughput is greatly improved.

3.5.2 UV Patterning of Cellulose Acetate

Cellulose acetate is degraded when exposed to ultra-violet light with a wavelength of less than 254nm. In a vacuum the photolytic changes involve deacetylation, chain scission and crosslinking. Analysis has shown that the six main products formed are ketene(CH_2=C=O), CO, CO_2, H_2, H_2O and acetic acid (CH_3COOH) [17]. It has been concluded that certain molecules are formed after cleavage of the molecule, namely :

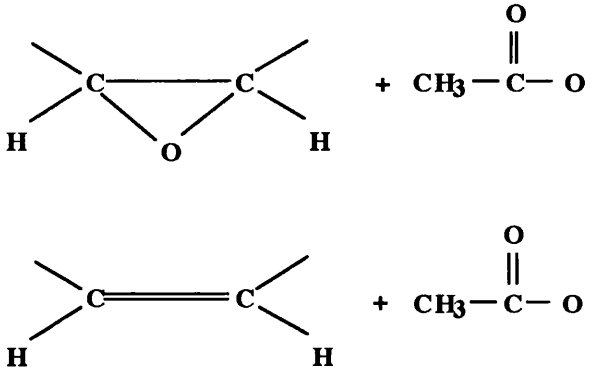

Therefore, because of this breakdown the exposed areas can be easily dissolved in a suitable solvent. The solvent used here is Shipley photoresist developer which is a potassium hydroxide based alkali chemistry. If this photolytic effect on the cellulose acetate is controlled by masking certain regions of the plastic surface it is possible to pattern the polymer. Throughout the course of this work the mask used has been Shipley S1818 photoresist which is not baked before patterning, but is instead left for 24 hours to allow solvent evaporation. This is done to avoid heating the cellulose acetate to temperatures near its upper working temperature which would compromise its dimensional stability. The photoresist is patterned using standard photolithography after which the cellulose acetate is exposed using our electron beam evaporator. This source of UV was inadvertently discovered when overcoating polymer samples. The resist is then removed by flood exposure and development. During this development the exposed cellulose acetate is also removed thus producing a pattern in the sample.

The interesting application of this technique is that it facilitates the superimposing of a photolithography pattern on top of an embossed pattern as demonstrated in the next section.

3.5.3 Secondary Patterning of Plastic Devices

The principle behind two layered plastic devices makes use of the fact that it is possible to superimpose a photolithography pattern on top of a previously embossed pattern [18]. The embossed pattern is then recessed into the body of the material by the removal of the exposed cellulose acetate in developer, as shown diagramatically in figure 44.

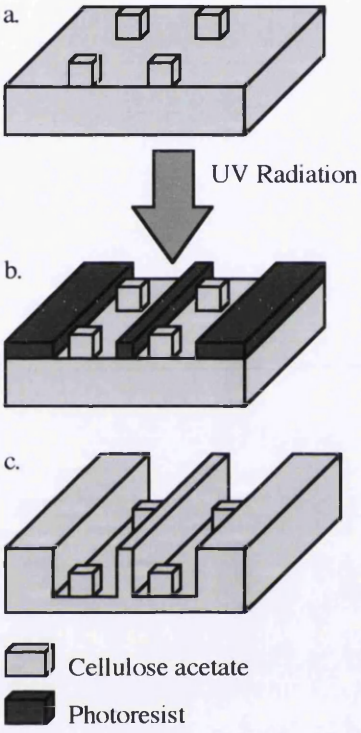

Figure 44. *UV patterning of embossed cellulose acetate. a) This figure shows embossed cubes on a plastic sample. b) The sample is then masked with photoresist and irradiated. c) The sample is developed and the resist is removed. The embossed features are recessed and not removed because of the penetration depth of the incident light.*

This phenomenon can be understood by considering the penetration depth of the UV radiation. It has been found that the measured UV penetration depth of cellulose acetate in our electron beam evaporator is approximately 250-300nm. Therefore, if a surface which has prominent features on it is exposed, then the top 300nm of the material is removed upon development but the surface topography is maintained. Consequently the features are simply recessed into the material by 300nm.

Using this process a sample which had been embossed with rows of 500nm linewidth 'U' shaped features was masked using photoresist and patterned with straight lines. The resist lines did not cover the rows of 'U' features but did cover the regions in between

the rows. The sample is then exposed and placed in Shipley photoresist developer. The photoresist is now removed. It is found that the irradiated polymer is removed and that the embossed 'U's are recessed into trenches as shown in the micrograph in figure 45 below.

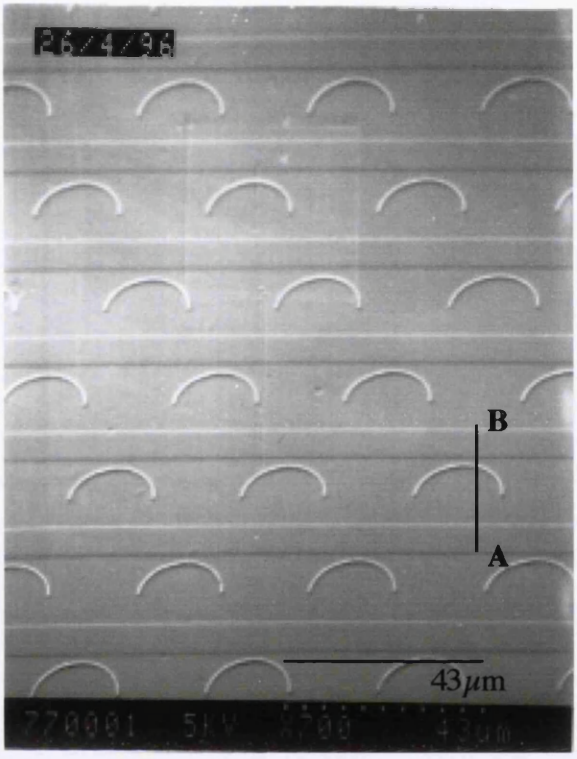

Figure 45. *The micrograph shows cup features recessed into trenches by UV exposure of cellulose acetate. Figure 46 shows a surface profile of the section AB in this micrograph.*

Thus, if an area is masked it will not be etched but the surrounding profile will be etched into the body of the plastic. Results have been obtained using this method which show embossed features in channels with walls 3 times the feature height. Figure 46 displays a plot from a Dek-Tak surface profiler which shows a 90nm high embossed feature in a 310 nm deep trench. There is no change in the embossed feature shape or profile after the UV patterning.

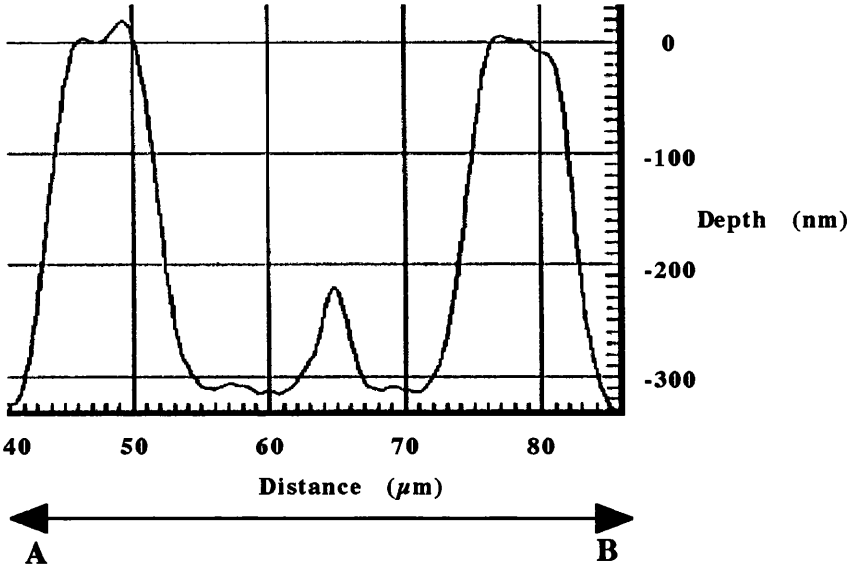

Figure 46. Surface profile of a cellulose acetate sample after embossing and UV exposure. The spike between 60 and 70μm is the embossed feature. This profile was taken on the surface of the sample between the points A and B as shown in figure 45.

This type of structure is very difficult to fabricate using standard lithography but it is just one of several potential applications for this technique.

3.6 The Advanced Fractionating Chamber

As explained in chapters 2 and 5 of this thesis there many parameters to be considered when designing and constructing a suitable retarding medium. It is essential that the fractionating chamber is capable of producing highly dispersive mobilities and that a suitable electric field can be produced within the lattice.

In the production of this device we have used electron beam lithography, dry etching, wet etching and electroplating to fabricate master dies for use in an embossing process. The embossing procedure facilitates the production of devices which are self contained, in that the structure array and the electrophoresis electrodes are on the same piece of material. However, in order to make working electrodes and a lattice with efficient conduction it is necessary to metalise the polymer samples. This is done using novel fabrication methods which allow nanofabrication on a plastic substrate.

In choosing the metals used, it is essential that they will adhere to the substrate when placed in aqueous environments and that any heating will not be a problem. It was found that a nichrome/gold layer structure was optimal for this purpose.

The final consideration when using the fractionating chamber is staining for the DNA. Since the method of observation of the DNA migration is fluorescence microscopy, it is essential that the DNA can be stained with a dye which will fluoresce brightly for several minutes without quenching or bleaching [20]. In the course of this work several dyes were tested for brightness, bleaching and background fluorescence. The results of these tests can be found in §5.5.

3.6.1 Chamber Fabrication

The plastic electrophoresis chamber is fabricated using the procedures described in this chapter. The polymer used for embossing is cellulose acetate which is an organic cellulose ester. The important characteristics of this plastic are that it has a smooth, gloss surface with good clarity and a relatively low embossing temperature. This plastic is known for its good moulding qualities and has a recommended compression moulding temperature of between 135-175^{o}C. Cellulose acetate also has good UV characteristics and is occasionally used in a gel form for electrophoresis. The fractionating device is replicated from a master die which is made using electron beam lithography, dry etching and electroplating. The full fabrication process is :

1)Clean 1mm thick glass substrate by immersing in an ultrasonic bath and successively washing in Opticlear™, acetone, methanol for 5 minutes each. Rinse in RO (reverse osmosis) water for 3mins.

2) Evaporate plating base and charge removal layer consisting of 8nm Ti, 8nm Pd and 60nm Au.

3) Spin resist adhesion promoter HMDS (hexamethyldisilazane) at 3000rpm for 35s.

4) Bake sample in an oven at 120^{o}C for 20 minutes

5) Spin resist layer. Pure AZ PN114 chemically amplified negative tone resist is used which gives a thickness of 1.6μm when spun at 3000rpm for 35s.

6) Soft bake resist on a vacuum hotplate at 120^{o}C for 2 minutes.

7) Pattern written on beamwriter. The pattern consists of the retarding area, two electrodes for application of the electrophoresis field and two alignment markers for photolithography. The job is run at 50kV and uses a dose of 15μC/cm^2 .

8) After the resist has been exposed the sample receives a post exposure bake at 105°C for 5 minutes.

9) The resist is then developed for 1 minute at 20°C in Hoechst AZ400K developer diluted 1:4 with RO water, rinsed in RO water and blow dried.

10) The sample is then cleaned using a CHF_3 dry etch for 1 minute. 20sccm is used at a pressure of 16mTorr and a rf power of 100W with a bias of -410V.

11) Electroplating. Electroplate sample with nickel at 54°C, pH 3 and 15 mA for 20 mins. This gives a Nickel thickness of 500nm.

12) Remove resist. The AZ PN114 resist is now removed by refluxing the sample in Opticlear-W for 1 hour at 100°C.

13) The sample is now a finished master die ready for embossing.

14) Goodfellow 0.5mm thick cellulose acetate is embossed using the electroplated die. The embossing process utilises a hinged clamp which is tightened to a known torque thus applying a constant force to the die/plastic/platen stack. Standard embossing times are 30 minutes at the elevated temperature of 135°C followed by a 15 minute cooling period.

15) The cellulose acetate sample is now selectively metalised to produce the electrophoresis electrodes and to coat the features of the retarding medium.

16) Spin Shipley S1818 photoresist at 4000rpm for 1 minute. The sample is then left in a fume hood over night to allow solvent evaporation. This is done instead of baking the resist to avoid heating the cellulose acetate to temperatures near its upper working temperature which would compromise its dimensional stability.

17) The resist is exposed and developed in 1:1 AZ developer : RO water for 75s.

18) The remaining resist pattern is flood exposed to allow lift off to be performed in developer rather than acetone which dissolves the plastic.

19) Evaporate 10nm NiCr and 50nm Au onto the sample.

20) The metal is lifted off by immersing the sample in neat photoresist developer for 15 minutes. This produces a pattern which has electrophoresis electrodes and retarding structures which are metalised in straight lines parallel to the electrodes. This is the final substrate for the chamber which can now be mounted and sealed.

Figure 47 below shows a schematic of the mask used to metalise the plastic features and a photograph of some 'U' shaped features metalised in rows with NiCr/Au from an actual device.

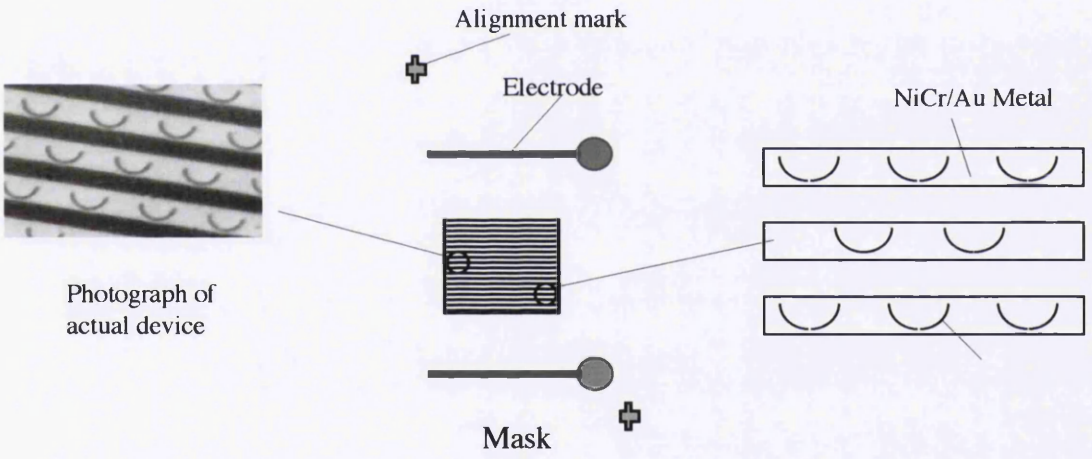

Figure 47. *'U' shaped retarding features metalised with NiCr/Au in lines parallel to the electrophoresis electrodes.*

3.6.2 Chamber Sealing and Mounting

Once the cellulose acetate sample has been fabricated by embossing and selective metalisation it is necessary to mount and seal the device before it is ready to use. A cover has to be placed on top of the fractionating array to produce a sealed environment for the electrophoresis. When using silicon devices this was done by anodic bonding, however this is not a suitable process when dealing with plastics because of the high processing temperature. Therefore, the cover is produced by sealing a plastic sheet on top of the structures. This is done by pressing a cellulose acetate sheet onto the structures and the electrodes and heating to the upper working temperature of the acetate sheet. At 95°C the plastic glazes but does not lose its shape or structure and therefore sticks to the metal electrodes and the feature array. This process works since at this temperature the polymer experiences slight relaxation before it reaches its glass transition temperature. The samples are pressed together using the same clamping system used for the anodic bonding process as shown in figure 6. The clamped samples are then heated in an oven.

Now that the device is sealed the sample is mounted on a glass slide using silicone sealant. This allows easy handling of the sample and makes it possible to anchor the device on the microscope stage. At this point the electrical connections are made to the device. Wires are attached to the slide using silicone sealant. The wires are connected electrically to the electrodes using silver loaded paint. The full experimental set up is shown below in figure 48.

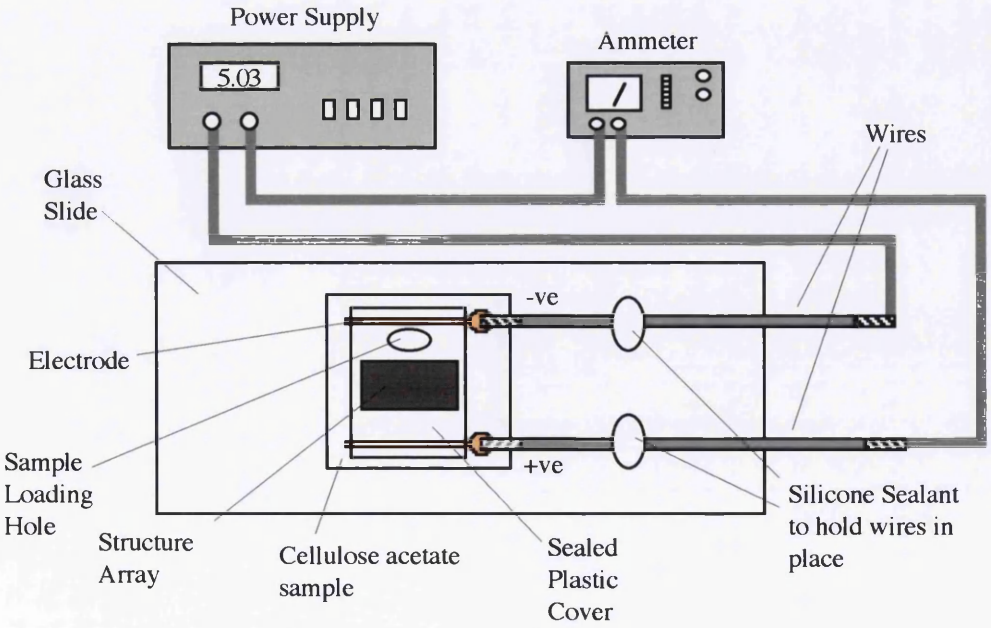

Figure 48. *Cellulose Acetate Electrophoresis Set up. The acetate device is sealed with a plastic cover. The cover has a hole at one side to facilitate loading of the DNA sample. The sample is then mountedon a glass slide to allow electrical connections and to allow easy mounting on the fluorescence microscope.*

3.7 Device Fabrication for Cell Adhesion Observations

In order to observe cell adhesion to topography, devices were made which consist of arrays of nanopillars. Two sizes of pillars were made using different fabrication processes.

15nm dots on 35nm centre to centre spacings were fabricated using the Jeol 100CXII. Silicon substrates (5mm by 5mm) were cleaned by successive ultrasonic agitation in Opticlear, acetone, methanol and RO water. PMMA (Elvacite Mwt 350000) resist was spun on the substrates from a 2.5% solution in xylene at 5000rpm for 1 minute. A pattern of holes was written on the Jeol over an area of 500μm by 500μm before being developed in a 3:1 mix of isopropanol : methyl iso butyl ketone. The resist was then used as a dry etch mask for the silicon. The silicon was etched using a Plasma Technology microP 80 reactive ion etching machine with a gas mixture of 50% $SiCl_4$ 50% HBr at a flow rate of 20sccm/20sccm, an etch pressure of 30mTorr, a rf power of 100W and a bias of -275V. The etch depth was 25nm after 5secs. The resist was removed in acetone and the silicon substrate is now used to emboss pillars into polystyrene at 97°C using the process described in §3.2. Figure 49 below shows an AFM micrograph image of the polystyrene pillars. These features were made using the silicon master die shown in figure 32b in §3.3.

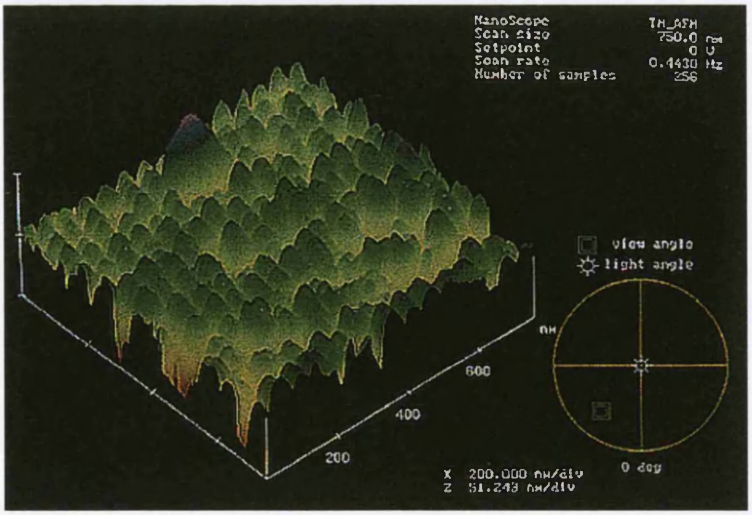

Figure 49. *The AFM image shows the 15nm polystyrene pillars produced from a silicon master by embossing.*

The second features used for cell adhesion tests were 60nm pillars on 300nm periods. The fabrication process for these devices utilised embossing. However, the method used differs from the other processes described in that the master die is also made from

a thermoplastic. The master embossing die is made using the process described in §3.5 whereby sheet PMMA is patterned using EBL. Polymethyl methacrylate sheet 1mm thick is cleaned with isopropanol before being coated with a 30nm evaporated nichrome layer. 150μm squares are written using the EBPG 5HR beamwriter with the resolution set to the required period (300nm) of the features and a spot size of 28nm. The exposure dose is 65μC/cm^2 which allows fast write times. This 150μm pattern is written repeatedly to produce an area of holes 5mm by 5mm in PMMA. The nichrome charge removal layer is wet etched away and the sample is developed in 3:1 isopropanol : methyl iso butyl ketone for 10s before being rinsed in isopropanol for 10s. The perspex sample is sputter coated with 5nm Au/Pd. Embossing is carried out into polystyrene at a temperature of 97°C for 9mins. A micrograph of these features is shown below in figure 50.

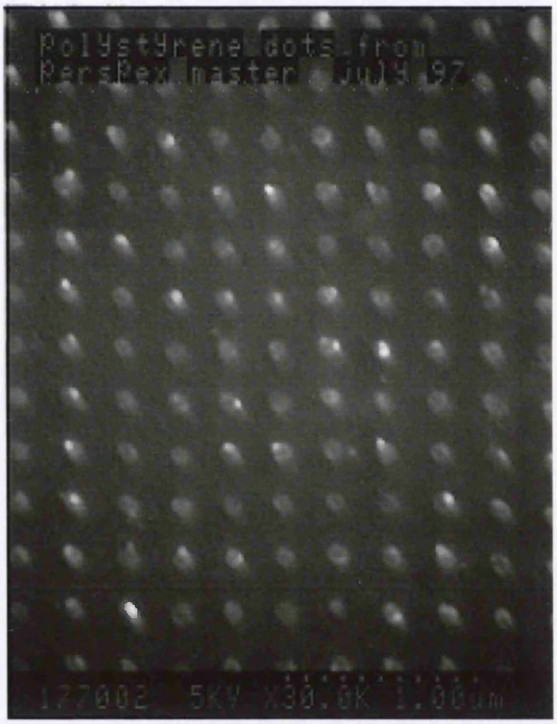

Figure 50. *Polystyrene pillars produced by embossing with a Perspex die. The features are 60nm in diameter and have a period of 300nm.*

The timing of this process is critical since both the polystyrene and the polymethyl methacrylate have glass transition temperatures of approximately 100°C. If the time is too long then the master will relax and the pattern definition will be lost. If the time is too short then there will be no pattern transfer since the polystyrene will not be pliable enough. The only reason that the process works is that the polymer relaxation time for perspex is longer than that for polystyrene. That is, it takes the polystyrene less time to soften than it takes the PMMA.

Now that the devices have been fabricated it is possible to test quantitatively the effect that rugosity has on the adhesion of biological cells to surfaces that they encounter.

3.8 References

[1] Broers, A. N., Fabrication Limits Of Electron-Beam Lithography and Of Uv, X-Ray and Ion-Beam Lithographies, Philosophical Transactions Of The Royal Society Of London Series A Mathematical Physical And Engineering Sciences, vol. 353, pp. 291-311, 1995.

[2] Chu, W., Smith, H. I., Rishton, S. A., Kern, D. P., and Schattenburg, M. L., Fabrication Of 50 Nm Line-and-Space X-Ray Masks In Thick Au Using a 50 Kev Electron-Beam System, Journal Of Vacuum Science & Technology B, vol. 10, pp. 118-121, 1992.

[3] Groves, T. R., Hartley, J. G., Pfeiffer, H. C., Puisto, D., and Bailey, D. K., Electron-Beam Lithography Tool For Manufacture Of X-Ray Masks, IBM Journal Of Research And Development, vol. 37, pp. 411-419, 1993.

[4] Reeves, C. M., Turcu, I. C. E., Stevenson, J. T. M., Ross, A. W. S., Gundlach, A. M., Prewett, P., Lawes, R. A., Anastasi, P., Burge, R., and Michell, P., Fabrication Of 200nm Field-Effect Transistors By X-Ray-Lithography Using a Laser-Plasma X-Ray Source, Microelectronic Engineering, vol. 30, pp. 187-190, 1996.

[5] Early, K., Tennant, D. M., Jeon, D. Y., Mulgrew, P. P., Macdowell, A. A., Wood, O. R., Kubiak, G. D., and Tichenor, D. A., Characterization Of Az Pn114 Resist For Soft-X-Ray Projection Lithography, Applied Optics, vol. 32, pp. 7044-7049, 1993.

[6] Kubiak, G. D., Hwang, R. Q., Schulberg, M. T., Tichenor, D. A., and Early, K., Chemically Amplified Soft-X-Ray Resists - Sensitivity, Resolution, and Molecular Photodesorption, Applied Optics, vol. 32, pp. 7036-7043, 1993.

[7] Chou, S. Y., Krauss, P. R.and P. J. Renstrom, Imprint Of Sub-25 Nm Vias and Trenches In Polymers, Applied Physics Letters, vol. 67, pp. 3114-3116, 1995.

[8] McCrum, N.G., Buckley, C.P., Bucknall, C.B., Principles of Polymer Engineering, Oxford University Press, UK, 1997.

[9] Brydson, J. A., Plastic Materials, Chapel River Press Ltd, UK,1969.

[10] Hoechst Celanese Corporation, Handling Recomendations for e-beam Negative - Tone Resist AZ PN114.

[11] Macintyre, D. and Thoms, S., High-Resolution Studies On Hoechst Az Pn114 Chemically Amplified Resist, Microelectronic Engineering, vol. 30, pp. 327-330, 1996.

[12] Personal Correspondance, Steve Thoms and Dave Cumming, Glasgow University, 1996.

[13] Brimi, M. A., Electrofinishing, American Elsevier Publishing Co., NewYork, 1965.

[14] Digital Instruments Nanoscope III Multimode AFM Instruction Manual.

[15] Cumming, D. R. S., Thoms, S., Beaumont, S. P., and Weaver, J. M. R., Fabrication Of 3 Nm Wires Using 100 Kev Electron-Beam Lithography and Poly(Methyl Methacrylate) Resist, Applied Physics Letters, vol. 68, pp. 322-324, 1996.

[16] Cumming, D. R. S., Khandaker, II, Thoms, S. and Casey, B. G., Efficient diffractive optics made by single-step electron beam lithography in solid PMMA, Journal Of Vacuum Science & Technology B, vol. 15, pp. 2859-2863, 1997.

[17] Casey, B. G., Cumming, D. R. S., Khandaker, I.I, Wilkinson, C. D. W., Nanoscale Embossing of Polymers using a Thermoplastic Die, To be published in Microelectronic Engineering, 1998.

[18] Ranby, R., Rabek, J.F., Photodegradation, Photo-oxidation and Photostabilization of Polymers, John Wiley and Sons Ltd., UK, 1975.

[19] Casey, B. G., Monaghan, W., and Wilkinson, C. D. W., Embossing of nanoscale features and environments, Microelectronic Engineering, vol. 35, pp. 393-396, 1997.

[20] Bustamante, C., Direct Observation and Manipulation Of Single DNA-Molecules Using Fluorescence Microscopy, Annual Review Of Biophysics And Biophysical Chemistry, vol. 20, pp. 415-446, 1991.

Chapter 4

Cell Adhesion On Patterned Substrata

The mechanism of cell adhesion has been studied by cell biologists for many years[1][2]. The mechanism is complex and not fully understood. The adhesion of cells to polymeric surfaces varies with the polymer[3]. Surfaces have been deliberately roughened in an attempt to promote cell adhesion. On the other hand some textured surfaces are less adhesive than their flat counterpart. In the body, biological cells adhere to each other and to non-cellular surfaces. Cell adhesion is important in tissue repair; in many cases it is desirable that cells adhere to each other and to other tissues. In certain situations it is essential that cells do not adhere to surfaces. A good example of this is in cardiac repair : here it is very important that platelet cells do not adhere to the inside of the plastic tube used to replace a diseased vascular moiety. In the work presented in this chapter devices were fabricated in polystyrene using a novel method of nano-embossing. These devices consist of large arrays of nanometre scale pillars of different diameter and centre to centre spacing. Cell adhesion to these patterned substrates is observed and compared to associated adhesion on a flat planar polystyrene surface. Possible mechanisms for the exhibited reaction are suggested and a course of further investigatory work detailed.

4.1 History of Topographical Cell Guidance and Adhesion

It has long been known that biological cells are greatly affected by their environment, whether it be in vivo or in vitro. However, it was in 1911 that Ross Harrison [4] first showed that cells responded to topographic cues on plasma clots and on spiders web fibres. Curtis and Vade [5] showed that cells were affected by curved surfaces and would align along a glass fibre. These were very interesting findings and it was the desire to understand these phenomena that led to the introduction of microfabrication techniques to produce artificial environments for testing cell response[6].

4.1.1 Cell Guidance

Initially devices used for cell guidance tests were made from the biocompatible materials quartz and perspex and utilised photolithography and reactive ion etching. The planar topographies used were cliffs, ridges, hills and grooves. It was found that cells did indeed respond to these cues. In the case of cliffs, it was found that the higher the face, the more difficult it was for a cell to climb down. With ridges, the cells accumulate on the top of the ridge and extend along it, a phenomenon known as ridge walking. The next topography tested was grooves. With these features it was found that cells aligned in the direction along the axis of the grooves and that guidance occurs. A great deal of analysis has been carried out on this type of environment to discover optimal conditions, such as groove depth, width and separation and can be found in [7][8][9].

The next main advancement in the area of cell guidance was on the engineering front. It was found that a faster, cheaper, and better method of producing these artificial environments was by using plastic substrates and a mechanical pattern transfer method known as embossing. The driving force behind this advancement was that it was necessary to use bio-degradable substrates for tendon repair. It was difficult to find a suitable lithographical process for such materials so it was decided to use embossing [10]. Figure 51 shows an example of an embossed groove pattern with cells aligned along pattern axis.

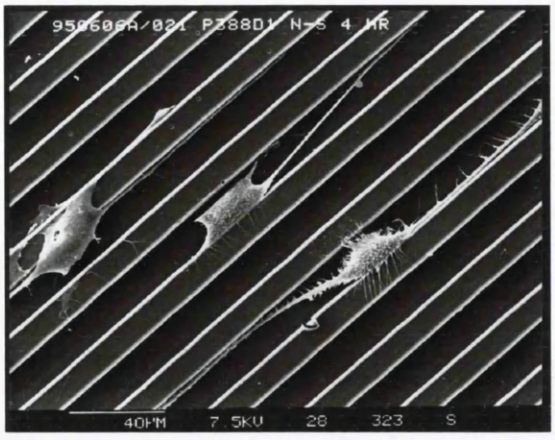

Figure 51. *BHK cells aligned along embossed grooves in PDS.*
Micrograph courtesy of Mr. Bill Monaghan.

This method of fabrication also offers the use of a more diverse range of patterns and materials; a great advantage when biocompatability and topographical area are of importance.

The applications for such guiding devices are as diverse as the topographies themselves. There is a great deal of interest for such devices in many areas of biomedical science, most notably for tendon regrowth [10] and tooth implants [11].

4.1.2 Cell Adhesion

The area of cell adhesion is closely related to that of cell guidance, and is extremely important in understanding the affect of topographical cues. Essentially, in a topographic cue environment, cell adhesion is controlled by surface roughness [12]. This roughness or rugosity is a random array of objects of varying height and size and of much smaller scale than the fabricated topography. Studies have been carried out to observe the affect of rougher and smoother polystyrene surfaces made by ion beam bombardment [13]. However, the method used to produce the roughened surfaces produces reactive oxygen at the cell - substrate interface which may in itself promote adhesion. Curtis showed that it is possible to smooth a polystyrene surface utilising wet chemical oxidation and that the smooth surface improved the adhesion of certain cell types [14]. Thus, there is not one unique answer as to what type of surface promotes adhesion. In this thesis a method of rendering a surface non-adhesive will be presented.

4.2 Design Ideas

Cell adhesion is affected by surface roughness, or rugosity [11]. The evidence [12][13] is inconclusive as to whether a smooth surface or a rough surface promotes adhesion: some of the difficulty coming from the problem of characterising a rough surface. It is therefore of great interest to discover if cells can indeed react to regularly spaced topographic features of known shape at the nanometric scale on a substrate.

It is known that when a variety of cells are placed in a micro or nano-structured environment, there are changes in adhesion and orientation of attached cells [14]. This is accompanied by cytoskeletal re-organisation and tyrosine phosphorylation, the activity of which varies with the type of substrata on which the cell rests [15]. The cellular cytoskeleton is an internal framework which gives a cell its distinctive shape and causes the cell to have a high level of internal organisation. The cytoskeleton consists of a network of tubules and filaments which give the cell shape. It controls the position of organelles and directs their movement, but more importantly from a cell adhesion viewpoint, it enables the whole cell to move or to change its shape. Figure 52 below shows a cartoon of a cell on a nanofabricated surface with features of importance to adhesion shown.

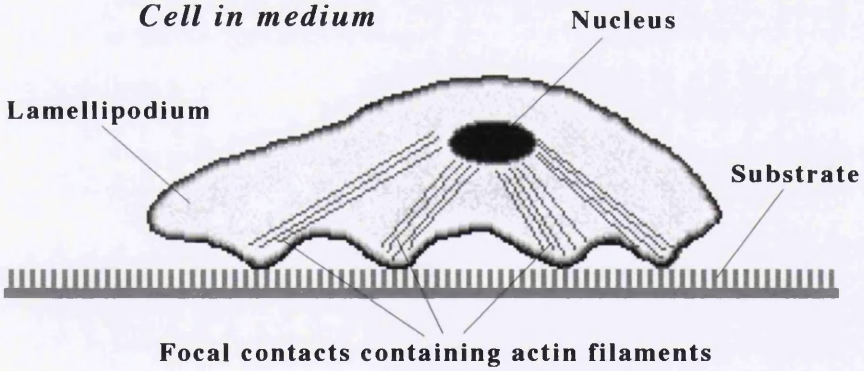

Figure 52. *Cartoon of a biological cell on a nanotextured surface. The important parts of the cell associated with movement and adhesion are shown.*

Initially when a cell is placed on a substrate, it has a rounded morphology similar to that of a cell suspended in an aqueous medium. However, once it contacts the substrate it sends out projections which form stable attachments to the surface. After a period of time the cell flattens and spreads itself out on the surface. This spreading is accompanied a dramatic change in the cytoskeleton.

The migration of animal cells is an extremely difficult process to explain at a molecular level. Different parts of the cell change at the same time and there is no obvious

organelle responsible for movement. However, it is known that cells on a substrate contact the surface at certain areas known as focal contacts [17].

In general, there is a gap between a cell and a surface of more than 50nm, however at focal contacts this is reduced to 10nm. At these points the plasma membrane of the cell is attached to parts of the extracellular matrix which have become adsorbed onto the substrate. These sites are known to be regions where the ends of stress fibres attach to the plasma membrane. These stress fibres or micro-filaments are prominent components of the cytoskeleton of fibroblast cells and are composed of contractile bundles of actin filaments. These actin filaments can polymerise and depolymerise and they do this during cell motion. It is these actin filaments that form the basis of animal cell migration by assembling into lamellipodium, associating with focal contacts and forming stress fibres. It is also at the focal contacts that the previously mentioned tyrosine is localised, the phosphorylation of which is indicative of a reaction to surface topography. Figure 53 shows the action of actin in a moving cell.

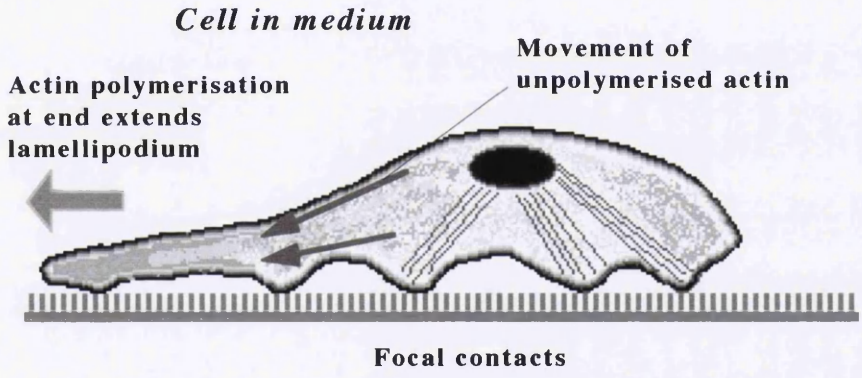

Figure 53. *Movement and location of actin in a moving fibroblast cell.*

Since the reaction of cells to surface stimulus changes subtly with feature dimensions, it is of interest to see how small a feature can induce a reaction in a cell.

In this chapter, the reaction of cells to small pillar structures, the fabrication of which is explained in §3.7, is examined. These devices are made using nanofabrication and therefore provide a means of controlling the roughness of the surface quantitatively, a feature missing from previous studies. The ability to fabricate devices with any size of feature spacing also facilitates the observation of focal contact interactions with a densely patterned surface. The use of these devices should therefore provide results which will allow further insight into cell adhesion and motion on topographic surfaces.

4.3 Cell Adhesion Results

Two types of cells were used to test adhesion to dotted surfaces. Firstly a macrophage line P388D1 was used which was grown in RPMI 1640 medium. Secondly, epitena cells were used which were grown from cultures isolated from rat flexor tendon in the same medium, grown for 2-3 passages. The cell culture work presented in this section was performed by Adam Curtis and Graham Tobasnick.

The polystyrene samples are sterilised by rinsing in 70% ethanol and are then blown dry. The cells were fixed using 4% buffered formalin and stained for microscope observation using Coomassie brilliant blue. 1.25g of Coomassie brilliant blue R-250 is made up in 225ml methanol, 50ml glacial acetic acid and 225ml water. The mixture is stirred for 30 minutes before being passed through a Whatmans No 1 filter. The cells and the nanostructured samples are covered in the stain for 5 minutes after which they are repeatedly washed in destain. The destain is 250ml methanol, 75ml glacial acetic acid and 675ml water. The rinsing is performed until only the cells are stained. Cell attachment results for the two pillar structures tested are shown in tables 1 and 2.

The 15nm pillar structures were tested using macrophage-like cells P388D.

Macrophage-like cells P388D1
Cells attached in 1 hour as percentage of cells in system per unit area

	Controls (Planar Surface)	Pillar
	55	7
	59	5
	60	7
	54	8
	57	6
Means	57.0	6.6
Standard deviation	2.5	1.15

Counting Area 340000μm^2

Table 1. *Macrophage-like cell P388D1 adhesion to 15nm diameter dots on 35nm pitch and smooth polystyrene surfaces.*

The 60 nm diameter pillars were used to observe the adhesion of rat epitenon cells, the results of which are shown in table 2 below.

Attachment of epitenon cells to pillar topographies 60nm in diameter, 300nm centre to centre repeat and 50nm high.

Rat Epitenon cells Cells attached in 1 hour as percentage of cells in system per unit area	Controls (Planar Surface)	Pillar
	74	11
	64	14
	60	14
	73	10
	72	13
	63	13
Means	67.6	12.5
Standard Deviations	6.02	1.64
Counting area 340000μm^2		

Table 2. *Rat Epitenon cell adhesion to 60nm diameter dots on 300nm centre to centre spacing and smooth polystyrene surfaces.*

Figure 54 shows two photographs of sample regions taken on a polystyrene substrate patterned with 60nm diameter posts and cultured with epitenon cells. The polystyrene used was sectioned from a bacteriological grade culture dish. The top picture is of a patterned area and the bottom one is of a planar area. The magnification is x20 (objective) and the cells are stained with Coomassie blue. It can be seen that there are far fewer cells on the pillared region than on the smooth area. This effect is observed for both feature sizes tested and for both cell types cultured.

From these results it is clear that the presence of these pillar arrays of either size seriously hinder cell adhesion to the surface. The reason for this is not completely understood, however, a possible explanation is given in the following section.

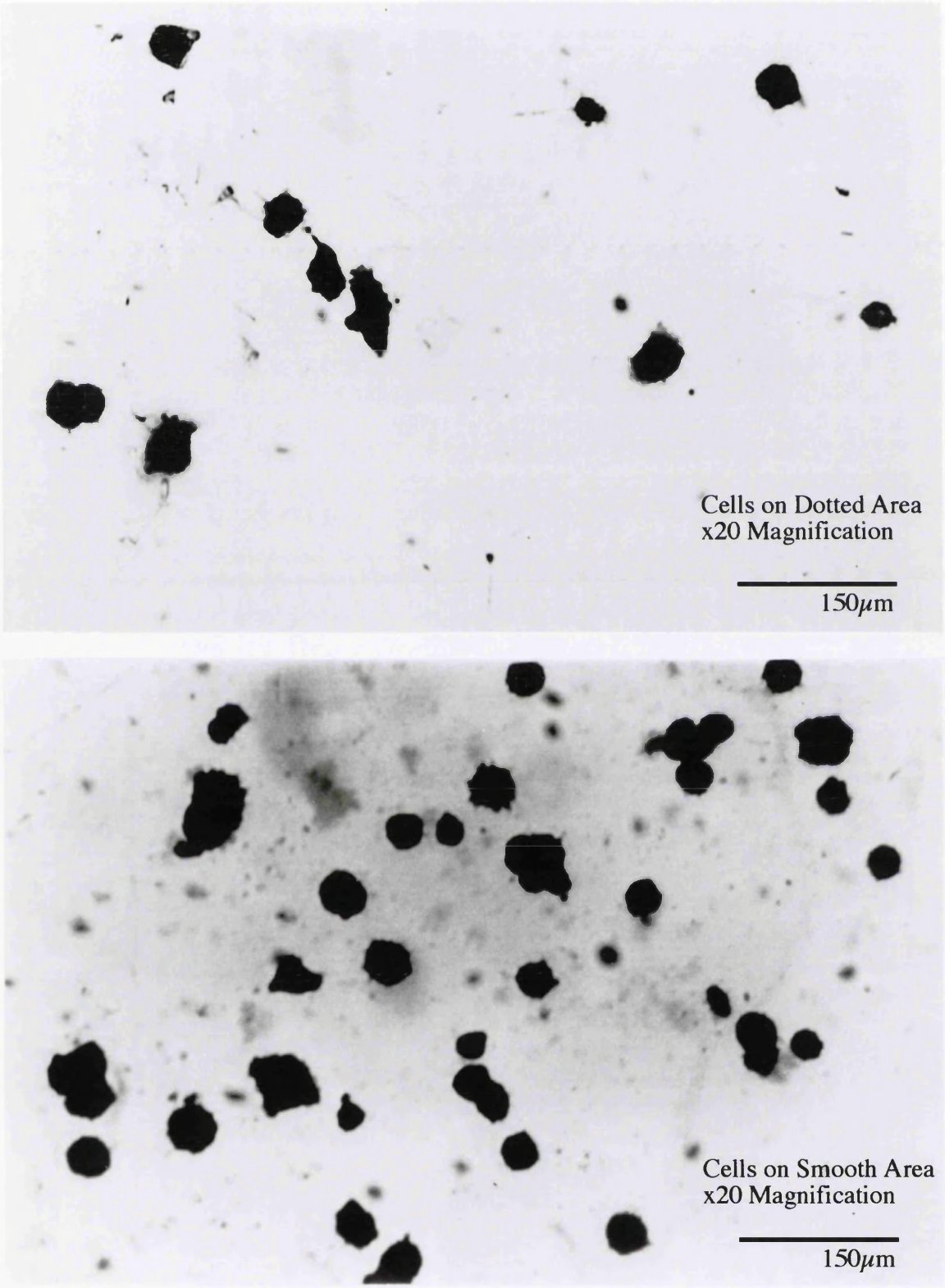

Figure 54. *Epitenon cells fixed to polystyrene surfaces. The top photograph shows cells on a surface pattered with 60nm diameter pillars on a 300nm pitch. The bottom picture is of cells on a smooth polystyrene surface. It can seen that there are far fewer cells on the patterned surface than on the smooth one. The cells are stained with Coomassie brilliant blue R-250.*

4.4 Conclusions

From the results obtained using the devices consisting of dense pillar arrays it is apparent that cells exhibit extremely poor adhesion to these structures. It is unclear as to why this phenomenon occurs, however there are several possibilities. It is likely that the reaction to the substrate topography is caused by a signalling system triggered by tyrosine phosphorylation. It is also possible that the cytoskeletal reaction and the phosphorylation are interrelated and can only form at a standard minimum spacing, perhaps due to the kinetics of polymerisation.

Secondly, it has been suggested that the cell is stretching itself between two or more points of attachment. Massia [18] stated that focal contacts can be as far apart as 140nm for fibroblast adhesion and spreading to develop. However other studies reviewed in this paper [18] suggest that minimum spacing between contact points must be between 10nm and 80nm for cell spreading, depending on the environmental conditions. Possibly the adhesion points, the focal contacts, are prepositioned and can only adhere at set intervals. This would suggest that there is a particular threshold spacing which the cell can detect.

Finally, Curtis [19] has suggested that cells may be their own scanning probe microscopes using the lamellipodium to identify the surrounding area.

It is clear that there is still a great deal of work required to understand the adhesion reaction of cells to different surfaces. The logical continuation from the tests presented here would appear to be to fabricate pillars of varying diameter and centre to centre spacing and observe cell adhesion to these surfaces. The reason for this being that it should be possible to uncover any relation between focal contact positioning and adhesion. Thus, if the adhesion points in a cell are prepositioned, an array of pillars of the correct dimensions should reveal this. It is also of interest to alternate patterned areas with smooth ones to see if it is possible to utilise this cell repulsion of rough areas to position the cells on a particular part of a surface.

4.5 References

[1] Curtis, A. S. G., Pitts, J. D., Cell Adhesion and Motility, Cambridge University Press, UK, 1980.

[2] Bellairs, R., Curtis, A. S. G., Dunn, G. A., Cell Behaviour, Cambridge University Press, UK, 1981.

[3] Curtis, A. S. G., Wilkinson, C. D. W., Topographical Control of Cell Migration, Motion Analysis of Living Cells, Wiley-Liss Inc., UK, 1998, 141-156.

[4] Harrison, R.G., On The Sterotropism Of Embryonic Cells. Science 1911;34:279.

[5] Curtis, A.S.G., Varde, M., control of cell behavior : topological factors, Journal of the National Cancer Institute, 1964, 33, 15.

[6] Curtis, A.S.G., Wilkinson, C.D.W., patent application U.S. 220413, Microstructures, 1983.

[7] Clark, P., Connolly, P., Curtis, A.S.G., Dow, J.A.T., Wilkinson, C.D.W., Topographical Control Of Cell Behaviour - I Simple Step-Cues. Research Development Biology 1987; 99: 439-448.

[8] Clark, P., Connolly, P., Curtis, A.S.G., Dow, J.A.T., Wilkinson, C.D.W., Topographical Control Of Cell Behaviour: II. Multiple Grooved Substrata. Development 1990; 108: 635-644.

[9] Clark P, Connolly P, Curtis A.S.G, Dow J.A.T, Wilkinson C.D.W. Cell Guidance In Ultrafine Topography in Vitro. Journal of Cell Science 1991; 99: 73-77.

[10] Wojciak, B., Crossan, J., Curtis, A. S. G., Wilkinson, C. D. W., Grooved substrata facilitate in-titro healing of completely divided flexor tendons, Journal Of Materials Science Materials In Medicine, vol. 6, pp. 266-271, 1995.

[11] Brunette, D.M., Kenner, G.S., Gould, T.R.L., Grooved titanium surfaces orient growth and migration of cells from human gingival explants, Journal of Dental Research, 1983, 62, 1045.

[12] Curtis, A.S.G., Clark, P., The effects of topographic and mechanical properties of materials on cell behaviour, Critical Reviews in Biocompatability, 1990, 5, 4, 343-362.

[13] Lydon, M.J., Clay, C.S., Substratum topography and cell traction on sulphuric acid treated bacteriological-grade plastic, Cell Biology Intl. Reps., 1985, 9, 911.

[14] Curtis, A.S.G., Forrester, J.V., McInnes, C., Lawrie, F., Adhesion of Cells to polystyrene Surfaces, Journal of cell Biology, 1983, 97,1500.

[15] Becker, W. M., et al., The World of the Cell, Third Edition, The Benjamin/Cummings Publishing Company Inc., USA, 1996.

[16] Alberts, B. et al., Molecular Biology of the Cell, Third Edition, Garland Publishing Inc., London UK, 1994.

[17] Karp, K., Cell and Molecular Biology : Concepts and Experiments, John Wiley and Sons Inc., New York, 1996.

[18] Massia, S. P., and Hubbell, J. A., An Rgd Spacing Of 440nm Is Sufficient For Integrin Alpha-V-Beta-3- Mediated Fibroblast Spreading and 140nm For Focal Contact and Stress Fiber Formation, Journal Of Cell Biology, vol. 114, pp. 1089-1100, 1991.

[19] Curtis, A. S. G., Macdonald, K., Wojciak-Stotard, B., Casey, B. G., Wilkinson, C. D. W., The Reaction of Cells to Nanometric Topography, To be published 1999.

Chapter 5

DNA Electrophoresis

By applying the fabrication techniques described in chapters 2 and 3, devices were fabricated to allow observation of DNA conformational changes during electrophoretic induced migration. This chapter details the biology and biochemistry of DNA and explains the biophysics of DNA migration during electrophoresis. Simple devices consisting of SiO_2 pillars were tested before focusing attention on a fractionation chamber which has all of the features proposed by the modelling to produce highly dispersive molecular mobilities. This new sequencing device was made using the embossing technique developed within the department and completed by applying a selective metalisation process to allow improved conduction [1]. The chamber was then sealed to produce a restrictive environment suitable for DNA visualisation using fluorescence microscopy. The results obtained using these SiO_2 and cellulose acetate flow chambers are presented here. Once the results from these devices had been considered, conclusions as to the function and operation of such devices are discussed. A plan for future work and chamber modifications are then detailed.

5.1 Basic DNA Biochemistry

The human body is made up of billions of individual cells, with DNA being the control centre of each of these biological building blocks. The DNA is stored in the form of several chromosomes which are arranged in homologous pairs thus producing a backup for the functional information contained within. Human cells contain 46 chromosomes in 22 homologous pairs plus the non-homologous X and Y chromosomes which determine sex.

DNA, or deoxyribose nucleic acid is a linear, unbranched polymer whose monomers are called nucleotides. Each nucleotide is composed of three parts : A:- a nitrogen containing base, B:- a five carbon sugar and C:- a phosphate group which can have one, two or three phosphates. In DNA the sugar present is deoxyribose and there are four options for the base. These are Adenine(A), Guanine(G), Cytosine(C) and Thymine(T). A structure of a standard nucleotide is shown in figure 55.

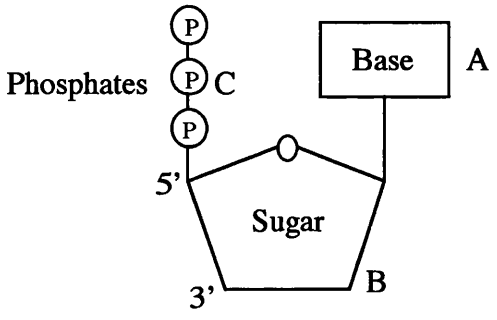

Figure 55. *General Structure of a nucleotide. The nucleotide may have 1,2 or 3 phosphates and the base can be Adenine, Guanine, Cytosine or Thymine. The 3' and 5' refer to specific carbon atoms which are involved in the polymerisation of the molecule.*

The nucleotide is the basic repeat unit of DNA and consists of a nitrogenous base covalently bound to the 1' carbon atom of the sugar. This nitrogenous base can be either a pyrimidine (cytosine or thymine), or a purine (adenine or guanine). When these nucleotides polymerise, the phosphate of one sugar on the 5' carbon atom links to a sugar on a second nucleotide via the 3' atom of that sugar. This type of bond is known as a phosphodiester bond. Due to this form of bonding in DNA there is a polymer backbone consisting of a repetitive sugar-phosphate-sugar pattern with the bases attached at the sides. This is represented schematically in figure 56.

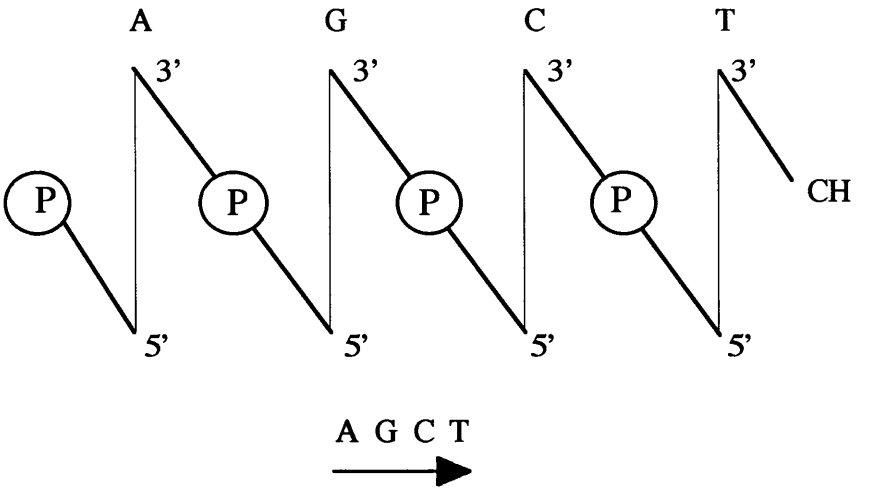

Figure 56. *Schematic representation of a polynucleotide chain. The figure shows the phosphodiester bond between the 3' carbon atom of one nucleotide and the 5' atom of another one. The base sequence is read as shown.*

The sugar-phosphate strand is polar due to the polarity of the phosphodiester bond and therefore the molecule is considered to have a 3' and a 5' end as shown in figure 56. The so-called 5' end has a terminal sugar which is not linked to a neighbouring sugar and the 3' end is defined by the absence of a phosphodiester bond on the 3' carbon atom of that end sugar. A full DNA molecule consists of two sugar phosphate backbones, like that shown in figure 56, running in opposite directions with the bases on the inside forming pairwise interactions which join the two strands weakly together by hydrogen bonding. This is known as the DNA duplex and is shown schematically in figure 57.

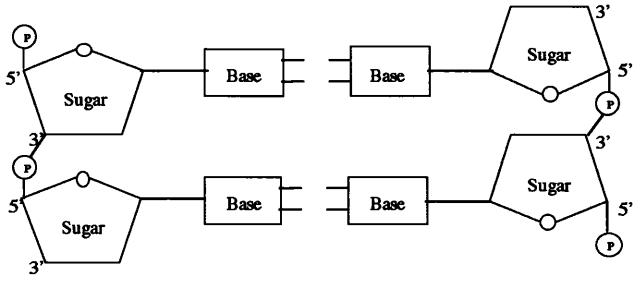

Figure 57. *Schematic representation of a DNA molecule showing two base pairs. The sugar - phosphate chains are antiparallel and enclose the bases which are held together by hydrogen bonds.*

The way in which the bases adhere together was solved in 1953 by James Watson and Francis Crick, whereby they produced a set of rules for base pairing. They said that the most stable pairings would be A-T and C-G, as shown in figure 58.

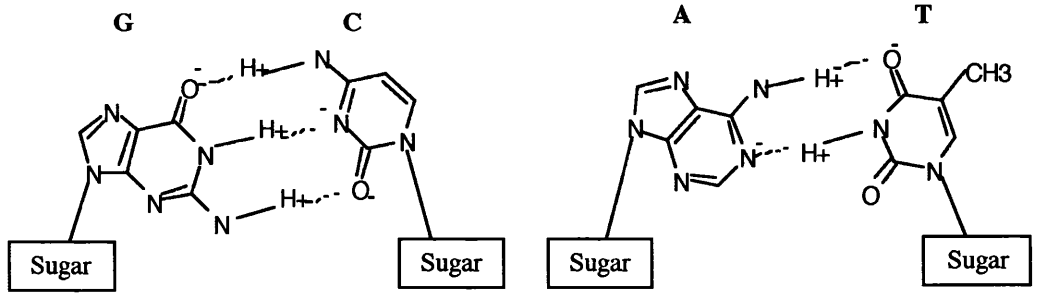

Figure 58. *Watson and Crick base pairings. The two figures above show the chemical bonding present between the bases A-T and C-G. Surplus charges responsible for the hydrogen bonding are also shown.*

The advantage of this set up, as opposed to Hoogsteen base-pairs[2], is that the four possible combinations A-T, T-A, C-G and G-C are all the same size, thus easily fitting in with the double helix geometry. However, the bonding can be explained chemically by considering that within a DNA base there is a small surplus of negative charge on oxygen and nitrogen atoms which are not attached to hydrogen atoms. Conversely, there is a small surplus of positive charge on these same atoms when they are attached to hydrogen. Thus, by considering the charges on each base it can be seen that the base pairings lend themselves well to the production of hydrogen bonds which in turn hold the duplex together.

In order to understand the physical shape and mechanics of DNA, it is necessary to consider the chemical constituents of the molecule. DNA consists of phosphates, sugars and bases chemically linked together in a particular way. Phosphates and sugars are soluble in water, however the base part of the molecule is hardly soluble. Adenine, guanine, cytosine and thymine are all hydrophobic molecules, however it has been shown that adenine dissolves in weak acid and that thymine dissolves in ammonia. This hydrophobicity of the bases is an extremely important factor in determining the conformation of the DNA molecule. Most of the volume within a cell is filled with water which has a neutral pH and therefore will not present a suitable environment for the bases. Therefore, in order for the molecule to be stable within the cell, the bases have to be hidden away within the centre of some form of folded structure so as to be out of

contact from the water. The sugar and the phosphates would thus be on the outside acting as a shield for the bases.

It has been shown that adjacent sugars within the DNA chain are 0.6nm apart and that the thickness of a single DNA base is 0.33nm. This suggests that there is a space of 0.27nm between the bases which cannot be filled with water due to their hydrophobicity but must be filled with something otherwise there would be a vacuum. Thus, the bases are attached to a sugar-phosphate chain which is twice as long as the thickness of the bases themselves.

This space between the bases can be removed if instead of considering the duplex as a simple ladder like structure as in figure 57, we have a skewed ladder as in figure 59. This would in fact would remove the spaces, however such a conformation would lead to unacceptably close contact between neighbouring atoms.

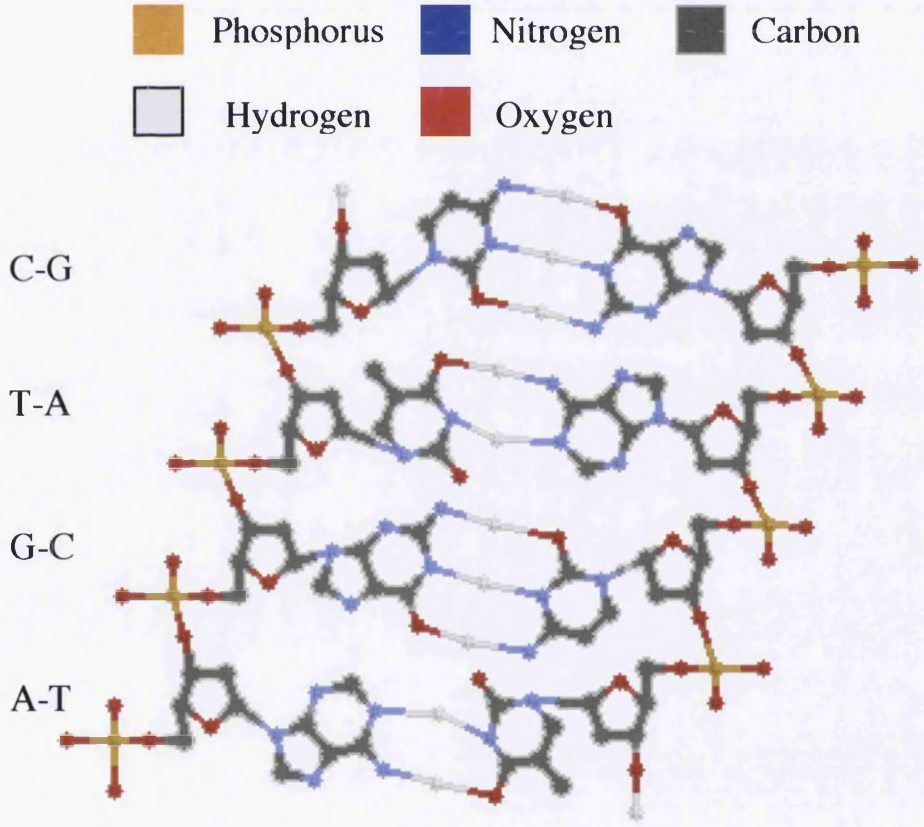

Figure 59. *Atomic representation of a skewed DNA ladder showing base hydrogen bonding drawn using ISIS/Draw. In order to remove the spaces between the bases completely the angle of tilt should be 30 degrees. The base pairings are shown on the left hand side of the figure.*

This is overcome in nature by the DNA strands rotating such a skewed ladder round an imaginary vertical axis, thus leading to the spiral or helix shape. It is therefore in its attempt to maintain a stable chemical structure that the DNA strands wind into their famous helix shape as shown in figure 60 below.

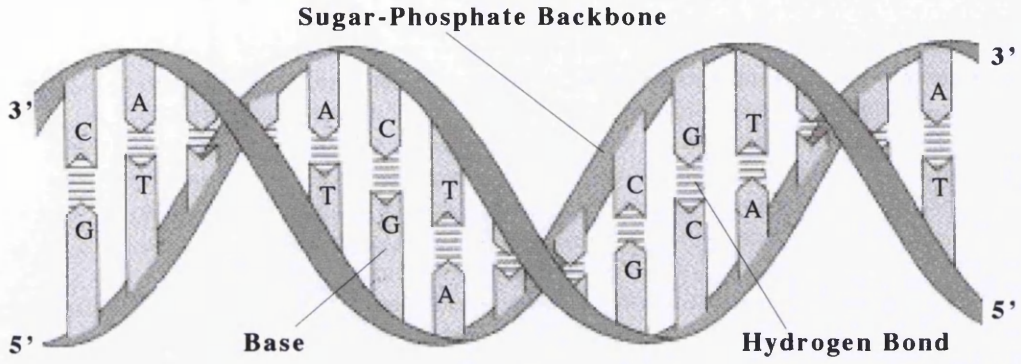

***Figure 60**. DNA helix showing the bases and the sugar-phosphate backbone [18].*

It has been found that almost all DNA double helices have between 10 and 12 phosphates per turn of helix. Research has also shown that in nature most duplexes are right handed in order to satisfy chemical constraints within the structure, such as bonding distances. It is for this reason also that the two strands of the duplex are antiparallel. Thus, by considering chemical structure and molecular separations it has been shown that the most common structure for DNA is a right handed helix with 11 phosphates per turn.

The DNA strand length is measured by the number of bases in the molecule and at present the size limit for fractionation in a gel using constant field electrophoresis is 50 kilobase pairs. The reason for this constraint is non-trivial and an explanation of the biophysics relating to it can be found in §5.2.1 of this thesis. In the polymer chain the sequence of bases is variable, and it is the order of these bases which is the concern of DNA sequencing.

The final point for consideration in this section is : what happens to DNA when it is stained for visualisation? In the work presented in chapter 5 of this thesis the DNA is stained with a substance called ethidium bromide (EtBr). EtBr fluoresces a bright red-pink colour when it is exposed to ultra-violet light and is therefore used to visualise DNA motion in conjunction with fluorescence microscopy. Ethidium bromide is a hydrophobic molecule which escapes from solution by intercalating into the

DNA. Essentially this means that the molecule inserts itself between neighbouring base pairs as shown in figure 61.

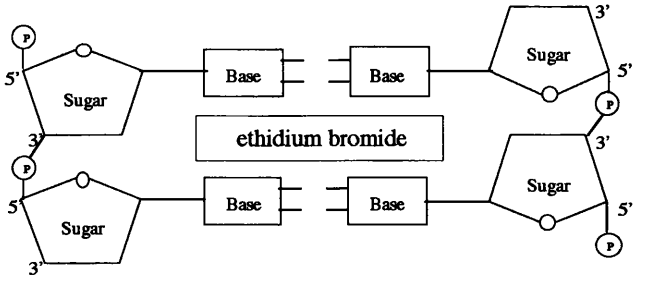

Figure 61. *Ethidium Bromide molecule intercalated between two sets of base pairs. In order for the intercalation of the EtBr molecule, the duplex chain must unwind locally at the point of insertion.*

In order for this to happen the DNA duplex must experience localised unwinding of the chains. Therefore, intercalated EtBr will cause length changes in the DNA molecule since the helix will become largely unwound producing a simple ladder type formation as shown in figure 57. It is the flexibility of the sugar - phosphate chains which allow them to change from spiral to straight ladder, and it is this flexibility which allows DNA to form various conformation when under the influence of an electric field and a retarding medium. Further, it is the size change caused by intercalation which is of great concern when designing retarding geometries for fractionation chambers and this problem will be discussed later in chapter 5.

5.2 Sequencing DNA

However difficult and complex it may appear to chart DNA due to the strand lengths involved and the large number of bases concerned, there is a standard procedure which is capable of doing so for relatively small strand lengths and which has been advanced by Maxam and Gilbert [3]. This method uses gel fractionation and is shown schematically in figure 62 (see over). The method involves labelling the 3' ends of DNA with radioactive phosphorous ^{32}P, and then separating the double strand into two single strands. Only one of the strands is kept and care is taken to ensure that it is the same strand for all the molecules being used. This produces a population of identical strands all labelled on the same end, which is then divided into four samples each of which is subjected to a different enzyme that destroys one or two specific bases. The first reagent destroys only guanine, the second adenine and guanine, the third thymine and cytosine and the fourth reagent destroys only cytosine. The loss of a base makes the sugar-phosphate backbone more likely to break at that point. However, the reagent concentrations are adjusted so that only one in fifty of the target bases are destroyed, thus resulting in a mixture of different sized pieces carrying the ^{32}P label (or a fluorescent label). The gel acts as a retarding medium for the DNA and has a length separation effect since big molecules travel with slower velocities than smaller molecules. When these molecular strands are separated in the different lanes of a gel, they can be arranged in order of length and the destroyed base at each site can be determined by noting in which lane or lanes the band appears. Thus the sequence of the bases in the strand can be quite simply read from the pattern of bands in the gel.

The biophysical reasons for this separation effect are detailed in the next two sections of this chapter and a detailed account of the present understanding of the electrophoretic induced migration which is used for sequencing the genetic code contained within the strands is described. Initially the molecular conformations induced under the application of an electric field are discussed. These motions are then reconsidered for the scenario whereby a retarding medium of some form is placed in the path of the migrating DNA. Following on from these considerations a model system is presented which describes the optimal conformation for length retardation and therefore fractionation of biological molecules of this type. Therefore, by comparing the biological conformations and the migrating environment it is possible to develop a system capable of sequencing the genes contained within the DNA strands.

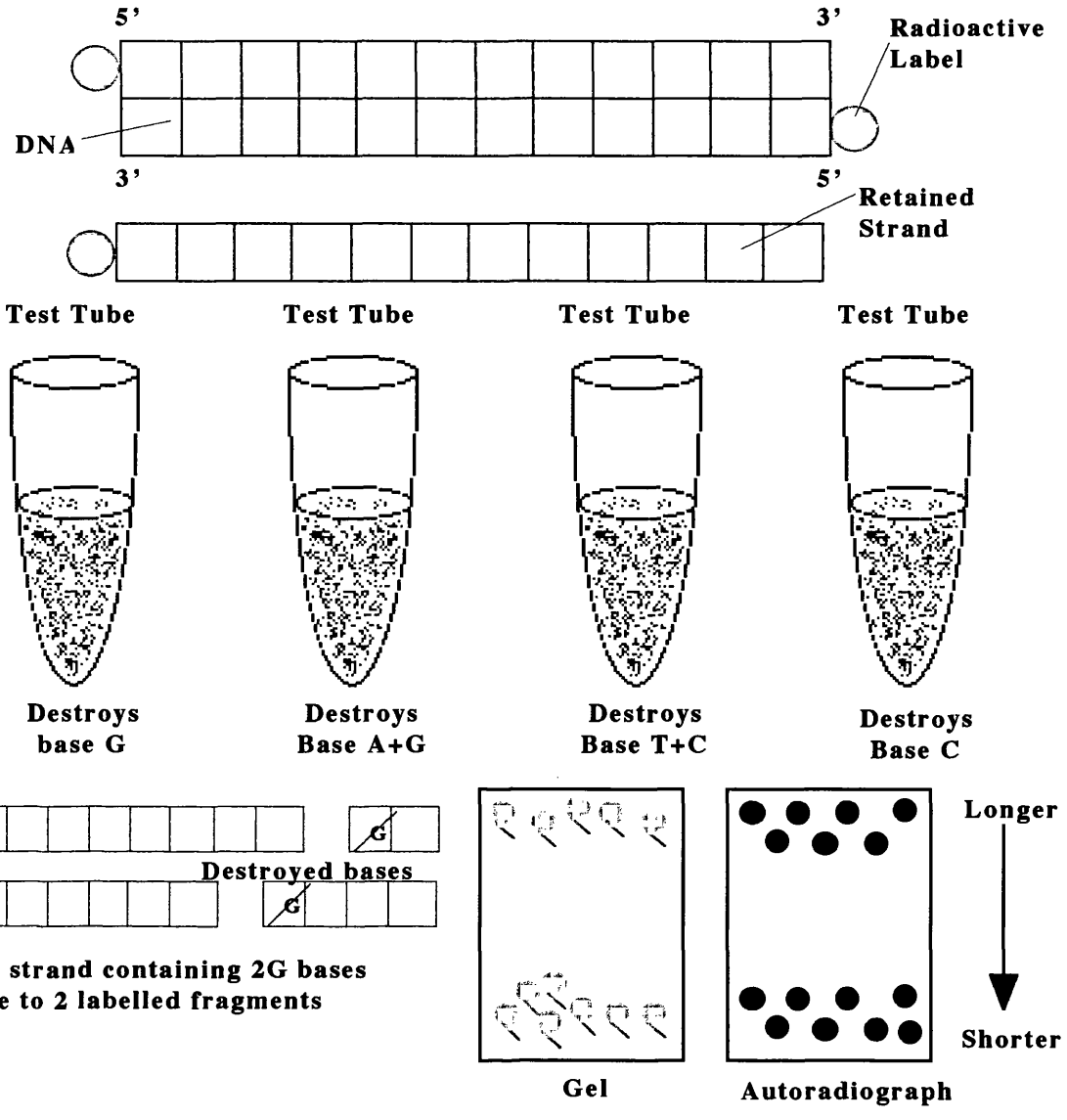

Fragments are separated in a gel and then identified by autoradiography

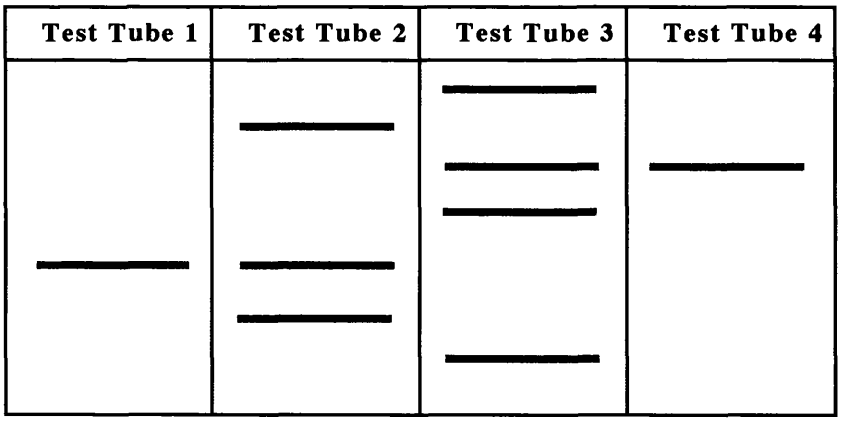

Destroyed Base	
T	1
A	2
C	3
T	4
G	5
A	6
T	7

Comparison of the bands produced by the labelled fragments allow calculation of the base sequence.

Sequence of the bases in the above DNA is :

T	A	G	T	C	A	T

Figure 62. *Gel Electrophoresis Procedure for Sequencing DNA [3]*

5.2.1 DNA Behaviour during Electrophoretic Migration

The mobility of DNA in free solution under the influence of an electric field is molecular size independent and given by

$$\mu_o = Q/\zeta \qquad (1)$$

where μ_o is the mobility of DNA in free solution, Q is the total electric charge and ζ is the friction coefficient of the DNA molecule. However this is not the case if electrophoresis is carried out in the presence of a gel. As already mentioned gel electrophoresis can be performed in either polyacrylamide or agarose gel and both methods are very similar. Agarose is capable of fractionation of stand lengths from 100bp(basepairs) to 50kbp in the presence of a constant electric field and polyacrylamide can separate lengths from 10bp - 2kbp. Either gel can be used to separate strands with a length difference of only 1bp. This length resolution depends mainly on the pore size of the retarding medium and the molecular size of the DNA. These gels are very porous materials and it is possible for substances to travel through the entire length of the gel by passing through these holes. For separating DNA the gel is placed in a buffer solution and a sample of strand lengths is loaded into small wells in the gel. The buffer used, usually a Tris buffer, has a pH of approximately 8 and in these alkali conditions the DNA has a net negative charge. The charge responsible for the migration of the DNA in an electric field is known as the electrokinetic charge and is the total charge of the sugar-phosphate backbone plus non-specifically bound counterions, charged molecules bound at specific sites on the strand and the charge of intercalated dye molecules. As a general guide this gives the molecule a charge in the region of $2e^-$ per base pair, therefore if a potential is applied across the gel the DNA duplex will migrate towards the positive anode. As the strands move through the gel they get caught on the solid parts of the agarose between the holes and therefore the gel retards the migration of the molecules. The long strands have greater difficulty passing through the holes, while short molecules can pass faster and more freely. Thus, it is possible to observe the strands separating due to their different rates of travel through the gel.

The DNA conformation which facilitates this form of fractionation is known as random walk and is shown in figure 63.

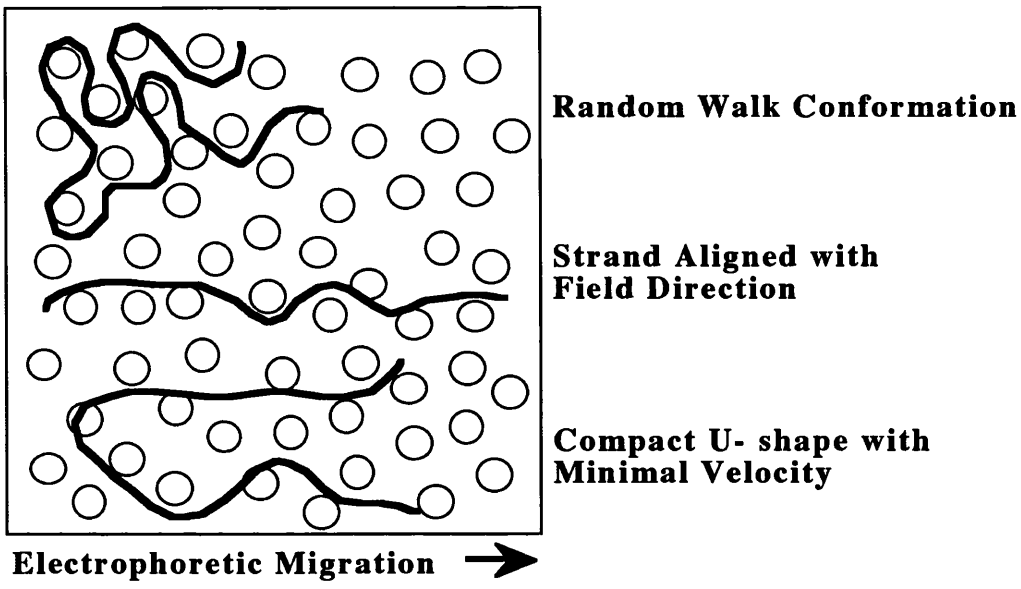

Figure 63. Conformations of migrating DNA strands under various field conditions.

In solution or a low concentration gel, DNA molecules have a random walk conformation with a radius of gyration given by

$$R_g^2 = 1/3\ pL\ [\ 1\text{-}p/L + p/L \exp(-L/p)] \qquad (2)$$

where L is the contour length of the molecule and p is the persistence length. It has been shown that for small L, where $L>>p$ and $R_g \leq a$, where a is the average pore size of the gel, that

$$\mu/\mu_o \cong \exp[-(R_g/a)^2] \qquad (3)$$

μ is the mobility and μ_o is the mobility in free soln. This form of migration is known as Ogston Sieving[4] since the globular DNA is smaller than the average pore size and therefore the gel sieves the molecules as they migrate. Related theory can also be found in references [5][6] and [7]. Equation 3 predicts the mobility relation that is required for good quality fractionation, namely

$$\mu/\mu_o \sim 1/L \qquad (4)$$

However, equations 3 and 4 do not hold for DNA strands longer than 50kbp because the relation $R_g \leq a$ is no longer true. Therefore in order for these molecules to move through the gel a great deal of molecular deformation is required and the mobility

reaches a constant value irrespective of molecular size. The conformation responsible for such mobilities can be seen in the two lower formation shown in figure 63. This mobility problem leads onto the theory of molecular reptation through the gel pores which is the principle used for long strand fractionation in agarose. This has been shown experimentally by Noolandi [8] and Deutch [9] and theoretically by Duke and Viovy [10] and [11].

In the reptation model the migrating DNA strand is considered to be contained within a tube defined by the molecule's path through the gel obstacles, as shown in figure 64.

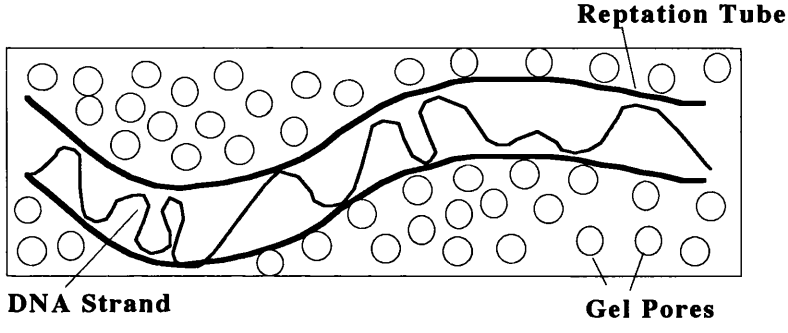

Figure 64. *Schematic representation of a DNA strand confined within a reptative tube.*

The motion of the chain between obstacles is assumed to be similar to that of the section in front and eventually the molecule may be considered as a primitive chain made up of N-1 freely jointed primitive segments each of length a. This model essentially describes the duplex as a bead-spring chain moving in a confined environment in the direction of the field. This model can be extended further by considering the biased reptation model which neglects variations in spring lengths, thus assuming that $a_i(t) = a$ for all times t. This model is the most useful for considering continuous field electrophoresis and can be defined as follows.

If each pore contains the same contour length of DNA then the force on the molecule can be written

$$F_1 = qEh_x/a \qquad (5)$$

where $h_x = a\sum u_{ix}$ is the end to end distance of the molecule in the field direction. For a molecule of fixed length migrating through the tube, the friction coefficient ζ is proportional to the length where $\zeta = \zeta_o L$ and ζ_o is the friction coefficient per unit length. From this the instantaneous velocity along the tube is

$$v_1 = F_1/\zeta = (qE/\zeta)(h_x/a) \qquad (6)$$

The electrophoretic mobility is then given by

$$\mu = \langle v_1(h_x/L)\rangle/E = \mu_o\langle(h_x)^2\rangle/L^2 \qquad (7)$$

The <..> brackets represent an average over a large number of identical chains at a given time. Equation 7 shows that the electrophoretic mobility is proportional to the average of the end to end vector and it can be seen that for small molecules or small electric fields the DNA migrates in the random walk conformation. This is reptation without stretching and gives the result that $\langle(h_x)^2\rangle \propto L$ which leads to the expected relation $\mu \propto 1/L$. However if the field or the molecules are large then stretching occurs and the relation $\langle(h_x)^2\rangle \propto L^2$ holds. This gives the relation $\mu \propto L^0$ = constant and therefore the mobility is independent of length.

This means that for stretched molecules the electric force and the opposing friction scale with the length, so that the mobility is determined by the force per unit length which is itself independent of the actual length.

5.2.2 Theory of Nanofabricated Media for Electrophoresis

The physical explanation of DNA migration in gels has long been an area of biophysical research [12][13][14][15]. However, it is only recently that there has been any work into DNA molecular conformations during interaction with nanofabricated environments or single obstacles [16][17].

The microscopic observation of DNA migrating under the influence of an electric field and in the presence of a retarding medium has shown that the motion is governed by a solitary dominant obstacle. Therefore, by considering this scenario, it is possible to calculate the preferred migration path for a molecular strand and to postulate a suitable retarding geometry.

Firstly, let us consider the dimensions of a DNA strand in an open lattice. The molecule may be considered as a chain containing N segments. The Kuhn length (twice the persistence length) is represented by b and is approximately 1.5nm. In its random walk conformation the strand is at equilibrium and has a size given by

$$R \sim bN^{3/5} \qquad (8)$$

which is smaller than the overall contour length

$$L = bN \tag{9}$$

By considering these dimensions and assuming that the charge per Kuhn segment is q= -1, the mobility of the strand in free solution is

$$\mu_0 = q/\zeta \tag{10}$$

where ζ the fluid friction acting on the polymer. From this, it has been shown that under the influence of an electric field E, the migration velocity of the DNA is

$$v_0 = \mu_0 E \tag{11}$$

When a DNA strand migrates through a retarding lattice, the actual molecular conformation is controlled by the obstacle size *u*, and the strength of the field relative to some control value

$$E^* = (u/b)^3 E_0 \tag{12}$$

In the instance of a weak field ($E<E^*$) and for the condition $R<u$, the molecules are sieved according to their size thus giving dispersive mobilities. However, for fields larger than the critical value and for long strand lengths where $R>u$, the molecules reptate and form U shapes which have minimal velocity as in the case for gel electrophoresis. Therefore, no length fractionation occurs for this set of conditions.

With this in mind, it thus essential when designing a nanofabricated lattice to consider obstacle size, separation and the overall device dimensions. For an array of fabricated posts with diameters of 500nm the DNA migrational motion is repetitious and, as stated earlier, is controlled by a single obstacle. During a strand's movement through the lattice it collides with pillars resulting in a U shaped conformation. However, due to the randomness of these interactions the arm lengths of the U are predominantly different in size and therefore the longer arm experiences a greater force. Due to this occurrence, the strand simply slides round the obstacle and disengages after a period of being hooked. The unhooking time in such a case is controlled by the ratio of left arm length to right arm length. Therefore this retarding regime does not allow for high resolution fractionation, although it does give insight into useful array features to exploit hooking to its fullest. It is this unhooking time which is the key to producing nanofabricated arrays capable of producing length dependent fractionations and thus it is this parameter which must be considered in detail.

An array of pillars is a very useful topography to observe DNA conformations during migration but in itself is a poor medium for length separations. When designing a useful lattice feature we must consider the migrational conformations that we require the DNA to exhibit. Firstly, we want the molecules to interact with the fabricated features. Therefore, if the separation between features is x, then the probability that a strand with random walk coil size R interacts with an obstacle in the array is

$$p_{collision} \sim R/x \tag{13}$$

In order to maximise the probability of hooking, the inter-obstacle distance in the axis perpendicular to the field direction should be equal to the coil size of the largest strand in the electrophoresis sample. This size choice also minimises the possibility of a DNA molecule being caught on more than one obstacle at a time.

In contrast to this, the separation of obstacles in the direction parallel to the electric field lines should be greater than the largest coil size. The reason for this is that in order for each row of obstacles to perform its task, the DNA strand which has undergone deformation by one feature must be allowed to return to its random walk before it has another interaction. In addition to this, the field strength and shape between rows of features is critical to allow the re-establishment of random walk conformations which in turn produce highly dispersive mobilities. Thus, after hooking in our devices, the molecule extends a distance past the feature given by

$$d \sim Nb - w \tag{14}$$

where w is the obstacle width.

After disengaging the molecule returns to its original conformation in a time Tr (relaxation time). This time is controlled by two main phenomena. Firstly, the time associated with the Brownian motion of a strand length b, which is given by

$$\tau = \zeta b^2 / kT \tag{15}$$

The second important consideration is the field strength where the thermal forces acting on the same length b become of comparable size to the electric forces [11][15], as shown by

$$E_0 = kT/qb \tag{16}$$

Ignoring hydrodynamic interactions this gives

$$T_R = \tau N^2 / 3\pi^2 \tag{17}$$

From this it can be seen that it is extremely important to design a fractionating array which has a low field strength between rows of obstacles. It is thus a combination of row separation and field pattern which control the strand shape between retarding interactions and which are the critical parameters when fabricating a retarding medium.

Assuming that these fabricated obstacles have a purely physical interaction with the DNA strands, then the relation below holds

$$v_o T_R \sim Nb \tag{18}$$

Equation 18 shows that the relaxation time is length dependent and therefore these electrophoresis conditions should produce suitable molecular motions for length separation. However, the strand motion depends greatly on the obstacle shape and whether it has more than a purely physical interaction with the molecule as discussed in chapter 2.

Finally, the array size is dependent on strand length, field strength and assay size. However as a rough guideline the lattice length required is similar to the gel length required for capillary electrophoresis. For most purposes this length is approximately 5mm.

Once a nanofabricated retarding medium has been made it is necessary to observe the DNA conformational changes during migration using some form of microscopy. The technique used throughout the course of this work is fluorescent microscopy and this is the subject addressed in the following section.

5.3 DNA Staining and Visualisation

Fluorescent dyes absorb light at one wavelength and emit light at a longer wavelength. If the dye is illuminated at its excitation wavelength then it will emit at its emission wavelength. Therefore, when the illuminated dye is viewed through a beam splitting mirror , which allows only the longer wavelength to pass through, then it is possible to see the fluorescent molecules against a dark background. This can be accomplished using a fluorescence microscope as explained in figure 65 below.

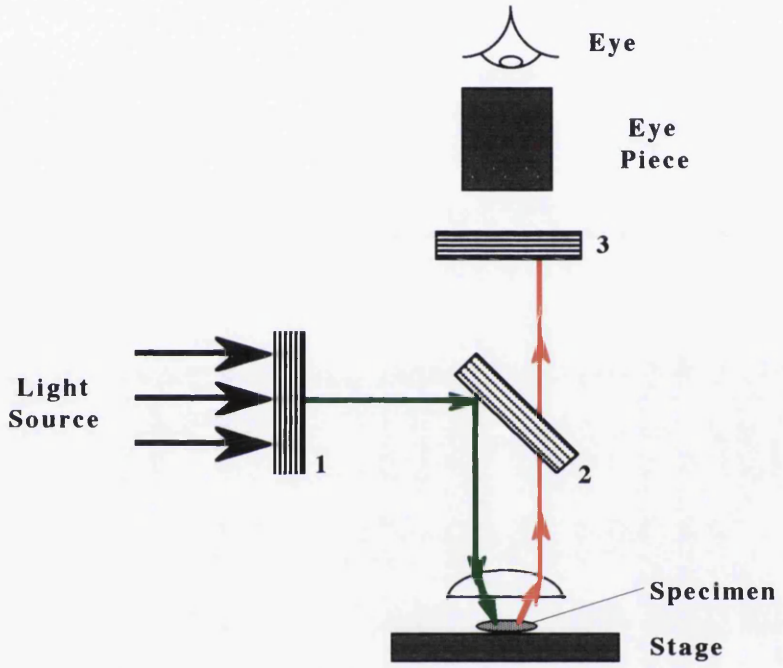

Figure 65. *Optical elements of a fluorescence microscope. 1: First Barrier Filter. This filter only allows the transmission of light of the correct wavelength to excite the fluorescent dye. 2: Beam-Splitting Mirror (Dichroic Mirror). This mirror reflects all light waves below a specified wavelength. The actual cut-off wavelength depends on the specific system being used. 3: Second Barrier Filter. This filter only allows transmission of the light emitted from the excited fluorophore. The UV light source is a Mercury lamp. The dye used in these experiments is Ethidium Bromide which emits a deep red colour when excited by green light.*

A Nikon Microphot microscope is used in these electrophoresis experiments to observe the fluorescently stained DNA. This microscope has high numerical aperture objective lenses which allow the observation of a bright image with good resolution at the

expense of a short working distance and small depth of field. The visualisation procedures were modified from references [18][19][20] and [21]. The samples of DNA used are highly purified Micrococcus Luteus (Sigma Chemical Ultra-pure) which are of uniform length 145kbp or 96×10^6 daltons. A number of different loading dye methods were tried but it was found that the best procedure is to add 2ml of Tris-borate buffer to 0.05mg of DNA and then add 0.1 ml of the fluorescent stain Ethidium Bromide at a concentration of 500μg/ml. This sample is then left in darkness overnight before being dialysed against the Tris buffer at a pH of 8. This procedure allows the removal of unbound dye molecules thus minimising the amount of background fluorescence from the sample. Ethidium Bromide has a maximum excitation wavelength of 524nm and a maximum emission wavelength of 584nm and quenching of its fluorescence is greatly reduced by adding 1% DABCO (1,4-Diazabicyclo[2.2.2]octane). DNA stained using this method is placed in the loading area of the silicon sample using a syringe before applying an electric field of 1V/cm.

When fluorescent observations were made using the SYTO and DAPI dyes, the relevant filter blocks for each dye were used[28][29].

5.4 DNA Conformations in Nanofabricated Lattices

Using a silicon dioxide flow chamber and the electrophoresis set up described previously, DNA migration was observed using fluorescent microscopy. It was found that it is possible to observe DNA being hooked on pillars before sliding off. Two photographs of migrating DNA molecules are shown below in figures 66 and 67.

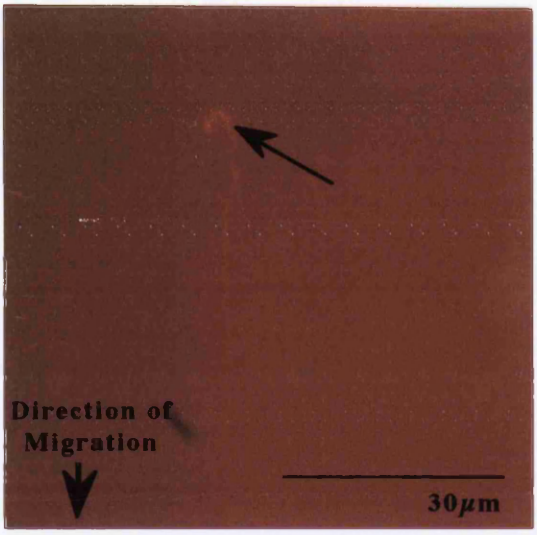

Figure 66. *Photograph shows a single DNA strand hooked on a 500nm diameter post. The strand segment can be seen to be slipping off the right hand side of the pillar and is reptating through the array. At this point the strand is being stretched to its full contour length since the unhooked end is travelling with a much greater velocity than the hooked section. This type of motion is in good agreement with that described by the theory in sections 5.2.1 and 5.2.2 of this thesis.*

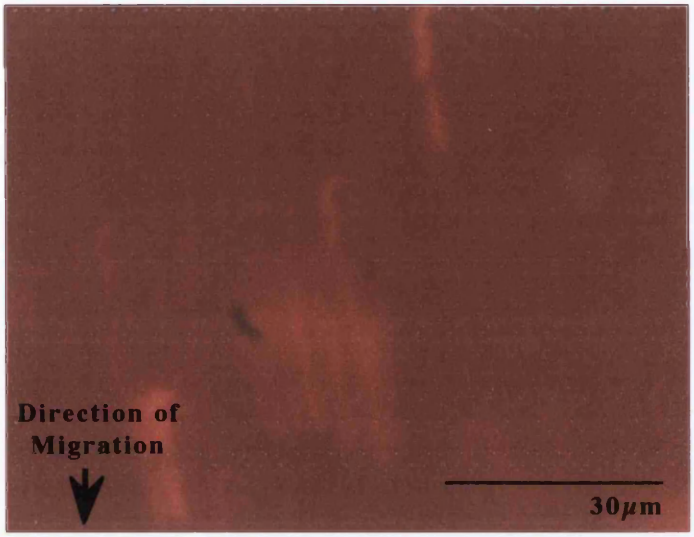

Figure 67. *This photograph shows several 30μm long DNA strands migrating through an array of 500nm diameter pillars. The back section, or top in the photograph, of the DNA strand appears slightly brighter than the front. This is because the back section travels with a greater velocity than the front, since it merely follows the front and has little interaction with the pillars. This is a common phenomena during reptative motion and is known as bunching.*

The results obtained using the silicon dioxide pillar samples were as expected. The DNA molecules migrate in a reptative motion and become hooked on the posts. This is the same type of motion which strands of this size (30μm) exhibit within a gel. This is encouraging since it shows that the theoretical motion explained in §5.2.1 holds true and that it is indeed possible to fabricate retarding media which have the same effect on DNA molecules as gel fibres. Therefore, by considering these results and the theory of electrophoretic migration within a nanofabricated lattice, as explained in §5.2.2, a new obstacle must be designed which will produce a non-reptative motion for long DNA strands.

5.5 Requirements for an Advanced Fractionating Chamber

The requirements for an advanced fractionation chamber are that it should produce dispersive mobilities for a variety of polymer lengths, should be cheap, easy to use and allow a constant field to pass through the bulk of the retarding environment. As explained in §5.2, it is essential that the chamber in conjunction with the electric field allow the DNA strands to migrate in their random walk conformation thus keeping reptation to a minimum.

The results obtained using simple pillar structures fabricated in SiO_2 showed that such obstacles caused the long molecular strands to migrate in the same reptative way as in a gel. To overcome this problem a new feature geometry had to be designed. The feature shape chosen was a simple 'U'. Concurrently, Volkmuth et al.[22] chose a 'V' shape to continue their exploration of molecular fractionation in microfabricated lattices. Both of these structures fractionate DNA in the opposite way to gels, i.e. long strands migrate faster than shorter ones. This is because shorter polymers have a longer escape time as they move through the array and so the electrophoretic mobility of the DNA increases with length. Devices with these features were fabricated and modelled simultaneously to observe their effectiveness for length fractionation of long chain DNA molecules.

The mobility in the obstacle courses is given by the simple scaling theory

$$\mu/\mu_o = N/(N^*+N) \qquad (1)$$

where N is the number of Kuhn segments and one Kuhn random flight length is equal to two persistence lengths. N^* is the resolution limit and depends on the electrostatic potential of the 'V', as described by Volkmuth[23].

Initially, the devices which utilise these features were fabricated in SiO_2 using the same fabrication processes as those used for producing the pillars. However, it was found that these devices did not work. The reason for this is that during the electrophoresis the field lines do not pass through the obstacle but instead fringe round, therefore forcing the DNA past the trap. To remedy this, it was decided that metal features should be fabricated which have less effect on the field. After considering several fabrication procedures to make such devices, metal coating of embossed features was chosen as the optimal process. These devices were fabricated using the processes described in §3.6.1 and §3.6.2 and consisted of 'U' shaped features. These devices are more sparse than the pillar arrays and therefore more suitable for large DNA. The type of DNA used here and the staining methods used for these samples are the topics discussed in the following section.

5.6 DNA Handling Procedures

The DNA used to test the cellulose acetate fractionating chamber is pulsed field marker DNA. This is DNA from chromosomes of Saccharomyces Cervisiae and consists of a number of strand lengths from 225 - 2200 kilo bases. The DNA is supplied by Sigma Chemical and comes in an agarose gel plug. Therefore, before use the DNA is removed from the plug by ultra centrifugation and ethanol precipitation before being made into 20μL aliquots in buffer. DNA of this length can only be sequenced conventionally using pulsed field electrophoresis with a gel [24]. Therefore, it is ideal to test the fidelity of the cellulose acetate device. By considering the theory of DNA migration and the modelling of the retarding medium it is thought that the nanofabricated array should be capable of separating DNA of this size using a constant field.

In order to visualise the DNA, fluorescence microscopy is again used [25][26]. The DNA is made up in the Tris-borate electrophoresis buffer. The buffer having been previously made up into a working solution which is composed of 89mM Tris-borate, 89mM Boric acid and 2mM EDTA (Ethylenediaminetetraacetic acid). The fluorescent stain used is ethidium bromide at a concentration of 50μg/ml. From Figures 68 and 69 in §5.4 it can be seen that using ethidium bromide as the stain produces a great deal of background fluorescence. This makes observation of the DNA extremely difficult. Therefore, two other stains were tested to see if the DNA visualisation could be improved.

Firstly a fluorescent dye called DAPI (4',6-diamidino-2-phenylindole) was used [27]. This was added to the DNA at a variety of concentrations ranging from 1μg/ml to 5μg/ml. Using this stain very little could be observed using fluorescent microscopy on our Nikon Microphot microscope. Therefore, another group of probes were tested. These probes are supplied by Molecular Probes and are called SYTO green fluorescent nucleic acid stains [28][29]. The SYTO dyes are cell-permeant DNA stains that differ from each other by one or more characteristic such as cell permeability or fluorescent enhancement. From this family of dyes two in particular are of interest in our application. These are SYTO 12 and SYTO 16. These stains exhibit large fluorescent enhancement upon binding to nucleic acids and can be viewed with a fluorescent microscope equipped with a standard fluorescein filter set. When bound to DNA SYTO 12 and SYTO 16 absorb at 499nm and 488nm and emit at 522nm and 494nm respectively. The stains are supplied as solutions in dimethylsulfoxide(DMSO) at a concentration of 1mM. The dyes are added to the marker DNA at concentrations between 10nM and 1μM. The samples were vortexed and incubated for 2 hours. It was

found that the optimal stain was SYTO 16 at a concentration of 50nM. However, this dye bleaches extremely quickly and allows only 20s visualisation before the molecule completely disappears. This problem could not be overcome by the addition of bleaching agents.

Staining and visualisation of single strand DNA is an extremely difficult task and requires a microscope with good optics and image capture capabilities as well as a molecular dye which fluoresces brightly but exhibits little background fluorescence and slow bleaching. During the course of this work it has been found that finding a dye with all of these characteristics is difficult. The most promising are the SYTO dyes, however these fade very quickly. It is possible that this problem arises in our experimental set up because we are using the dyes for a purpose different from the one that they were designed for. The SYTO probes are inter cellular dyes designed to stain the nucleus of live cells and are therefore optimised for this process. The other problem which arises from the DNA staining protocol is that it is possible to have an aliquot which contains little or no DNA. This is an unavoidable problem brought about by the necessity to remove the DNA from its agarose plug. This is the only way in which such DNA is supplied and means that there is large scope for molecular shearing or loss during the centrifugation and ethanol precipitation.

There is a lot of work required to develop an effective protocol for staining and visualising large single strand DNA molecules using our experimental set up. There are several modifications and options to improve the current process which will be discussed in §5.8.

5.7 Cellulose Acetate Electrophoresis

Using the fluorescent stains described in the previous section, electrophoresis was performed using the cellulose acetate fractionating chambers. It was hoped that using these devices it would be possible to observe single DNA strand conformations as they migrate through the retarding medium and compare these conformations with those predicted by the theory and the modelling. However this proved to be extremely difficult.

Using ethidium bromide and DAPI the background fluorescence made observation of the DNA strands almost impossible. It is possible to see the molecules migrating using fluorescence microscopy, but it is very faint and impossible to image.

By changing the dye to one of the more selective SYTO stains it is easier to see the DNA strands since there is no background fluorescence. However, these dyes bleach very quickly and allow only a short period of imaging time. This makes photographing or image capture impossible and does not allow any observation of the molecular migration.

As in the previous section there is also the problem that some sample aliquots tested contain little or badly sheared DNA which makes it very small and hard to image. Due to these imaging and molecular damaging problems few results have been obtained using the cellulose acetate flow chamber in the time available. It is felt that it should be possible to improve this situation and produce a working device but that either a better stain should be found or a different approach to the experimental set up is required. This will be discussed in the following section.

5.8 Conclusions

With pressure and interest mounting in the Human Genome Project it is essential that novel and successful processes be developed to increase the rate of genomic sequencing [30]. The approach taken during the course of this work was to design and fabricate a nanotextured substrate to act as a retarding medium during electrophoretic induced DNA molecular migration. The medium was designed with careful consideration of the theoretical response that DNA would have to such an open lattice and by modelling of the electrophoretic environment. The electrophoresis flow chamber was then fabricated using nano-embossing and sealed and mounted ready for use. The DNA was stained and fluorescence microscopy used to observe the molecular conformations during electrically induced motion. This is the point where the problems arose.

Using a variety of fluorescent dyes it was found that it was extremely difficult to visualise the molecules for any length of time or with any acceptable resolution. Within the time constraints of the project this problem was not resolved and few results were obtained to confirm or disprove the retarding medium design. By consultation with more experienced researchers in the field of fluorescence microscopy and by comparison with other work in this field [31] it has been concluded that observation of single DNA strands randomly positioned and oriented is, to say the least, difficult. However, with a view to future work, there are options which could alleviate the problems faced during the fluorescent observation section of this project.

The main problem with the current experimental set up is that it relies on the ability to image individual DNA strands. There is, however, a very good reason why the system was designed like this. In order to understand the molecular migrational conformations and the function of the chamber it is necessary to be able to compare the experimental motion of a molecule with the theoretical response and with the environments modelled effect on the motion. If this form of observation is to be pursued there are two problems to be addressed. Firstly, a usable dye must be found which allows visualisation of single molecules for a relatively long period and with minimum adverse fluorescent effects. At present, Molecular Probes produce a huge number of dyes, such as YOYO and TOTO, some of which are reportedly capable of producing good quality images with single stranded DNA molecules [28]. However, these dyes are expensive and would require a great deal of characterisation to optimise them for this application. It is felt, however, that this could be time and money well spent if it produces acceptable resolution and observational characteristics for the large DNA molecules under investigation in this thesis. The molecular staining is the most important aspect of this

work which needs to be addressed. The choice of polymer sample is also of great importance. Cellulose acetate may not be the best choice of substrate due to its chemical and autofluorescent properties. This material was chosen as a demonstrator since it has a history in electrophoresis, albeit in proteins. Consideration should be given to surface chemistry, autofluorescence, pH, rugosity, surface charge, water absorption and hydrophobicity or hydrophilicity when choosing a suitable material. It is felt that the fluorescence experiments could therefore be improved by a more selective choice of polymer substrate. This choice of polymer is intrinsic to the operation of the fractionating chamber, however an alternative experimental set up is possible which could reduce the need for such a high quality fluorescent dyes.

With hind sight it may have been useful to produce a device with comparable dimensions to a standard electrophoresis gel. That is approximately 15cm long and 7cm wide. With a retarding medium of this size it would not be necessary to observe individual strands but instead one could view size bands as in a normal gel. A device like this would not allow direct observation of the migration and would therefore not facilitate comparison of experimental migration with theoretical motion. This would, however, at least allow some form of conclusion to be made as to the operation of the chamber on a macroscopic scale. The difficulty with an artificial gel like this is that we do not have the capability of producing such a device at Glasgow. However, as a line of work to run along side improving staining methods it would appear to be an extremely useful experiment for gaining insight into the function of the flow chamber.

After consideration of the results obtained using electrophoresis in cellulose acetate devices it is felt that there is reason for optimism in this work. Certainly, little in the way of results were obtained but this is due to a localised problem in one area of the work which is possible to fix in a reasonable time scale. From a positive viewpoint, the theoretical response and modelled environment response of the chamber have been described and the full fabrication process has been developed and optimised. Therefore, with some future work in this field it should be possible to solve the fluorescent problem and gain some results and insight into the operation of the devices. This in turn would allow application of the chambers to genomic separation and hopefully facilitate an increase in gene sequencing throughput.

5.9 References

[1] Casey, B. G., Monaghan, W., and Wilkinson, C. D. W., Embossing of nanoscale features and environments, Microelectronic Engineering, vol. 35, pp. 393-396, 1997.

[2] Calladine, C.R., Drew, H.R., Understanding DNA : The molecule and how it works, Academic Press, London, 1997.

[3] Suzuki, D.T., Griffiths, A.J.F., Miller, J.H., Lewontin, R.C., An Introduction to Ginetic Analysis, W.H. Freeman and Company, New York 1986.

[4] Ogston, A.G., The Spaces in a Uniform Random Suspension of Fibres, Transactions of the Faraday Society, 1958, 54, 1754-1757.

[5] Wilding, P., Pfahler, J., Bau, H.H., Zemel, J.N., Kricka, L.J., Manipulation and Flow Of Biological Fluids in Straight Channels Micromachined in Silicon, Clinical Chemistry, 1994, 40, 43-47.

[6] Simonson, T., Kubitsa, M., DNA Orientation in Shear Flow, Biopolymers, 1993, 33, 1225-1235.

[7] Manning, G.S., Limiting Laws and Counterion Condensation in polyelectrolyte Solutions I. Colligative Properties and II. Self-Diffusion of the Small Ions, The Journal of Chemical Physics, 1969, 51, 924-938.

[8] Noolandi, J., Theory of DNA Gel Electrophoresis, Advances in Electrophoresis Vol. 5, Edited by Chrambach, A., Dunn, M.J., Radola, B.J., VCH Publishers Inc., New York 1992.

[9] Deutch, J.M., Theoretical Aspects of Electrophoresis, Electrophoresis of Large DNA Molecules: Theory and Applications, Edited by Lai, E., Birren, B.W., Cold Spring Harbor Laboratory Press, New York 1990.

[10] Duke, T.A.J., Viovy, J.L., Simulation of Megabase DNA Undergoing Gel Electrophoresis, Physical Review Letters, 1992, 68, 542-545.

[11] Duke, T.A.J., Semenov, A.N., Viovy, J.L., Mobility of a Reptating Polymer, Physical Review Letters, 1992, 69, 3260-3263.

[12] Duke, T.,"Computer-Simulation Of Dna Electrophoresis," Analusis, vol. 21, pp. M 29-M 31, 1993.

[13] Viovy, J.L.,and Duke, T.,"Dna Electrophoresis In Polymer-Solutions - Ogston Sieving, Reptation and Constraint Release," Electrophoresis, vol. 14, pp. 322-329, 1993.

[14] Rentzeperis, D., Ho, J. and Marky, L.A.,"Contribution Of Loops and Nicks to the Formation Of Dna Dumbbells - Melting Behavior and Ligand-Binding," Biochemistry, vol. 32, pp. 2564-2572, 1993.

[15] Porschke, D., Schmidt, E.R., Hankeln, T., Nolte, G., and Antosiewicz, J.,"Structure and Dynamics Of Curved Dna Fragments In Solution - Evidence For Slow Modes Of Configurational Transitions," Biophysical Chemistry, vol. 47, pp. 179-191, 1993.

[16] Masubuchi, Y., Hidehiro, O., Akiyama, T., Matsumoto, M., Doi, M., Dynamics of a DNA Molecule Hanging over an Obstacle in Gel Electrophoresis, Journal of the Physical Society of Japan, 1995, 64, 1412-1420.

[17] Duke, T., Monnelly, G., Austin, R.H., Cox, E.C., Sequencing in Nanofabricated Arrays : A Feasibility Study, Electrophoresis, 1997, 18, 17-22.

[18] Alberts, B. et al., Molecular Biology of the Cell, Third Ed., Garland Publishing Inc., New York, 1994.

[19] Morikawa, K., Yanagida, M., Visualisation of individual DNA molecules in solution by light microscopy : DAPI staining method, Journal of Biochemistry, 1981, 89, 693-696.

[20] Smith, S. B., Bendich, A. J., Electrophoretic Charge Density and Persistence Length of DNA as measured by fluorescence microscopy, Biopolymers, 29, 1167-1173, 1990.

[21] Bustamante, C., Direct observation and manipulation of single DNA molecules using fluorescence microscopy, Annual Review of Biophysics and Biophysical Chemistry, 20, 415-446, 1991.

[22] Volkmuth, W.D., Strick, W., Duke, T., Austin, R.H., Cox, E.C., Separation of DNA and observation of bands in microfabricated arrays, Biophysical Journal, 66, A280, 1994.

[23] Personal Correspondence, Wayne Volkmuth, 1995.

[24] Bendich, A. J., Structural-Analysis Of Mitochondrial-Dna Molecules From Fungi and Plants Using Moving-Pictures and Pulsed-Field Gel-Electrophoresis, Journal Of Molecular Biology, vol. 255, pp. 564-588, 1996.

[25] Reese, H. R., Effects Of Dna Charge and Length On the Electrophoretic Mobility Of Intercalated Dna, Biopolymers, vol. 34, pp. 1349-1358, 1994.

[26] Beattie, K. L., Beattie, W. G., Meng, L., Turner, S. L., Coralvazquez, R., Smith, D. D., McIntyre, P. M., and Dao, D. D., Advances In Genosensor Research, Clinical Chemistry, vol. 41, pp. 700-706, 1995.

[27] Larsson, A., Akerman, B., and Jonsson, M., Dapi Staining Of Dna - Effect Of Change In Charge, Flexibility, and Contour Length On Orientational Dynamics and Mobility Of the Dna During Agarose-Gel Electrophoresis, Journal Of Physical Chemistry, vol. 100, pp. 3252-3263, 1996.

[28] Haughland, R. P., Molecular Probes : Handbook of Flourescent Probes and Research Chemicals, Molecular Probes Inc., 1996.

[29] Molecular Probes, Web Page : www.probes.com.

[30] Strachan, T., The Human Genome. UK: BIOS Scientific Publishers Limited, 1992.

[31] Bakajin, O.B., Duke, T.A.J., Chou, C.F., Chan, S.S., Austin, R.H., Cox, E.C., Electrohydrodynamic Stretching of DNA in Confined Environments, Physical Review Letters, 80, 12, pp. 2737-2740, 1998.

Chapter 6

Conclusions

6.1 Summary

Bioelectronics and cell engineering are rapidly growing areas of research which are attracting large amounts of interest from academic and industrial institutions. At Glasgow University there is a long history of work in bioengineering, however if this field is to advance at an appreciable rate it is important that a department with such diverse research interests as the Electronics Department contributes its expertise and resources.

One of the most valuable contributions that electrical engineers can make to bioengineering is the technology and skill to fabricate environments, electrodes, manipulators and potentially whole laboratories on a scale capable of direct interaction with biological molecules and cells. It is this nanofabrication and its applications in biological sciences that have been at the centre of the work carried out during the course of this project.

There are essentially three strongly related main areas of research which have been investigated here and which can be considered independently of each other. These are : mechanical pattern transfer methods, DNA fractionation and cell guidance and adhesion. The pivotal technology for the biological application mentioned here is undoubtedly embossing and its donor processes of electron beam lithography and reactive ion etching.

One of the main problems in nanofabrication is the patterning of large surface areas in a reasonable time scale and at an acceptable cost. Embossing of thermoplastics is a process which can alleviate this problem. Plastics are excellent materials for pattern transfer simply because they can be patterned in so many different ways. Many thermoplastics such as cellulose acetate can be patterned using temperature, light, radiation and even mechanical force, thus allowing itself to be fashioned in various forms.

The results obtained with plastics during the course of the work have, however, shown that feature sizes comparable with those produced at the limits of electron beam lithography can be fashioned into a polymer using a simple embossing technique. Dense patterns of 15nm dots can be easily transferred over large areas with good uniformity.

Progress has been made to overcome the problem of multiple layered plastic devices. It has been found that using plastic photolithography allows patterns to be superimposed on top of one another, a potentially very useful effect. Leading on from this, work has been done to discover the effect of direct writing of plastic samples using e-beam lithography. This proved to be an extremely useful process for the fabrication of efficient diffractive optics and in the production of devices for cell adhesion tests.

In conclusion to this section of work it is felt that embossing and plastic patterning are extremely useful processes for many applications but particularly in the fields of bioelectronics and optoelectronics where devices utilising these methods are currently being fabricated for use within and outwith the department.

The primary application of nanofabricated devices in this project was in DNA fractionation using nanostructure lattices and electrophoresis. It was found that using simple pillar structures, DNA conformations could be seen using fluorescence microscopy that were in good agreement to those predicted by reptation theory and modelling. Thus, using this information and modelling prospective devices an obstacle configuration was designed which is capable of producing DNA conformations conducive to length fractionation. These devices were fabricated using embossing but due to problems with fluorescent staining of the DNA little in the way of experimental results were obtained in the allowed time scale.

The final area of research under consideration in this thesis is the application of embossed devices in the observation of biological cell adhesion to patterned substrata. Dotted substrates were fabricated in polystyrene and it was found that cells do not adhere well to these surfaces. This is a very interesting finding since it has long been an

area of uncertainty as to what effect rugosity has on a cell. From a practical point of view it means that it is possible to control the positioning of cells on a surface, a potentially useful phenomenon for clinical implants and vascular prosthetics.

6.2 Further Work

It is felt by this researcher that mechanical pattern transfer is a technology which has a great deal to offer. As such, work is required to optimise this process and to standardise it for use as a service rather than a purely research technology within the department. There is also scope for work in the areas of high aspect ratio embossing and embossing into materials other than polymers.

As for work into DNA fractionation using artificial retarding media and electrophoresis it is felt that there is cause for optimism that this could become an everyday procedure in life science laboratories. However, in order to achieve this goal it is necessary to continue development and design of the medium to produce and optimise the separation.

More importantly from our viewpoint it is essential that a suitable visualisation method is found. It is possible that by increasing the size of the retarding medium to be in the order of a few centimetres in length, we would not require to view individual DNA strands but could instead view bands as in a gel. This would appear to be the logical progression in this work, but in order to fabricate such devices they would have to be produced by an external source since we do not have such a capability in house. This is the reason that such steps have not already been taken.

Lastly, more work is required to obtain a fuller understanding of the mechanism for cell adhesion to different nanometric topographies. At present, understanding of this effect is uncertain but with the ability to produce almost any feature shape using nanofabrication it should be possible to clarify this area.

Appendix

A1 Units

amu	atomic mass unit
kbp	kilo base pair (1 kbp = 6.6×10^5 daltons $\approx$ 0.3nm)
μC/cm^2	micro Coulombs per centimetre squared
micron, μm	10^{-6} m
nm	10^{-9} m
sccm	Standard cubic centimetre per minute

A2 Abbreviations

AFM	Atomic force microscope
DABCO	1,4-Diazabicyclo[2.2.2]octane
DNA	Deoxyribonucleic acid
EBL	Electron beam lithography
EBPG	Electron beam pattern generator
ECR	Electron cyclotron resonance
EDTA	Ethylene diamine tetra acetic acid
HMDS	Hexamethyldisilazane
Mwt	Molecular weight
PAC	Photo active compound
PMMA	Polymethyl methacrylate
RIE	Reactive ion etching
RO	Reverse Osmosis
RPM	Revolutions per minute
SEM	Scanning electron microscope
UV	Ultra violet

A3 Manufacturers

AZ Photoresist Products
Business Unit Electronic Materials
Clariant Corporation (USA)
70 Meister Avenue
Somerville
New Jersey 08876, USA

Goodfellow
Goodfellow Cambridge Ltd.
Cambridge Science Park
Cambridge
CB4 4DJ
England

Hoechst
Hoechst Celanese Corporation
70 Meister Avenue
Somerville
New Jersey 08876
USA

Opticlear™
National Diagnostics
Unit 3, Chamberlain Road
Aylesbury
Bucks HP19 3DY
England

Shipley Europe Limited
Herald Way
Coventry
England
CV3 2RQ

A4 Material Compositions

Cellulose Acetate
Goodfellow sheet cellulose acetate code AC 311400

Density	1.3g cm^{-3}
Refractive Index	1.49
Specific Heat	1.2-1.9 kJ kg^{-1} K^{-1}
Thermal Expansivity	80-180 x10^{-6} K^{-1}

Corning 7740 Pyrex Glass
Composition : 80.5% SiO_2, 12.9% B_2O_3, 2.2% Al_2O_3, 3.8% Na_2O, 0.4% K_2O

Chrome/Nichrome Wet Etch (As used in this project)

1l water, 150g ceric ammonium nitrate, 35ml acetic acid(98%)

Hoechst AZ 400K Developer

Aqueous potassium hydroxide based chemistry

Hoechst AZ PN114 Chemically Amplified Resist

Novolak matrix insolublised in an acid a catalysed cross linking reaction. Upon radiation, a strong Bronsted acid is produced which activates a melamine type crosslinking agent

Hoechst EBX Thinner

Ethyl lactate

Novolak

Phenolic or cresylic type resin [1]

PAC (Photo Active Compound)

O-naphthoquinonediazide based chemistry [1]

Polymethyl methacrylate (PMMA)

Goodfellow sheet polymethyl methacrylate code ME 303010

Density	1.19g cm^{-3}
Refractive Index	1.49
Specific Heat	1.4-1.5 kJ kg^{-1} K^{-1}
Thermal Expansivity	70-77 x10^{-6} K^{-1}

Shipley Microposit S1800 Series Photoresists (e.g. S1818)

Commercial solvent based photoresist consisting of a photoactive compound in a Novolak type resin. The solvent is propylene glycol monomethyl ether acetate [2]

---

[1] Pacansky, J., Lyerla, J.R., Photochemical Decomposition Mechanisms for AZ Type Photoresists, IBM Journal of Research Development, Vol 23, No 1, 1979.

[2] Shipley Microposit S1800 Series Datasheets.